**University of Aveiro**
**2015**

Department of Materials Engineering and Ceramics

**Mathieu Paradis**

# Plataformas de Ácido Poli-L-Lático para aplicação em engenharia de tecido ósseo: desenvolvimento e caracterização

**University of Aveiro**
**2015**

Department of Materials Engineering and Ceramics

**Mathieu Paradis**

# Plataformas de Ácido Poli-L-Lático para aplicação em engenharia de tecido ósseo: desenvolvimento e caracterização

# Development and Characterization of Poly(L-lactic acid) (PLLA) platforms for Bone Tissue Engineering

Tese apresentada à Universidade de Aveiro para cumprimento dos requisitos necessários à obtenção do grau de Mestre em "Ciência e Engenharia de Materias", realizada sob a orientação científica da Doutora Paula Vilarinho e Doutora Maria Helena Fernandes, ambas Professoras associadas do Departamento de Engenharia de Materiais e Cerâmica da Universidade de Aveiro

**O júri**

Presidente

Prof. Dr. Ana Margarida Madeira Viegas de Barros Timmons

Assistant Professor of the University of Aveiro

Prof. Dr. Maria Helena Figueira Vaz Fernandes

Associate Professor of the University of Aveiro

Prof. Dr. Maria Ascensão Ferreira Silva Lopes

Assistant Professor of the Faculty of Engineering of the University of Porto

**Agradecimentos**

First of all I would like to thank Mrs. Paula Vilarinho who introduced me this biomaterial subject and hosted me in her research group. I also would like to thank her, as well as Mrs. Maria Helena Fernandes for the guidance they provided me and their whole trust in me.

Then a special acknowledgment to my collaborator Marisa Maltez, who made my internship, and also my stay in Portugal really pleasant. I am very grateful for all her patience, her advices, and all the explanations she gave me during throughout the internship, and even throughout the every day life. Because her experience and her advices helped me a lot to fulfill the objectives of the project, as well as define more my professional project I would never be grateful enough.

I also acknowledge my collaborator Ana Roque, from the Institute of Biomedicine (IBIMED) for the great job done with cells, as well as all technicians and researchers from and out of the Department of Materials and Ceramics of the University of Aveiro who contributed to the success of the project.

Another special thank goes to the other FAME students Antoine Lopez, Louise Saidi, Hannes Radenbach, and Manon Wilhelm for the great time spent with them.

Finally I would like to thank my family, my parents and my brothers, who are trusting and supporting me in all situations.

**Palavras-chave**

Biomateriais, osso, regeneração, ácido poli-L-láctico, piezoelectricidade, resposta celular.

**Resumo**

O desenvolvimento de *scaffolds* baseados em biomateriais é uma estratégia promissora para a engenharia de tecidos e entrega de fármacos. Este trabalho centra-se na engenharia de tecido ósseo, o objectivo é desenvolver biomateriais electricamente modificados, com diferentes valores de cristalinidade e propriedades eléctricas, e estudar o seu impacto no comportamento biológico da célula de modo a prever o efeito desses materiais na regeneração do tecido.
É já amplamente conhecido o fato de o osso possuir características piezoeléctricas, e reconhecido que estas contribuem para os mecanismos de regulação do crescimento e reparação do tecido ósseo. Além disso é um facto aceite que a estimulação eléctrica também influencia o crescimento e reparação do osso. Os materiais piezoeléctricos apresentam assim vantagens quanto à sua utilização em engenharia de tecido ósseo, e têm vindo a ser estudados para esse efeito.

No presente trabalho foram desenvolvidos filmes de ácido poli-L-láctico (PLLA), um polímero sintético semi-cristalino que é biocompatível, biodegradável, e piezoeléctrico, que se apresenta como promotor da regeneração óssea. O PLLA é um material aceite para implantes em humanos pela "Food and Drug Administration" (FDA), e está já a ser utilizado em várias estratégias e produtos para uso clínico. O presente estudo consiste numa primeira fase de preparação e caracterização de filmes de PLLA em termos de propriedades estruturais e de superfície, e numa segunda fase de avaliação do comportamento celular em termos de viabilidade, proliferação, morfologia e mineralização, para cada uma das configurações de PLLA obtidas. Os filmes foram preparados pelo método de evaporação do solvente com molde, e submetidos a diferentes tratamentos térmicos de forma a obter diferentes valores de cristalinidade. Estas plataformas foram depois electricamente polarizadas, positiva e negativamente, por meio de descarga de corona para modular as suas propriedades eléctricas. Os ensaios celulares foram realizados utilizando duas linhas celulares osteoblásticas, em contacto direto com as superfícies de PLLA: Osteoblastos Humanos - Hob, cultura primária de células, e linha de Osteosarcoma Humano - MG-63.

Este trabalho também inclui uma introdução teórica para área da Engenharia de Tecido Ósseo, e resume o trabalho de investigação realizado nesta área até hoje incluindo aquele relacionado com a piezoelectricidade do tecido ósseo. A parte experimental dedica-se aos efeitos do grau de cristalinidade e da polarização nas propriedades de superfície do material e nos ensaios biológicos. Foram estudadas nove configurações, originadas por três valores de cristalinidade: 0, 7 e 35%, e três tipos de polarização: positiva, negativa e neutra (apenas com o tratamento térmico análogo).

**Key words**

Biomaterials, bone, regeneration, Poly (L-lactic) acid, polarization, piezoelectricity, cellular response

**Abstract**

The development of scaffolds based on biomaterials is a promising strategy for Tissue Engineering and cellular regeneration. This work focuses on Bone Tissue Engineering, the aim is to develop electrically tailored biomaterials with different crystalline and electric features, and study their impacts onto cell biological behavior, so as to predict the materials output in the enhancement of bone tissue regeneration. It is accepted that bone exhibits piezoelectricity, a property that has been proved to be involved in bone growth/repair mechanism regulation. In addition electrical stimulations have been proved to influence bone growth and repair. Piezoelectric materials are therefore widely investigated for a potential use in bone tissue engineering. The main goal is the development of novel strategies to produce and employ piezoelectric biomaterials, with detailed knowledge of mechanisms involved in cell-material interaction.

In the current work, poly (L-lactic) acid (PLLA), a synthetic semi-crystalline polymer, exhibiting biodegradibility, biocompatibility and piezoelectricity is studied and proposed as a promoter of enhanced tissue regeneration. PLLA has already been approved for implantation in human body by the Food and Drug Administration (FDA), and at the moment it is being used in several clinical strategies. The present study consists of first preparing films with different degrees of crystallinity and characterizing these PLLA films, in terms of surface and structural properties, and subsequently assessing the behavior of cells in terms of viability, proliferation, morphology and mineralization for each PLLA configuration. PLLA films were prepared using the solvent cast technique and submitted to different thermal treatments in order to obtain different degrees of crystallinity. Those platforms were then electrically poled, positively and negatively, by corona discharge in order to tailor their electrical properties. The cellular assays were conducted by using two different osteoblast cell lines grown directly onto the PLLA films: Human osteoblast Hob, a primary cell culture and Human osteosarcoma MG-63 cell line.

This thesis gives also a comprehensive introduction to the area of Bone Tissue Engineering and provides a review of the work done in this field in the past until today, in that same field, including the one related with bone's piezoelectricity. Then the experimental part deals with the effects of the crystallinity degrees and of the polarization in terms of surface properties and cellular bio assays. Three different degrees of crystallinity, and three different polarization conditions were prepared; which results in 9 different configurations under investigation.

# Table of contents

**Index of figures .....XVII**

**Index of tables .....XIX**

**List of abbreviations .....XXI**

**Chapter 1: Introduction to Bone Tissue Engineering .....1**

1 Tissue Engineering.....3
1.1 Principles and practice of Tissue Engineering.....3
1.2 Current applications.....5
1.2.1 Tissue Engineering for the regeneration of damaged tissues.....5
1.2.2 Tissue Engineering for modeling human physiology.....6
1.3 Conclusion.....6
2 Tissue Engineering approaches for the regeneration of bone.....7
2.1 Bone Biology.....7
2.1.1 Chemical composition of bone.....8
2.1.2 Bone cells.....8
2.1.3 Development of bone and regeneration.....10
2.2 Bone tissue engineering.....12
2.2.1 Current treatments for damaged bone.....12
2.2.2 Biomaterials and alternative solutions.....13

**Chapter 2: Piezoelectric PLLA for bone regeneration .....17**

1 Bioelectricity.....19
2 Piezoelectricity .....20
2.1 Definition.....20
2.2 Piezoelectricity in bone.....21
2.3 Piezoelectric materials for the regeneration of bone.....22
3 Poly (L-lactic) acid.....24
3.1 The molecules of PLA and PLLA .....24
3.2 PLLA as a piezoelectric material .....25
4 Objectives.....26

**Chapter 3: Materials and methods .....29**
1 Materials.....31
2 Preparation of the films of PLLA .....31
2.1 Film assembly.....31
2.2 Crystallization.....33
2.3 Summary.....34
3 Polarization.....36
4 Characterization of the films of PLLA.....39
4.1 Micro-structural characterization.....39
4.1.1 Optical microscopy.....39
4.1.2 Scanning Electron Microscopy.....40
4.2 Surface roughness measurement.....41
4.3 Wettability – contact angle measurement.....42
4.4 X-Ray diffraction – XRD.....42
4.5 Differential Scanning Calorimetry.....45
5 Cellular biological assays.....48
5.1Preliminary steps .....48
5.1.1 Preparation of the wells and cutout of the samples.....48
5.1.2 Sterilization.....49
5.1.3 Hob culture.....51
5.2 Assays.....51
5.2.1 Cell viability: adhesion and proliferation.....51
5.2.2 Cell morphology.....52
5.2.3 Cell mineralization.....53

**Chapter 4: Results and discussion .....55**
1 PLLA film characterization results.....58
1.1Micro structural study.....59
1.2 Surface roughness measurement.....64
1.3 Thickness measurement.....65
1.4 Wettability – Contact angle measurement.....66
1.5 Thermal analysis.....67
1.6 X-ray diffraction studies.....71
1.7 Cellular bio assay results .....73
1.7.1 Cell viability onto PLLA films .....73
1.7.2 Assessment of the morphology by immunofluorescence and scanning electron microscopy analysis .....7§
1.7.3 Mineralization study.....77

**Conclusion and prospects .....81**
1 Conclusion.....83
2 Future work .....84

**References .....85**

**Annexes .....95**
Annex A: Film assembly protocol.....97
Annex B: Crystallization protocol .....99
Annex C: Polarization protocol.....101
Annex D : Surface roughness measurement protocol.....105
Annex E: Wettability measurement protocol .....107
Annex F: Sterilization protocol.....109
Annex G: Cell culture protocol.....111
Annex H: Viability and proliferation assay.....113
Annex I: Morphology assay .....115
Annex J: Mineralization assay.....119

# Index of figures

Figure 1: Microscopic structure of bone .....7

Figure 2: Osteoblast life cycle .....10

Figure 3: Bone repair mechanism .....11

Figure 4: The dowsing reaction .....20

Figure 5: The stereo-isomers of lactic acid .....24

Figure 6: Schematic representation of the film preparation setup .....32

Figure 7: Example of PLLA film obtained after drying .....32

Figure 8: Schematic representation of the experimental setup used for the crystallization step .....33

Figure 9: Processing cycle of a) amorphous; b) semi-crystalline and c) crystalline PLLA films .35

Figure 10: Corona setup .....37

Figure 11: Polarization cycle .....38

Figure 12: Different SEM signals .....40

Figure 13: Schematic representation of the surface roughness experimental setup .....42

Figure 14: Contact angle measurement systems .....43

Figure 15: Static contact angle measurement with the sessile drop method .....44

Figure 16: Schematic representation of the goniometer used for the contact angle measurement ..45

Figure 17: Typical DSC thermogram .....46

Figure 18: Schematic representation of the wells box .....48

Figure 19: Resazurin used as colorimetric assay for cell viability .....52

Figure 20: HOB after mineralization in vitro .....53

Figure 21: Schematic representation of the processing cycles for amorphous, semi-crystalline and crystallines samples .....57

Figure 22: Schematic representation of the poling step for standard, non poled and poled (positively or negatively) samples.....58

Figure 23: Topographic pictures of PLLA films before and after thermal treatment varying the degree of crystallinity .....61

Figure 24: Electron micrographs of PLLA films before and after thermal crystallization varying the degree of crystallinity .....63

Figure 25: DSC curves of amorphous, semi-crystalline and crystalline PLLA films for standard and non poled configurations .....68

Figure 26: Standard amorphous DSC thermogram.....69

Figure 27: X-Ray diffractogram for amorphous, semi-crystalline and crystalline samples, in standard configuration, i.e. as prepared .....71

Figure 28: X-Ray diffraction patterns for non poled, poled positive, poled negative and standard for different cases a) amorphous, b) semi-crystalline, and c) crystalline samples .....72

Figure 29: Graph of resazurin measurements for 8 days for HOB cells were grown on different PLLA films polarized and non-polarized, and plastic .....74

Figure 30: Graph of resazurin measurements for 8 days for MG-63 cells grown on different PLLA films polarized and non-polarized, and plastic.....74

Figure 31: Fungus attack on cells .....76

Figure 32: Images of HOB grown on different surfaces for 21 days .....78

Figure 33: Images of MG63 grown on different surfaces for 21 days .....79

Figure 34: Equipment used for the preparation of the sample for polarization .....101

Figure 35: Schematic representation of the different steps of preparation of the sample for polarization .....102

Figure 36: Corona polarization setup including a Faraday cage (a), a Corona needle and a Corona plate (b & c), a multimeter (d), and and a power supply unit (e) .....103

# Index of tables

Table 1: Cell sources and biomaterials used in different areas of Tissue Engineering .....5

Table 2: List of FDA approved drug delivery products using PLA polymer .....25

Table 3: Summary of primary sterilization methods employed in biomaterials ..... 49

Table 4: Surface roughness results .....64

Table 5: Thickness measurements .....65

Table 6: Contact angle results in water .....66

Table 7: Enthalpies and degrees of crystallinity of PLLA films.....70

# List of abbreviations

ALP – Alkaline Phosphate

BTE – Bone Tissue Engineering

BSE – Backscattered Electrons

CaP – Calcium phosphate

DDS – Drug and Delivery System

DSC – Differential Scanning Calorimetry

EBSD – Electron Backscattered Diffraction

EDX – Energy Dispersive X-ray spectroscopy

FDA – Food and Drug Administration

HAp – Hydroxyapatite

Hob – Human Osteoblast

HPGP – Hydrogen Peroxide Gas plasma

PGA – Poly (glycolic acid)

PLA – Poly(lactic acid)

PLLA – Poly(L-lactic) acid

PVDF – Polyvinylidene Fluoride

SE – Secondary Electrons

SEM – Scanning Electron Microscopy

TE – Tissue Engineering

XRD – X-Ray Diffraction

# Chapter 1

Introduction to Bone Tissue Engineering

# 1 Tissue Engineering

## 1.1 Principles and practice of Tissue Engineering

The term tissue refers to the intermediate organizational level between cells and organs. In living organisms, cells group together to form tissues. Organs are then formed by the functional grouping of several tissues. Tissues provide the numerous functions of organs necessary to maintain biological life. The structure and the function of tissues are different for each organ. But these tissues can be damaged and undergone trauma. In order to repair tissues, tissues engineering has been developed [1].

Tissue engineering is an interdisciplinary domain that creates functional three-dimensional tissues combining scaffolds, cells and/or bioactive molecules [2]. This field involves scientific areas such as cell biology, material science, chemistry, molecular biology, engineering and medicine. It applies the principles of engineering and life sciences toward the development of biological substitutes that restore, maintain, or improve tissue functions [1] in order to trigger the self-healing of the human body.

Moreover, tissue engineering exhibits some advantages in terms of tissues damages, compared to the actual medicine [3]. Indeed, medical therapies such as transplants, mechanical devices or surgical reconstruction have saved and improved patients' lives, but they present associated problems. For example, organ transplants show important limitations such as transplant rejection and lack of donor to cover all the worldwide demand. Mechanical devices are not capable of accomplishing all the functions associated with the tissue and cannot prevent progressive patient deterioration. Finally, surgical reconstruction can result in long-term problems. Therefore tissue engineering arises from the need to provide more definitive solutions to tissue repair in clinics and aims to achieve this goal by the development of in vitro devices that would repair in vivo the damaged tissue. To succeed in these purposes, tissue engineering uses nature as an inspiration source by mimicking native human tissues in order to obtain better response of the host. For example, the human liver will regrow to its original size even when more than 50% of its mass is excised [4]. Several tissues as bone and skin for example, also have an innate capacity to regenerate to fill injuries below a critical size [5].

Tissue engineering involves three basic elements: scaffolds, cells and biomolecules. A suitable combination of these three elements allows performing a wide range of applications.

***Scaffold***

Scaffolds are three dimensional (3D) elements that serve as temporary substrate for supporting and guiding tissues formation allowing cell attachment and migration by recreating the in vivo environment [3]. It can also be functionalized in order to answer some specification like drug delivery or other biological agents [6].

To achieve the goal of tissue reconstruction, scaffolds must fulfill some requirements as biocompatibility and biodegradability. Moreover parameters as scaffold dimension, its stiffness, the percentage of porosity, and the size of the pores have great importance [3]. The design of the scaffold will influence the cell seeding and diffusion throughout the whole structure of both cells and nutrients.

After a certain time, the scaffold disappears or is removed by medical surgery. Scaffolds only serve as template, to hold and guide cells in 3D space until they produce their own physiological matrix environment, while the scaffold gradually degrades [2].

***Cells***

Tissue engineering uses living cells as engineered materials. For instance, fibroblasts in skin replacement, chondrocytes for the repair of cartilage, and osteoblast for the repair of bone.

***Biomolecules***

Biomolecules play an important role, they control the biology of cells from proliferation to apoptosis. For example, in the cellular environment, the presence and gradient of biomolecules such as growth factor, chemokines, and cytokines play an important role in biological phenomena such as chemotaxis, morphogenesis and wound healing [3]. In particular, these signals are tightly controlled and unique to each organ.

## 1.2 Current applications

### 1.2.1 Tissue Engineering for the regeneration of damaged tissues

The regenerative medicine, defined as the combination of living cells and biocompatible scaffolds, is one of the scope of application of tissue engineering [7]. The aim is to create engineered and functionalized living tissues capable to sustain itself, allowing the replacement or the regeneration of damaged cells, tissues and organs in order to restore normal function. The regeneration is done by stimulating, at the cellular scale, the mechanisms of repair. The strategy is to induce the body to heal itself using cells.

The regenerative medicine is applied to repair a wide range of tissues: skin, bone, cartilage, pancreas, heart and nervous tissues. Depending on the applications, the kind of cells used is different. Table 1 summarizes the materials and the cells employed depending on the area. However there are many issues to consider in the creation of a functional, and implantable tissue. Most important, it must be easily accessible, a readily abundant cell source with the capacity to express the desired tissues' phenotype, i.e. the suitable characteristics such as the morphology, the behavior, the biochemical and physiological properties, the cell components, etc; and a biocompatible inert scaffold to deliver the cells to the damaged region [7].

***Table 1**: Cell sources and biomaterials used in different areas of Tissue Engineering [3]*

| Scaffold | | | | Cells | |
|---|---|---|---|---|---|
| **TE area** | | **Bioceramics** | **Polymers** | **Self-assembling peptides** | |
| Bone | Autologous grafts, Alginate, Chitosan, Collagen, Fibrin, Gelatin | Hydroxyapatite | PCL, PEG, PGA, PLA, PLG, PLGA | RAD16-I | Adipose Stem Cells, Bone Marrow Stem Cells |
| Articular Cartilage | Alginate, Agarose, Chitosan, Collagen, Fibrin, Gelatin, Hyaluronan | — | elastin-based polymers, PCL, PEG, PGA, PLA, PLGA, polyurethane | RAD16-I, KLD-12 | Chondrocytes, Adipose Stem Cells, Bone Marrow Stem Cells |
| Heart | Agarose, Alginate, Chitosan, Collagen, Elastin, Fibrin, Gelatin, Hyaluronan, Laminin, Matrigel™, Platelet gel, Silk, Starch, Vitronectin | — | PCL, PEG, PGA, PLA, PLGA, Polyesters, PPF | RAD16-I | Resident Cardiac Stem Cells, Cardiac Myocites, Skeletal Myoblasts, Embryonic Stem Cells, Bone Marrow Stem Cells, Adipose Stem Cells, Endothelial Pluripotent Cells, Umbilical Cord |
| Pancreas | Agarose, Alginate, Collagen, Chitosan, Laminin, Matrigel | — | Acrylonitrile copolymers, NIPA, PEG, PLA , PLGA, | — | β-cells, Embryonic stem cells, Stem/Progenitor cells of the Ductal Epithelium, Adult Ductal or Acinar Cells, Bone Marrow Stem Cells, Hepatic Cells |
| Vasculature | Agarose, Alginate, Chitosan, Collagen, Elastin, Fibrin, Gelatin, Hyaluronan, Matrigel™ | Hydroxyapatite, Silica-based mocrospheres | PEG PGA, PGLA, PLA, Polycarbonate, Polyethylene oxide, Polyester, Polypropylene oxide, Polyuretane | RAD16-I | Adipose-derived stem cells, Endothelial cells, MSCs, Smooth muscle cells |
| Cancer | Alginate, Collagen, Gelatin, Hyaluronan, Laminin, Matrigel | — | PEG, PLA, PLG, PLGA | RAD16-I | Tumoral Cells |

### 1.2.2 Tissue Engineering for modeling human physiology

The knowledge and the understanding of mechanisms involved in tissue growth are key parameters for regenerative medicine. Therefore the creation of models which will help to identify and understand the mechanisms that drive cellular processes are of major importance. The strategy is to cut out the complex cellular microenvironment into simpler systems in order to study the role of different chemical, mechanical and physical factors [3]. Using algorithms like the finite elements method correlated to in vivo and in vitro results we should be able to understand better the physiological cellular environment and to predict the effect of medical therapies and also the propagation of diseases such as cancer in order to improve the therapeutic approaches (disease modeling) [3].

## 1.3 Conclusion

Tissue engineering is a new challenging area in bioengineering at the frontiers between several domains. It offers a promising approach for the regeneration of damaged tissues, by triggering the self-healing of the body. Great advances have been done, especially in the last two decades, in all of the domains of tissue engineering. However, further research is still needed. Indeed, tissue engineering involves living organisms organized in complex architecture. Therefore the need for models is growing but a lot of influencing parameters are still not well known. Moreover, the selection of the material appears to be a major challenge: the exact interaction between cells and biomaterials is far from being understood. Indeed, cell adhesion is affected by the surface properties of the biomaterial such as wettability, roughness, surface charge and chemical functionalities. Understanding how cells and biomaterials interact will drive the development of the next generation of biomaterials for repair and replacement of defective tissues [8].

# 2 Tissue Engineering approaches for the regeneration of bone

## 2.1 Bone Biology

Bone is a living organism made of cells having their own lifecycle. Architected at several scales (see figure 1), the bone exhibits a wide range of properties making it a complex and fascinating material.

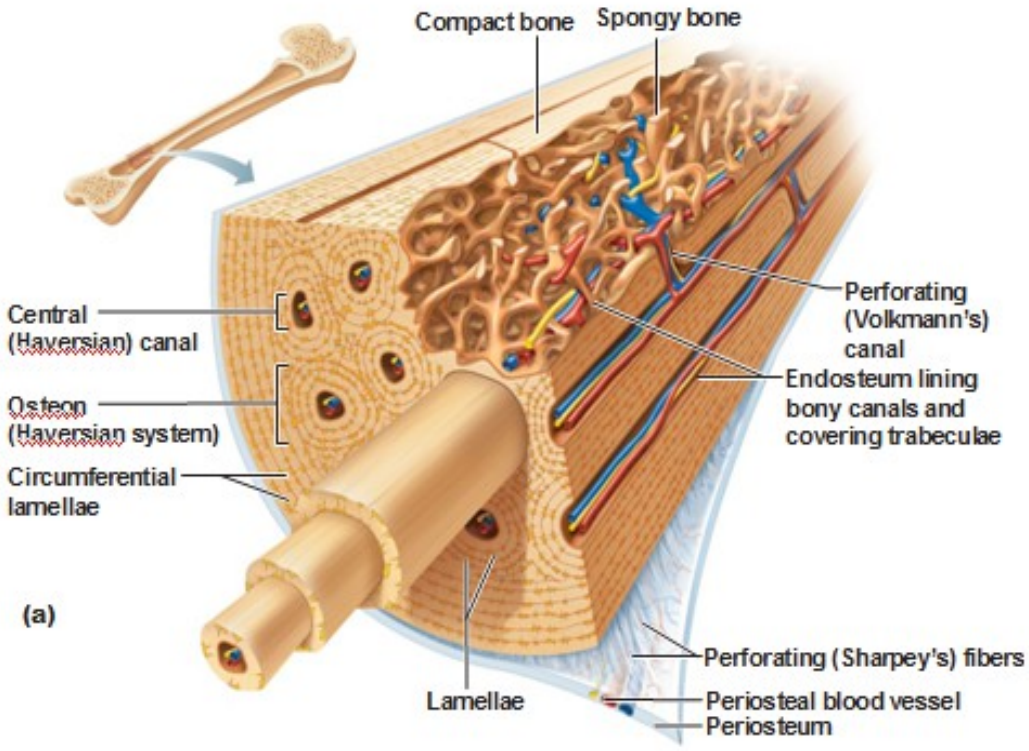


***Figure 1**: Microscopic structure of bone [9]*

Bones of the human body provide a framework where the mussels are attached and thus allow the support and the mobility of the body [7, 10, 11]. Moreover bones serve as the storage of minerals such as calcium and phosphate [10]. Some bones, as bones from the skull and the vertebrae also ensure the protection of organs and marrow [7, 11, 12].

### 2.1.1 Chemical composition of bone

Bone is a composite material made of two major components; an organic part and an inorganic mineral phase. The organic part, mainly composed of collagen type I: about 90% by mass, provides a supporting matrix upon which the mineral phase grow [13, 14, 15]. The mineral phase is made of calcium phosphate crystals such as hydroxyapatite, having as chemical formula ($Ca_{10}(PO_4)_6(OH)_2$) [11]. It is this part that provides solidity and hardness to the bone [7]. However its exact structure and chemical composition are still not well known due to its continuous remodeling [11] and varies from one person to another one according to the age, gender, and also depends on factors such as nutrition and hydration of the body [16]. Bone tissues also include water and molecules such as enzymes and growth factors.

### 2.1.2 Bone cells

Despite its relatively simple outer appearance, bone is not a solid homogenous tissue. Bone is made up of solid material with spaces between its hard elements. The outer smooth portion of the bone is compact or cortical bone (80% of bone), and the inner spongy part of the bone is trabecular bone (20% of bone) (figure 1). Furthermore, within those regions are different types of cells making up the cellular structure of the bone itself: osteoblasts, osteocytes, bone lining cells, and osteoclasts [17]. The third three types: osteoblasts, osteocytes and bone lining cells, are bone-forming cells what means that they produce the matrix that composes the bone. Osteoblasts, osteoclasts and bone lining cells are located at the surface of the bone tissue, whereas osteocytes take place inside the bone matrix [17].

***Osteoblasts***

Osteoblasts are immature bone cells that produce the matrix of the bone by the process of osteogenesis: they mainly secrete collagen but also other proteins such as alkaline phosphate (ALP) [7, 12]. The future of osteoblasts can occur in several ways [17]: 1) transformation of osteoblasts into osteocytes; 2) differentiation into bone lining cells; 3) death by apoptosis. The figure 2 gives a good description of the cycle of life of osteoblasts from mesenchymal state to differentiation to osteocytes or bone lining cells.

***Osteocytes***

These cells are former osteoblasts. During the process of maturation and growth of bone, osteoblasts were progressively surrounded by the bone and trapped in lacunae between layers of this mineralized matrix; and they finally differentiate into osteocytes [12, 17], as observed in figure 2. Their function is to maintain the bone matrix [12, 17] and contribute to regulate the rate of calcium in bones calcium homeostasis [7].

***Osteoclasts***

Osteoclasts are bone's absorption cells. They are responsible for the resorption and remodeling of bone and the overall decrease in bone mineral density [7]. The osteoclasts secrete hydrochloric acid and collagen which decrease locally the pH and allow to dissolve the inorganic matrix. This activity is essential to maintain strong and healthy bones, in parallel to the activity of osteoblasts. Thus it is estimated that, the overall bone mass is replaced every 5-6 years [11].

***Bone lining cells***

The bone lining cells are osteoblasts at rest (inactivated osteoblasts that previously differentiate into bone lining cells) that are able, if necessary, to become active osteoblasts (see figure 2). These cells cover the surface of the bone which is not under remodeling or formation [12]. The function of these cells is still not clear but studies showed that they digest bone matrix that is not resorbed by osteoclasts what initiates bone remodeling performed by osteoclasts [18].

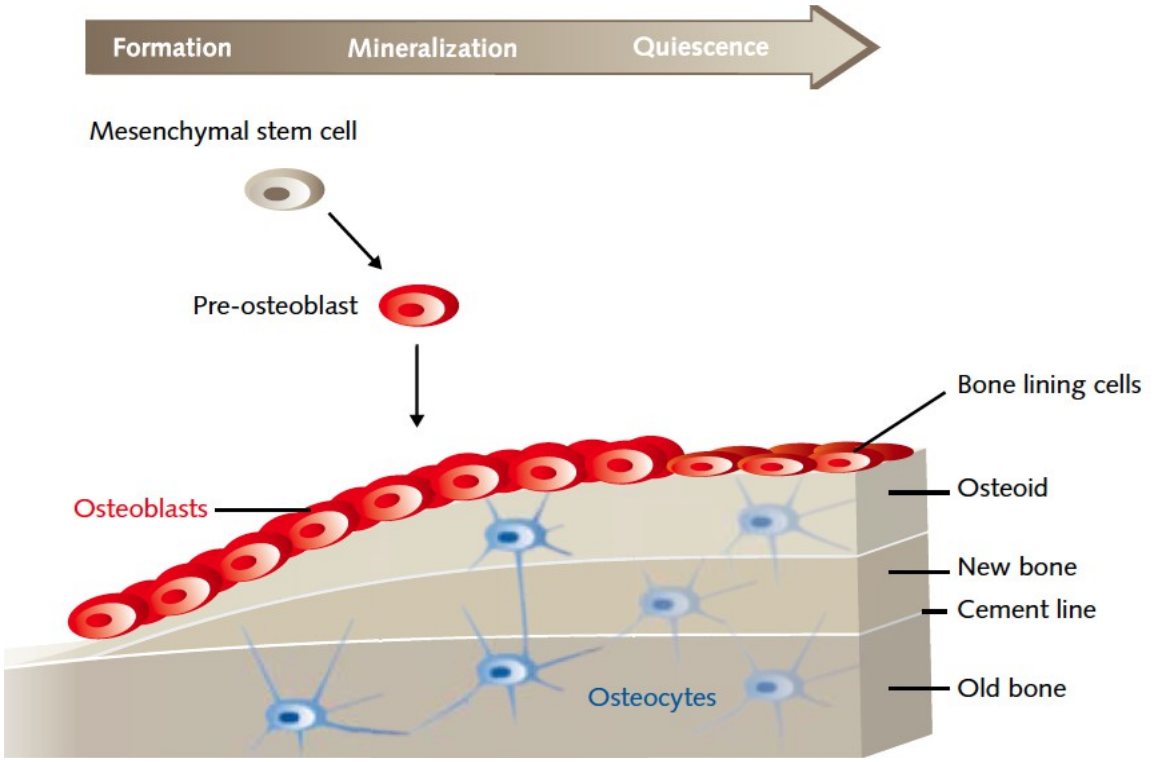


***Figure 2**: Osteoblast life cycle [15] – Osteoblasts are bone cells responsible for secreting and mineralizing the bone matrix. They develop from mesenchymal precursors*

### 2.1.3 Development of bone and regeneration

Within the body, the formation and growth of bone, also called osteogenesis, occurs by two processes: intramembranous and endochondral ossification; intramembranous ossification for flat bones and endochondral ossification for long bones [7, 10]. The intramembranous ossification refers to the formation of a bone via the replacement of a fibrous membrane [7, 19]. The formed bone is called intramembranous bone. They include certain flat bones of the skull and some of the irregular bones [19]. The endochondral ossification involves the replacement of hyaline cartilage with bone tissue. The formed bone is called cartilaginous bone [7, 10]. However, about bone formation, one needs to distinguish the process of ossification, which is the cellular synthesis of the organic matrix by osteoblast, and the process of mineralization, which refers to the deposition of a mineral phase within the organic matrix already synthesized [11].

Concerning bone regeneration, bone exhibits great properties and is thus able to heal itself after an injury. A healing cascade is then triggered to restore the tissue's original state [7, 10]. This healing cascade occurs in three phases, beginning with the inflammation of the tissues and then followed by the steps of repair and remodeling. This process is illustrated in figure 3. Briefly, the inflammatory phase results in hematoma formation as fibroblasts and cells from the inflammatory cascade (macrophages, monocytes, lymphocytes etc.) migrate into the injury site (hours to days). In the repair phase, collagen fibers and mineralized osteoid combine to form a soft callus around the injury site (4-6 weeks). As the callus ossifies it forms a disorganized structure known as woven bone. During the remodeling phase the disorganized woven bone is replaced by highly organized sheets of parallel collagen fibers called lamellar bone [7].

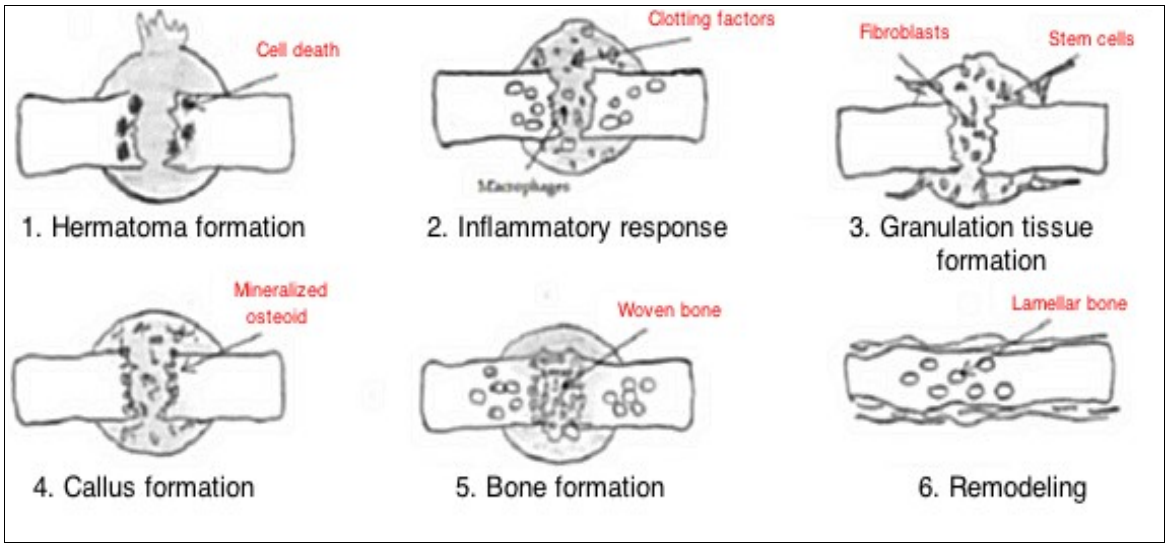


***Figure 3**: Bone repair mechanism [7]*

In this process of regeneration the mechanical environment is of large importance even though it is not the only one factor involved. In this context it has been shown that a mechanical stress helps to regenerate bone tissue. At the opposite a lack of physical activity causes bone loss and fractures because of tissues atrophy and bone loss [10, 20]. This can be explained by the body, which tends to improve the bone structure in order to adapt itself better to its mechanical environment [20, 21].

When one increases the mechanical load, the cellular activity increases as well. The body tends to adapt to its mechanical environment by improving the bone structure, leading to the reinforcement of the bone structure. This consequence is directly related to the piezoelectric effect of bone. One will discuss deeper this effect later in the report. Moreover, bone tissues are living tissues; they are continuously remodeled by the degradation of the matrix by the osteoclasts and the synthesis of new mineralized matrix by the osteoclasts [21]

## 2.2 Bone tissue engineering

As seen above, bone is capable of self regeneration in case of injuries or to remodel itself through mechanical load. However beyond a critical point, the natural self-healing process can be not enough important [19]. This may happen in case of severe injury, the fracture is too important and the repair mechanism can fail. In these circumstances the bone does not repair properly and therefore does not recover all its mechanical functions. Moreover bone tissues can suffer from several diseases, the most known being osteoporosis [14, 22, 23] and osteomalacia [23]. In that case a clinical intervention is required in order to help and assist bone in its healing process.

### 2.2.1 Current treatments for damaged bone

***Bone bracing***

The conventional approach for bone repair is bone bracing. It consists of immobilizing the bone in order to restrict its motion and therefore allow the injured area to heal [24]. This approach includes both surgical and non-surgical methods. Non-surgical alternatives such as external casts, bracing and splint are viable alternatives in cases with fracture displacements less than 2mm. This is the preferable method for bone healing, as it is non-invasive and minimizes risk of infection. Surgical approaches, such as open reduction internal fixation in which bones are set and held in place by nails, screws, or plates to guide and facilitate the healing process. Unfortunately, as with a surgical option, there is an increased risk of infection; however, surgical approaches are necessary in fracture displacements exceeding 2 mm [7]. Usually these fixation devices are metals, such as stainless steel, cobalt or titanium [25], which provide immediate mechanical support.

***Bone grafts***

Bone grafting is a surgical procedure by which new bone is placed into spaces between or around broken bone in order to aid in healing [26]**.** Bone grafts are used to enhance bone healing in specific injury zones. The advantages of this treatment is that the grafted tissues contain the cellular and matrix compounds necessary for the repair. The main types of grafts currently being utilized are autografts, allografts, xenografts, and synthetic grafts. Conventionally, autografts are the most effective grafts since they are harvested from the patient's own body, usually from the iliac crest, fibula, ribs, or mandible [7]. Moreover autografts do not represent risk of immune rejection [7, 10]. Although this approach is really efficient for bone repair, it presents few drawbacks: complications such infections, pain, etc; and supposes a second surgery for bone harvesting, and thus creates a secondary healing site and posses the associated risks. Allografts, on the other hand, are also natural human bone grafts, but unlike autografts which are harvested from the patient's own body, allografts are harvested from an external donor. Although the allograft eliminates the need for an additional surgery on the recipient, they also do not have the immunogenic properties of the autograft, and the risk of rejection increases [7]. Xenografts are grafts that are harvested from another species and are stripped down to just their calcium matrix. Synthetic grafts are artificial bone grafts that can be made of biologically active materials such as ceramics, bioglasses, or even calcium phosphate [7].

### 2.2.2 Biomaterials and alternative solutions

In cases where surgery is required, regenerative tissue engineering may offer alternatives solutions, reducing healing time and increasing bone strength. The use of bone substitutes such as bio-materials is one of the most explored strategy. The objective is to create a biocompatible scaffold, combined with living cells able to generate biologic substitutes capable of sustaining themselves and mimicking functional native bone, in order to restore functions of bone tissues. The bio-material used for the scaffold has to exhibit some properties to fulfill all the conditions necessary to be implanted in the human body. First scaffolds should be biocompatible and should have adequate mechanical properties. Further requirements include controllable biodegradability, as the degradation and resorption rates should match cell/tissue growth, and also a pore size >100 μm and good pore interconnectivity [12, 27].

***Hybrid materials***

A wide range of materials, mainly ceramics and polymers, have been developed for bone tissue engineering applications. In order to be used in the body, bone bio-materials have to possess some physical, chemical, and biological properties [28]. Although great strides have been made, it is difficult for any biomaterial to satisfy all of the listed requirements. Recent efforts have been aimed, in the direction of developing hybrid biomaterials. It now possible to combine two or more material types, to take advantages of all components and better mimic the bone structure. For instance, ceramics have low mechanical properties what can lead to fracture under load. Polymers are biodegradable. The most common composites are made of hydroxyapatite HA and a polymer that can be poly(lactic acid) PLA, poly(glycolic acid) PGA, gelatin, chitosan, or collagen [28]. These hybrid materials have demonstrated better results compared to the pure materials used separately [28].

***Hydrogels***

Hydrogels are hydrated polymers. When the polymer is in contact with water it swells and forms a three-dimensional network. The hyaluronic acid and vinyl phosphonic acid based hydrogels, gelatin, collagen and poly(ethylene glycol) are some examples [29-32].Their liquid forms make them injectable. Moreover hydrogels display many properties that make them useful for bone tissue engineering. Indeed, they are biocompatible, biodegradable and are able to mimic extracellular matrix surface and deliver required biomolecules in order to promote tissue regeneration [28]. By functionalizing their surface it is possible to allow the attachment of cells on it. In addition drugs can be incorporated in the polymer network for a controlled delivery. Until recently, hydrogels have been mainly considered for soft tissue regeneration. For hard tissue engineering applications, hydrogels are not yet well adapted. Indeed they exhibit a poor mineralization. A new trend in tissue engineering involves the development of hydrogels that possess the capacity to mineralize [32]. This is done by incorporating inorganic phases such as calcium phosphate into the hydrogel matrix. These inorganic particles act as nucleation sites that enable further mineralization, thus improving the mechanical properties of the composite material [32].

***Osteoinductive materials***

Osteoinductivity is the ability of inducing the differentiation of cells in order to synthesize the mineral bone matrix. Such materials present the advantage to promote new bone formation. Although the biological mechanisms are not fully understood, it has been observed that they provide a better integration on the host tissues and remodeling compared to other materials. Indeed they enhance the cellular response of the tissues what make them having a great potential for bone tissue regeneration. A wide range of biomaterials have demonstrated having osteoinductive properties such as natural and synthetic ceramics [28]. For example hydroxyapatite (HAp) and calcium phosphate CaP, two compounds naturally present in the bone are osteoinductive. Moreover, polymer/ceramic composites, such as PLGA/HAp, have been shown to be osteoinductive and to induce bone formation [28].

To summarize, the goal of bone tissue engineering is to assist the bone is the process of regeneration by using suitable bone substitutes in order to create new bone tissues. The strategy is to initiate the reconstruction of the bone and then gradually degrade the bio-material in order to allow the new bone to remodel and assume its mechanical function. They offer the advantages of limiting the secondary effects present in graft. However bone is a complex material that is very difficult to mimic. The substitutes have closed mechanical properties, but even small shifts in the chemical composition are of great importance. Moreover they do not have the proteinic and cellular compounds useful for the formation of new functional tissues. All these features make the fabrication of ideal bone substitute difficult and really challenging.

# Chapter 2

Piezoelectric PLLA for bone regeneration

This current chapter describes the main discoveries related to electrical phenomena in bone tissues, which inspire this study. Research about bioelectricity on bone led to several discoveries, in particular it has been noticed that both mechanical and electrical stresses are related through piezoelectricity of bone tissues. In addition one has shown that electrical potentials generated by mechanical stress alter cell proliferation and extracellular matrix secretion, in other words, electrical stimulus facilitate osteoinduction. These results have then led to the development of modified and smart materials, which are able to induce and accelerate bone regeneration in order to fix bone defects.

# 1 Bioelectricity

In 1792 Luigi Galvini discovered that the human body generates an endogenous electrical signal when he noticed that an accidental spark discharge caused frog muscle fibers to contract [16]. This has been the beginning of big discoveries in the field of bioelectricity. Since that it has been shown that all organisms, from bacteria to mammals are sensitive to electromagnetic fields and that this phenomenon affects cell division, tissue growth and wound repair [16]. In addition one has demonstrated that tissues, which generate electrical signals, have higher capacity to regenerate. Indeed when a tissue has been damaged, injury potentials create steady electric fields, which exist locally for days after the insult. Research has indicated that electrical gradients generated by injured tissue may be an integral part of the regeneration process [16]. It was only postulated much later, in 1980's that mechanical deformations of bone alter endogenous electrical signaling, and subsequent control bone cell activity. It is the beginning of the appearance of bone piezoelectricity.

Since the discovery of bone bioelectricity, electrical stimulations have shown great interest for accelerating bone repair. For example, in orthopaedics, the use of electric and electromagnetic fields has focused primarily on promoting healing of bony nonunions. Indeed during the consolidation of a fracture callus, there is a beneficial effect exerted by the redistribution of electric charges in the patient’s body [16]. However the electric properties of bone are not new, they have been utilized for centuries by dowsers to detect water sources. Sources in the ground emit strong magnetic fields. These are the magnetic

fields that water diviners detect. Indeed the piezoelectric properties of bone in the forearm could be the reason for involuntary muscle movements which cause the dowsing reaction. This could be explained both mechanically and electrically. In a relaxed arm an electromagnetic field change causes nothing except a small imperceptible volume change of the bone. Whereas in a strongly loaded arm of a dowser the piezoelectric effect causes both mechanical stress and electric voltage [33]. By holding the divining rod, the mussels of the arms are contracted what results in mechanical stress in the bone. In the presence of a magnetic field the volume of the bone changes what leads to a change of the mechanical stress and finally to the rotation of the arm (figure 4). To be effective the water diviner has to hold the rod with a constant force. One can note that they use of divining rods which have most of the time Y or L shapes, to magnify the electromagnetic signal.

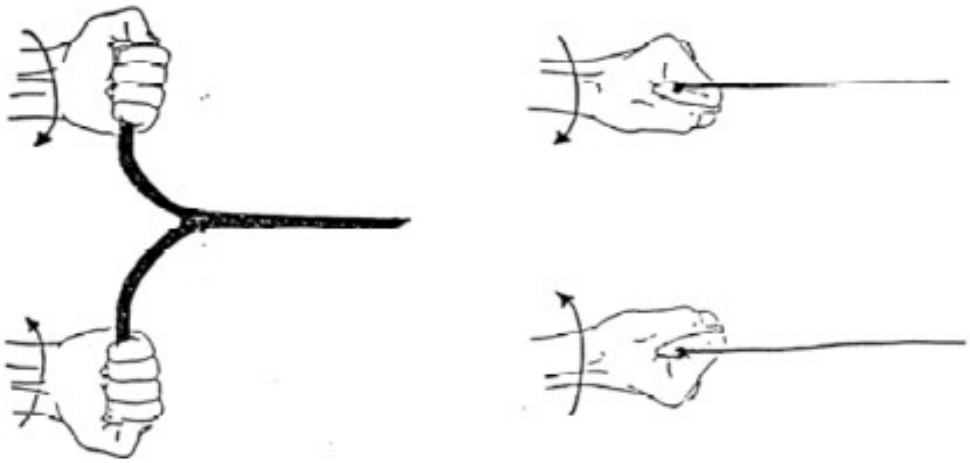

***Figure 4****: The dowsing reaction - wrist movements make Y-shaped rod bend vertically and L-shaped rod to move horizontally [33].*

# 2 Piezoelectricity

## 2.1 Definition

Piezoelectricity is the ability exhibited by some materials, to get polarized under a mechanical stress: there is then an accumulation of charges when materials are submitted to compression or tension. Reciprocally they deform under electrical field: one observes a change of the volume when the material is submitted to an electromagnetic field or current. The both effects are linked and inseparable. There is a considerable number of materials

that exhibit piezoelectricity, being one of the most known quartz. Due to their piezoelectric activity crystals of quartz are wide spread in the watch industry. Indeed, when electrically stimulated, quartz oscillates with a specific frequency what allows to measure time. The piezoelectric effect can also be noted in other groups of materials as ceramics or polymers - Polyvinylidene Fluoride (PVDF), Poly(L-Lactic acid) (PLLA) and Collagen. Bone shows piezoelectric properties as well [34].

## 2.2 Piezoelectricity in bone

In the 1950s, Eiichi Fukada and Iwao Yasuda, working on piezoelectricity, discovered that bone tissues have the ability to generate electrical signal under mechanical stress [16]. Yasuda inserted two electrodes inside the femur of a rabbit. When applying external electrical stimulations, he observed the formation of a callus after 3 weeks. These electrical stimulations were direct currents between 5 and 20 μA. He suggested then the hypothesis that an exogenous electrical stimulation could improve bone formation [35, 39]. He discovered as well the effect that he called “bone piezoelectricity”: bone generates electrical current under mechanical stress. Especially regions under compression generate a negative charge and the regions under traction generate positive charges [36].

The study of Yasuda was then completed by Fukuda, a japanese orthopedist. He confirmed the piezoelectric property of bone by applying a force along the axis of a long bone. He recorded an electrical signal at the surface of the bone. Other studies demonstrated the double effect of piezoelectricity in bones: the direct piezoelectric effect, which describes the generation of electrical signal in response to a mechanical stress, and the opposite piezoelectric effect, which relates a mechanical deformation with an applied electrical potential. In addition they shown that the polarization at the surface of bone depends on many factors such as the load, the frequency of the applied load, the water content, among others. Finally they observed that piezoelectricity is a collagen dominated phenomenon [16, 37].

## 2.3 Piezoelectric materials for the regeneration of bone

As stated before, it has been shown that piezoelectricity is present in some living tissues such as bone with piezoelectric collagen, dentin, tendon, nerves, cartilage and skin among others. From the recognition of the piezoelectric character of the bone, the idea emerged in the 1970s of using piezoelectric materials to correct bone defects. These materials present the advantage of accelerating bone regeneration compared to non-piezoelectric materials. These materials have undergone in vivo tests, and they have been shown to accelerate bone regeneration. Here is a non-exhaustive list of piezoelectric materials investigated for the regeneration of bone. These materials are classified in three families: ceramics, polymers an ceramic/polymer composites.

***Piezoelectric ceramics***

Barium titanate ($BaTiO_3$) is a ferroelectric ceramic, known historically as the first piezoelectric ceramic material. It was first used for bone repair in 1978. Sometimes combined with hydroxyapatite HAp or other polymers such as PVDF, $BaTiO_3$ thin films have shown interesting results on mouse and human cells. The cells were found to attach and proliferate on poled surface, showing a preference for negatively charged areas [38].

***Piezoelectric polymers***

This family is divided into two sub-categories: natural polymers such as collagen and synthetic polymers including polyvinylidene fluoride (PVDF), and poly(L-lactic) acid (PLLA).

*Natural piezoelectric polymer: collagen*

Collagen is the most abundant protein in the human body, but also in animals. Most of the time it has the form of elongated fibrils, which is present in the extracellular matrix of various connective tissues such as tendons, ligaments, skin, corneas, cartilage, bone, dentin and blood vessels. The type of collagen differs according to the organs. Indeed, 28 types of collagen have been identified, I, II, III and V being the most present types in bone, cartilage, tendon, skin and mussel [39]. For example in bone, collagen type I associated with hydroxyapatite, provides rigidity and resistance to shocks. In cornea it shows optical

properties such as transparency. Thus collagen plays an important role to maintain biological and structural integrity of the extracellular matrix in order to ensure proper physiological functions and is involved in a wide range of tissues [39]. It is therefore used as a biomaterial for many applications including tissue regeneration; research focusing on the development of biomaterials that mimic its natural form in order to replace native collagen. From an electrical point of view, its piezoelectric properties have been investigated for bone and tendon healing. However collagen is hard to synthesize because of its particular structure. Indeed the different collagen types are characterized by considerable complexity and diversity in their structure, their splice variants, the presence of additional, non-helical domains, their assembly and their function [40]

*Synthetic piezoelectric polymers: PVDF and PLLA*

Polyvinylidene fluoride (PVDF) belongs to the fluoropolymer family. It is a semi-crystalline thermoplastic polymer very hard. It is light weight, has a good flexibility, a good resistance against fire, corrosive chemical agents and has been first used for electrical isolation. In 1969, Kawaï and co-workers discovered the piezoelectric property of PVDF opening the door to new applications [41]. PVDF is being investigated as a potential scaffold for bone tissue engineering because of its proven biocompatibility and piezoelectricity.

Poly(L-lactic) acid (PLLA) is a biodegradable, biocompatible, and piezoelectric semi-crystalline synthetic polymer approved by the US Food and Drug Administration for clinical use (e.g. biodegradable sutures) and well known for its biocompatibility and adjustable physical and mechanical properties. It has been actively studied as a scaffold for tissue development and also as a vehicle for drug and gene delivery in the field of bone tissue engineering [42].

# 3 Poly (L-lactic) acid

## 3.1 The molecules of PLA and PLLA

Polylactic acid (PLA) is a rigid thermoplastic polymer that belongs to the family of polyesters. PLA is derived from the fermentation of renewable and degradable resources such as corn and rice [43]. PLA is produced through ring-opening polymerization of lactic acid [44]. Since lactic acid is a chiral molecule, it exists in two forms, D-PLA and L-PLA. PLLA is the result of L-PLA polymerization. L-lactic acid and D-lactic acid are isomers, i.e. that they have the same chemical formula but different chemical structure. In that case, as seen in figure 5, one notices that the stereo-representation around the first atom of carbon is slightly changed [43].

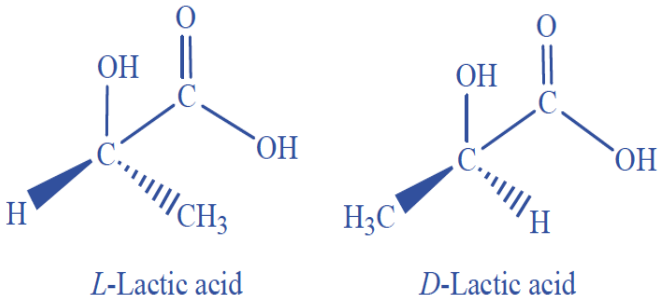


***Figure 5**: The stereo-isomers of lactic acid*

Due to its great thermal properties, PLA can be processed by film casting, extrusion, injection, blow molding and fiber spinning; contributing to the applications of PLA in industry in fields such as textiles, food packaging or floral wrap [45].

PLLA is a biodegradable and biocompatible polymer what means that it can be broken by certain enzymes once placed inside the body. PLLA and its degradation products, namely $H_2O$ and $CO_2$, are neither toxic nor carcinogenic to the human body [43, 46]. No significant accumulation amounts of PLLA degradation have been reported in any of the vital organs [45]. These properties make them excellent materials for biomedical applications including sutures, clips, and drug delivery systems (DDS) [43]. In the 1970's, PLA products have been approved by the US Food and Drug Administration (FDA) for direct contact with biological fluids [43, 44]. Table 2 gives some examples of drug delivery products using PLA polymer.

**Table 2**: List of FDA approved drug delivery products using PLA polymer [47]

| Product | Polymer | Active Ingredient | Indication |
|---|---|---|---|
| Atridox | PLA | Doxycycline hyclate | Periodontal disease |
| Lupron Depot | PLA | Leuprolide acetate | Prostate cancer, Endometreosis |
| Zoladex | PLA | Goserelin acetate | Prostate cancer, Endometreosis |

## 3.2 PLLA as a piezoelectric material

PLLA does not exhibit an intrinsic polarization. However, when a shear strain is applied to a PLLA molecule, the permanent dipole of C=O bond rotates slightly, and a change in the polarization appears in the direction perpendicular to the plane of the shear strain [48]. This is the piezoelectric effect of PLLA.

Piezoelectric properties of PLLA have been highly studied. Some of the most recent studies on PLLA as a piezoelectric material in TE have been conducted by Barroca et al. [34, 49]. First of all, in 2011, Barroca and co-workers demonstrated that a preferential adsorption of proteins, namely fibronectin, occurs at the surface of a polarized piezoelectric PLLA film [49]. A higher concentration of proteins on poled areas compared to non-poled ones was observed. This effect seems to be independent of the polarity of the polarization. Moreover in 2012, Barroca et al. investigated the decay of kinetics of polarization on PLLA for both α and α' crystalline forms, which have different mechanical properties [34]. The relationship between the electrical response and the crystalline form of the polymer is not studied yet but is suggested that different crystalline forms may have different polarization behaviors, mainly, regarding the polarization stability. Thus it was shown that at room temperature, both PLLA crystalline structures presented a rapid loss of the polarization but α -PLLA exhibited better results in terms of polarization stability along the time. The second interesting fact is that when poled at high temperature, i.e. above the glass transition temperature, dipoles are "frozen" resulting in a much more stable polarization; whereas when poled at room temperature the polarization is less durable [34]. All these results are of great importance for PLLA piezoelectric tissue engineering platforms

# 4 Objectives

The application of electrical stimuli has long been known to influence the way in which nerves, cartilage, skin and bone heal. Indeed electrical stimulation of cells via the attachment to a substrate might lead to improved cellular interaction and tissue growth compared with non-piezoelectric scaffolds by influencing cell behavior in some desired manner. However the mechanism underlying the facilitated bone growth by piezoelectric implants is far from being understood; and the direct relationship between the electrical response, the crystalline form of the polymer and the cell behavior is not studied yet. However it is assumed that different crystalline forms may have different polarization behaviors, and therefore different cellular response. Based on the knowledge already acquire and on the promising importance of PLLA as a biofunctional platform, PLLA, a synthetic semicrystalline polyester, combining adjustable biodegradability and physical properties, has been chosen for this study and to further explore its function as a platform supporting bone grow. Thus the main idea is to develop films as physical and osteoinductive support, where bone cells could be able to adhere, proliferate, grow and mineralize, stimulated by electric or mechanical clues. The final stage and ultimate proof of the project will be the use of these films to coat a prosthesis which will be subsequently implanted in the body in order to improve the acceptance by the body and the healing process.

Within this context, the present project is focused on the development and characterization of PLLA platforms with different degrees of crystallinity and poled under different conditions, for bone tissue engineering. It is then intended to use these films in different cellular biological assays in order to explore how the cellular response proceed and therefore gain a better understanding of the cell/material interactions. The relations between the degree of crystallinity and cell interaction will be established.

In the frame of these objectives, the main steps of the work are:

- Fabrication of PLLA films by solvent casting (Standard films);
- Inducing different degrees of crystallinity by thermal treatment of standard films (Amorphous and Crystalline);
- Poling by corona discharge in order to tailor their electrical properties
- Surface and structural characterization of the different films;
- Conduction of the cellular bio assays (viability and proliferation, morphology and mineralization) using human osteoblasts.
- Establishment of the correlations between the properties measured on the PLLA films and the cell performances in order to discriminate the treatments (crystallization and poling) which improve osteoinductivity.

# Chapter 3

Materials and methods

# 1 Materials

Poly(l-lactic acid) (PLLA) films were obtained by solvent cast of PLLA solution. The material used for the preparation of the solution are (Purasorb PL 38 – Purac): poly[(3S-cis)-3,6-dimethyl-1,4-dioxane-2,5-dione] with chemical formula $(C_6H_8O_4)_n$ and 1,4 dioxane (Scharlau). The weight average molecular weight $M_w$ of PLLA, calculated using the inherent viscosity of the polymer in the Mark Houwink equation, is superior or equal to 184 041g;mol$^{-1}$.

The solution was prepared by dissolving PLLA pellets in 1,4 dioxane at 80°C, which was then stabilized at 37°C. Prior the bio assays, some films were submitted to a thermal treatment in order to modify the degree of crystallinity and electrically poled via corona discharge. The cellular assays were then conducted by using two different osteoblast cell lines grown directly onto the PLLA films: Human osteoblast Hob, a primary cell culture and Human osteosarcoma MG-63 cell line.

# 2 Preparation of the films of PLLA

## 2.1 Film assembly

Films were prepared by solvent cast technique [50]. It consists of mixing the specie which one wants to dissolve: PLLA, with a solvent, here dioxane, and to heat the solution until the polymeric powder is dissolved inside the solvent. This is done by mixing both constituents in a flask with a magnetic agitator and placing it in a oil bath at 80°C (see figure 6). The oil is silicon oil, chosen for its good heat transfer capacity. The bath is warmed up with a hot plate controlled in temperature thanks to a thermocouple that measures the temperature of the oil. It is important to not go above 80°C in order to not evaporate the solvent. When preparing the solution and during heating up, it is important to pay attention about the top of the flask that has to remain fixed in order to keep the same amount of water inside. Indeed PLLA is very sensitive to water and a big change in the content of water can dramatically change the result. Finally after 2 h and 30 min, when the PLLA is dissolved in the solvent, the solution is poured in a petri dish in glass of 5cm in diameter and placed in the oven to dry at 37°C for at least 3 h. The experimental protocol is detailed in annex A.

Once completely dried, films are stored in a desiccator in order to avoid humidity to be absorbed at film's surface. Figure 7 provides an example of film obtained after drying.

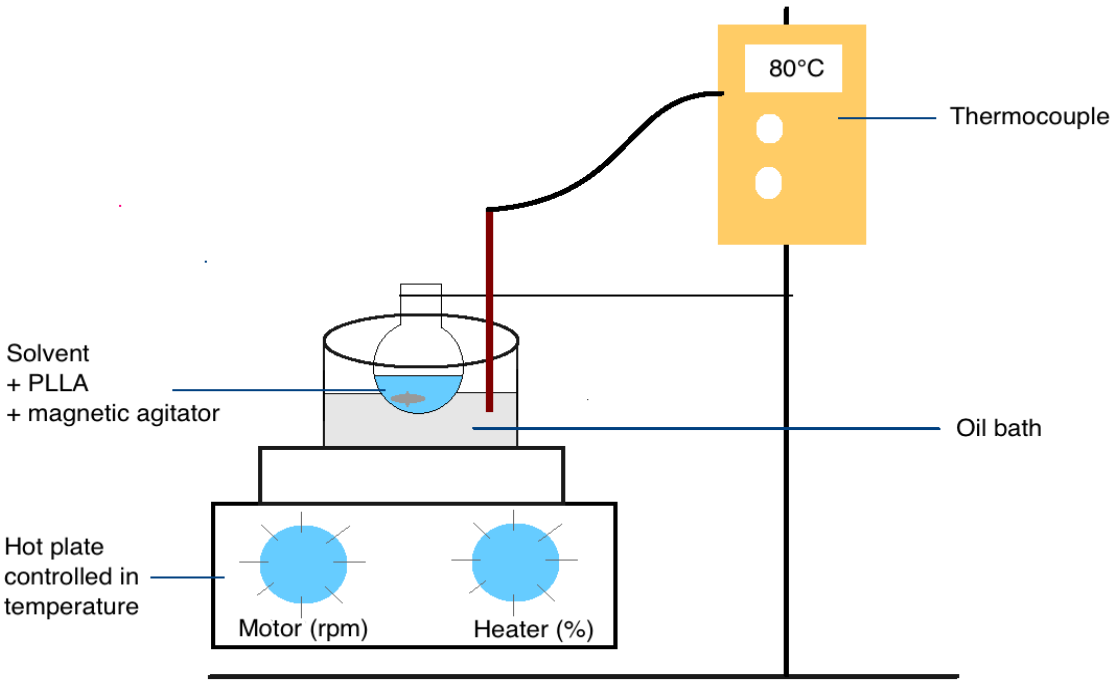


***Figure 6**: Schematic representation of the film preparation setup – the preparation is heated by a hot plate controlled by a thermocouple; and mixed for 2h30 at 80 °C*

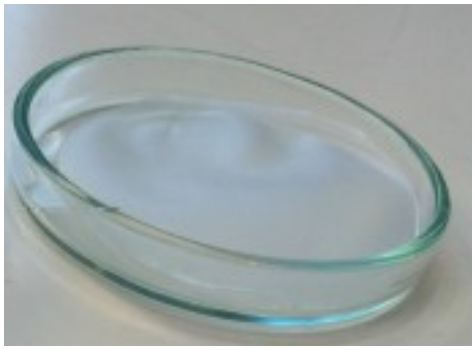

***Figure 7**: Example of PLLA film obtained after drying - The films were prepared by solvent cast technique*

## 2.2 Crystallization

Films with different degrees of crystallinity are needed in order to investigate the influence of the degree of crystallinity on the cell behavior. The goal of this step is therefore to prepare films with different degrees of crystallinity. However it is not really what one calls a crystallization process. The appropriated term is recrystallization. Indeed, at the end of the film assembly process the films are already crystallized (pellets of PLLA were dissolved in the solvent, dropped in a petri dish, and then allowed to slowly crystallize out as the solution cools). At the end of this cooling step, the degree of crystallinity is about 7 - 8%. Thus this "crystallization" step consists of modifying the films in order to change their degree of crystallinity. In this work, three degrees of crystallinity were tested, and the films were modified undergoing different thermal treatments.

The simplest crystallization method of a film is to heat it and then either to cool down slowly at a particular temperature, or to quench it in order to obtain amorphous samples. In this technique, one uses a hot plate on which the samples are placed to perform the recrystallization. The schematic representation of the setup is given in figure 8.

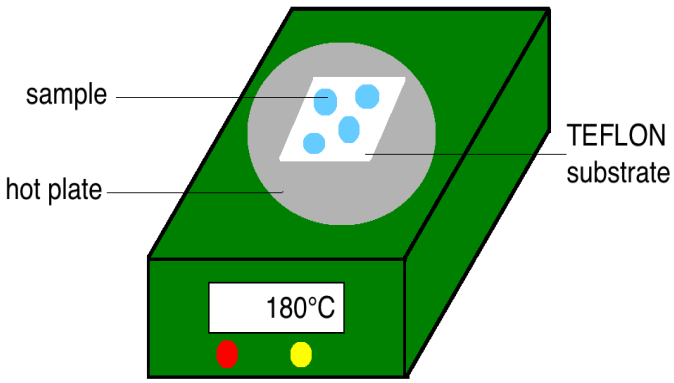


***Figure 8**: Schematic representation of the experimental setup used for the crystallization step*

The three different degrees of crystallinity will be called amorphous, semi-crystalline and crystalline. The synthesis process allows obtaining samples with a degree of crystallinity of about 8%, that will be called semi-crystalline. Thus semi-crystalline samples are "as-prepared films", what means that they do not undergo any thermal treatment, whereas amorphous and crystalline samples are made by modifying semi-crystalline films. The protocol is given in annex B.

The recrystallization is done at 180°C, which corresponds to a temperature slightly higher than the melting temperature of PLLA (170 °C) [51]. Working above this temperature would degrade the polymer change its structure and thus one would deal with a new phase [51].

## 2.3 Time-temperature schedules

The next figure illustrates the processing cycle for the three types of samples, from the film assembly to the crystallization step. The first 2h30, from t1 to t2, correspond to the dissolution of PLLA in the solvent. Then the film dried from 80 °C to 37 °C and the oven, and the to room temperature (from t2 to t3). Finally, according to the degree of crystallinity needed for the experiments the fills undergone an extra thermal treatment: the recrystallization step. Amorphous were heated at 180°C for three minutes (from t3 to t4); and quenched on water at room temperature (figure 9a). Semi-crystalline samples were kept as prepared (figure 9b). Crystalline samples were heated at 180°C for three minutes (from t3 to t4) and then crystallized slowly at 120°C for 45 minutes (from t5 to t6) before cooling down to room temperature (figure 9c).

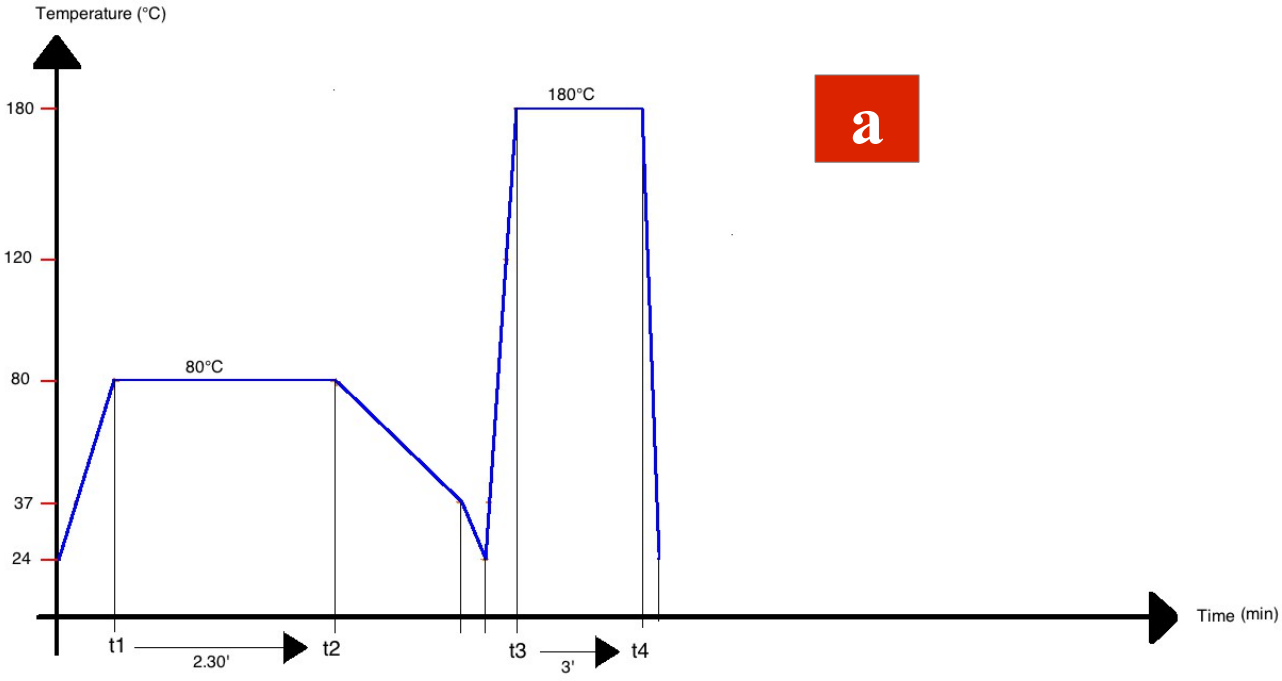

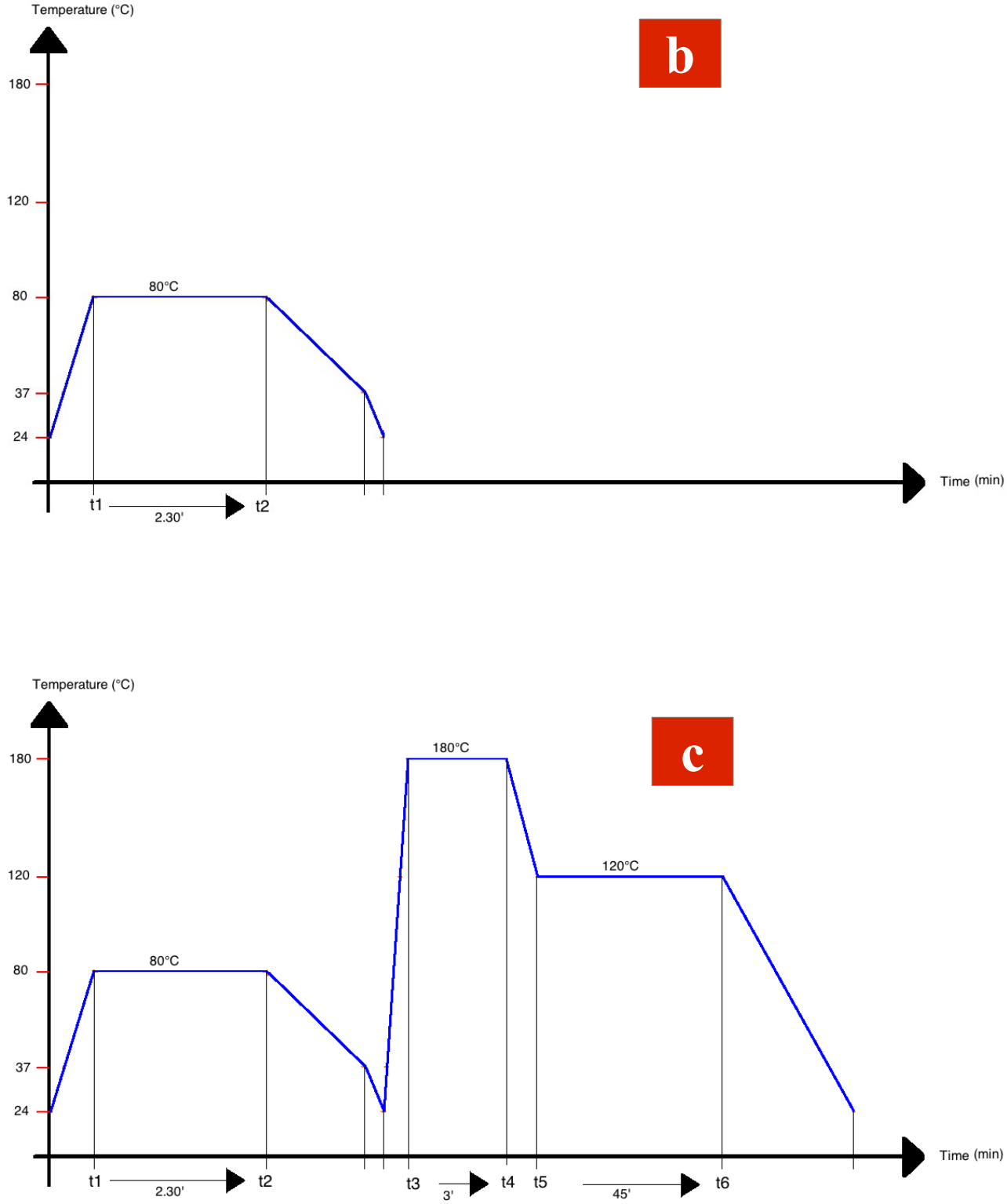


***Figure 9:*** *Processing cycle of* ***a)*** *amorphous;* ***b)*** *semi-crystalline and* ***c)*** *crystalline PLLA films*

# 3 Polarization

In order to investigate the influence of the polarization of PLLA substrate on the cells behavior, PLLA films were submitted to a poling step by CORONA method, by placing the films under an external electric field. Due to its crystalline structure PLLA is a non-polar molecule. And although it does not have any intrinsic polarization, when submitted to an electric field, the electronic cloud of each atom is slightly shifted leading to the formation of an induced dipole.

The polarization density or electrical polarization represents the density of permanent or induced electric dipole moments in the material. When placed in an electric field, the molecules of the material under the electric field, gain a non-zero total electric dipole moment and the material is said to be polarized. The electric dipole moment induced per unit volume of the dielectric material is called the electric polarization of the dielectric [52, 53]. The polarization density also describes how a material responds to an applied electric field as well as the way the material changes the electric field. It is the equivalent of magnetization, which is the measure of the corresponding response of a material to a magnetic field in magnetism.

There are several methods available nowadays to pole a material, such as the application of an alternating current between two electrodes [54, 55], and the corona discharge. The last one, used in this study, is one of the most popular methods for electrical polarization of thin films and ionizer in research and industry [56]. The other reasons of using corona in this study is also because poling can be performed without deposited electrodes, higher fields can be achieved than in the case of sandwich poling and it does require any immersion step in a bath oil; required in other methods [57], what is not compatible with bio-polymers.

*Corona discharge*

In electricity, the corona effect, is an electrical discharge phenomenon appearing when the intensity of the electric field at the surface of the conductor exceeds a certain critical value, leading to the formation of electron avalanches. These electron avalanches result in a partial discharge of electrical energy called corona discharge and in the ionization of the surrounding medium [56].

**Applications**

The corona process is used for years in order to pole and perform surface treatment of materials such as polymers and metals. For example coronas are widely used as chemical reactors for surface treatment. An industrial very important application is the surface treatment of polymers, in particular to increase their wettability and their adhesively to ease printing, painting, sealing, coating, etc [58]. The principle consists of placing one side of the sample on a plate related to the ground potential and the other side left free below the electrode. The setup called point-to-plate corona, is made of a needle (the point electrode) brought to a high potential (~10 KV) versus the ground potential, ionizing the surrounding media. Charges accumulate on the surface of the sample, thus creating a potential difference between the free surface and the surface connected to the ground. In some cases it is common using a hot plate in order to control the temperature and then control better the polarization [58]. Such a setup is represented in figure 10.

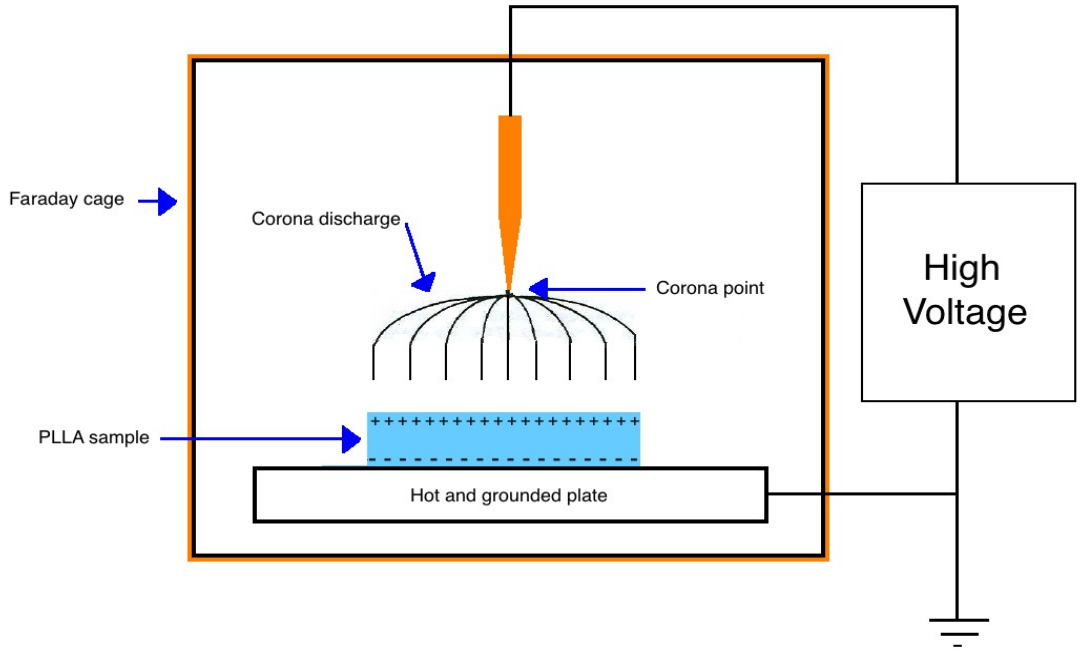


***Figure 10**: Corona setup – The device works as a shower of charges forcing the dipoles to orientate in the direction of the field. According to the polarity of the supply voltage the sample acquires a positive or negative polarization*

**Detection**

The corona discharge can be detected in several ways: visually, audibly, by radio influence and by gaseous effluent. Visually a purple glow appears, which comes principally from the recombination of nitrogen ions with free electrons [59, 60]. Audibly the sound is produced by the air disturbances around the discharge, caused by the movement of the positive ions [59]. Olfactively, corona activity in the air can produce very tiny amounts of gaseous effluents: ozone and nitrogen oxide [60].

The films were polarized via Corona discharge using a device made especially for the investigation group that can be seen in Figure 36, annex C. The films preparation consists on the attachment of PLLA samples into silver paper with carbon tape, as described in figure 35.

The polarization process is divided in three steps and is described in figure 11:

· Heating up until 80 ºC;

· Polarization at 80 ºC for 30 min ;

· Polarization upon cooling down until room temperature (24°C).

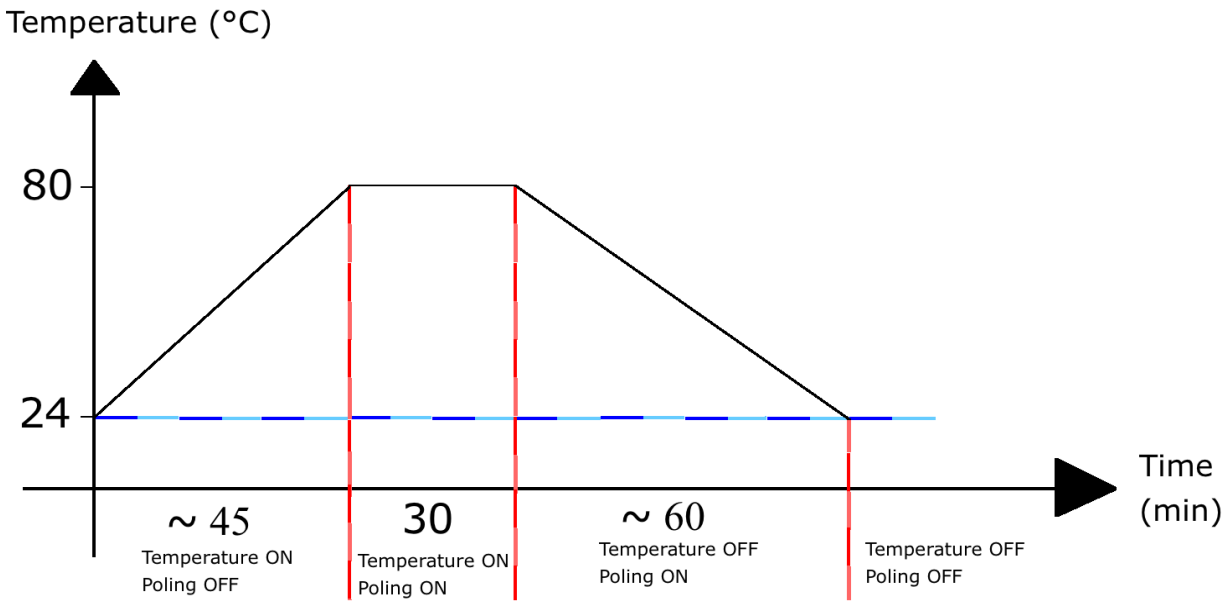


***Figure 11**: Polarization cycle*

The maximum temperature (80°C) was chosen based on the glass transition temperature Tg of the material. When the temperature approaches Tg, the dipoles gain sufficient mobility to contribute to the permittivity. Thus by working a little bit above the glass transition temperature of the polymer which is about 70°C, one enables the movement of the molecule and then dipoles rotation along the direction of the electric field [61, 62]. The current is maintained during cooling in order to freeze the dipoles. When room temperature is reached the voltage is switch off and the sample is then stored in a desiccator.

For the need of the study, both positive and negative corona are used. Moreover neutral samples are tested. In order to have all samples in exactly the same conditions, neutral samples, i.e. no poling step in the process, also undergo the thermal treatment (heating up to 80 °C and then 30 min at 80 °C without field); thus the cycle in figure 11 is the same, but “poling” is always OFF. One suspects that the thermal treatment changes slightly the degree of crystallinity of the films.

# 4 Characterization of the films of PLLA

Various types of artificial materials are being utilized as implants in all fields of medicine. The surface and structural properties of the implant determine its interactions with the surrounding host tissue. Physochemical properties of the surface, like wettability and surface topography, are of prime importance for the optimization of adhesion, spreading and proliferation of cells. This part describes quickly the techniques used to measured the physical properties of the films of PLLA

## 4.1 Micro-structural characterization

### 4.1.1 Optical microscopy

Optical microscopy allows observing microstructure with a resolution up to the micrometer. Thus the morphology can be observed, and the size of crystallite assessed.

### 4.1.2 Scanning Electron Microscopy

This technique is based on the different radiation effects on matter between a beam of electrons and the material. A beam of electrons scans the surface of the sample and the different kinds of emitted radiation are analyzed. The size of the probe allows going below the limit of the optical microscope (400nm) and thus strongly increases the magnification (up to 300 000 times) with a resolution in the nanometer scale. The depth of field is also better than the one of the classical microscope, what also allows observing porous and rough materials.

The SEM is a very versatile tool thanks to the wide range of available radiations allowing deep investigations. One of the biggest applications is the micro-structural analysis including the detection of grains, the determination of their size and shape.

Several modes that correspond to the different analyzed radiations are available on the SEM, as shown on figure 12:

- Secondary Electrons (SE): topographical contrast imaging
- Backscattered Electrons (BSE): chemical contrast imaging
- X rays (EDX): elements and impurities identification
- Electron Backscattered Diffraction (EBSD): crystallographic orientation imaging

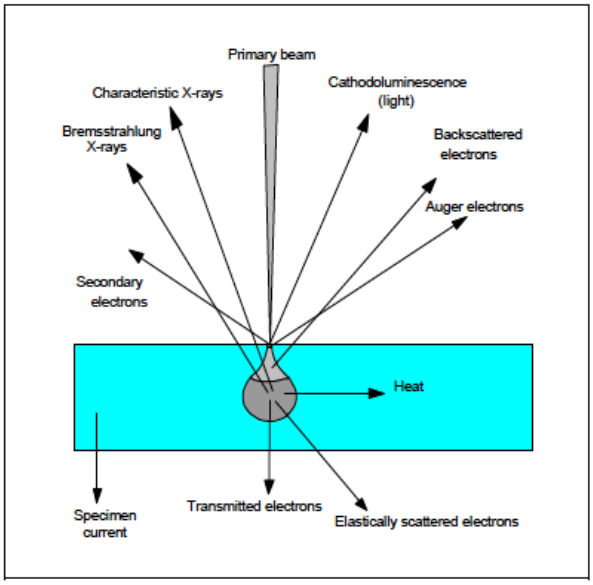


***Figure 12**: Different electronic signals emitted after the interaction of the electron beam with the sample surface [63]*

**Experimental setup**

The SEM consists of an electron gun that emits a beam of electrons which irradiates the sample. When the beam of electrons reaches the sample, it scans the surface and interacts with the sample by emitting different signals. Then the detectors collect the particles and provide images of the surface of the sample.

## 4.2 Surface roughness measurement

One calls surface roughness the curves and valleys of a surface measured versus the average surface locally associated to a plan [64]. Often gathered under the terms topography or rugosity, surface roughness is a component of surface texture. It is quantified by the variations of the normal vector along that plan. If the altitude variations are important, the surface is rough; whereas if the variations are small, the surface is smooth.

Surface roughness plays an important role in the determination of how a real object will interact with its environment. For instance, rough surfaces usually wear more easily and more quickly than smooth surface because of their higher friction coefficient. Moreover roughness is a good indicator of the mechanical performances of a material; irregularities may form nucleation sites for cracks or corrosion. However roughness can also be a good advantage by promoting the adhesion, like in the case of cells on a substrate.

Roughness can be measured in several ways including mechanical methods [65], and optical techniques based on light properties such as reflection and interference methods [65]. Other techniques more accurate, such as scanning probe microscopy and electron microscopy methods [65] can be used. The mechanical method is accurate enough for the need of the study. It is based on the utilization of an apparatus and performs mechanical profile measurement.

In the study, the roughness is assessed by the mechanical stylus method using a surface profilometer. The device, shown in figure 13, is working by physical contact of a stylus on the material. The stylus is a tip that probes the surface. The profilometer amplifies and records the vertical motions of the stylus displacing at a constant speed on the surface of

the material [65]. Then it computes the average height deviation in µm. The measurement protocol is given in annex D. The device used is a Hommel tester T1000.

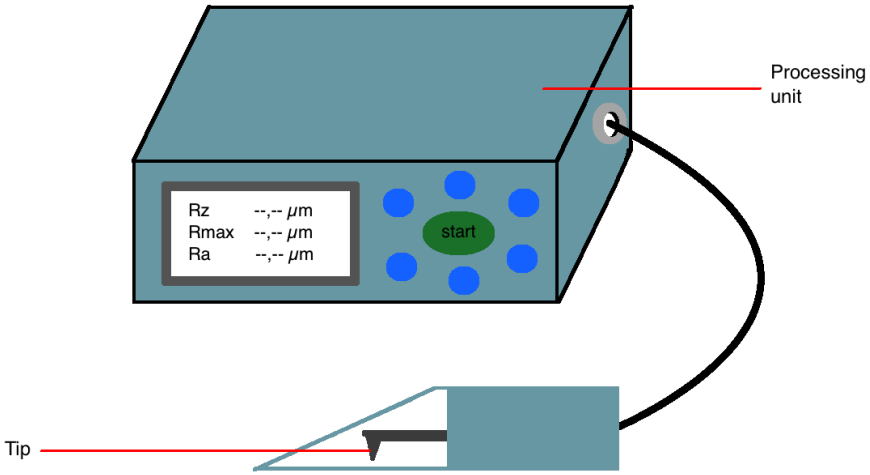


***Figure 13**: Schematic representation of the surface roughness experimental setup – a tip placed at the end of the device runs along the material surface and detects the ups and downs; and then computes the average roughness at the surface of the sample. In the end the measurement is presented in the monitor*

## 4.3 Thickness measurement

The cross section of the samples, before and after thermal treatment have been assess using a microscope (Leica EZ4 HD).

## 4.4 Wettability – contact angle measurement

When a drop of liquid, water for example, is placed on a solid surface, the liquid will either spread across the surface to form a thin, approximately uniform film or spread to a limited extent but remain as a discrete drop on the surface. The final condition of the applied liquid to the surface is taken as an indication of the wettability of the surface by the liquid [66]. Thus wettability measurements enable to characterize the affinity of a surface towards a liquid; and is performed by measuring the equilibrium contact angle θ between the drop of

liquid and the solid surface. Low values of θ indicate a strong liquid–solid interaction such that the liquid tends to spread on the solid, or wets well, while high θ values indicate weak interaction and poor wetting. If θ is less than 90°, then the liquid is said to wet (or sometimes partially wet) the solid. A zero contact angle (θ = 0) represents complete wetting. If θ is greater than 90°, then it is said to be non-wetting.

There are a variety of simple and inexpensive techniques for measuring contact angles. The most common direct methods (Figure 14) include the sessile drop (a), the captive bubble (b) and the tilting plate (c). Indirect methods include tensiometry and geometric analysis of the shape of a meniscus [66]. For solids for which the present methods do not work, such as powders and porous materials, methods based on capillary pressures, sedimentation rates, wetting times, imbibition rates, and other properties, have been developed [67].

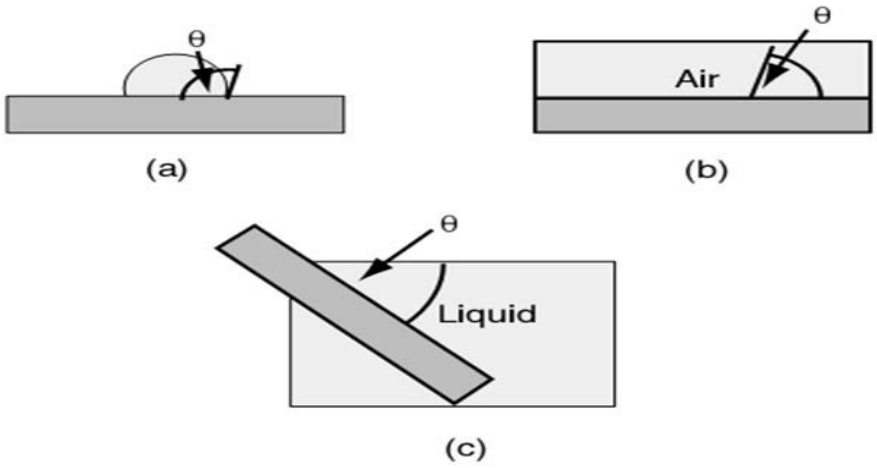


***Figure 14**: Contact angle measurement systems including the sessile drop (a), the captive bubble (b) and the tilting plate (c) - θ is the contact angle to be measured [66]*

The sessile drop method is the easiest contact angle technique. This method is described in details below.

**The sessile drop method**

It's a static contact angle measurement method, which consists in putting down a liquid drop on the solid plate we want to characterize its surface by measuring the contact angle made by the drop on this surface. Indeed, when a drop of a liquid is dropped down on a solid surface; three phases system occurs: solid, liquid and gas (Figure 15).

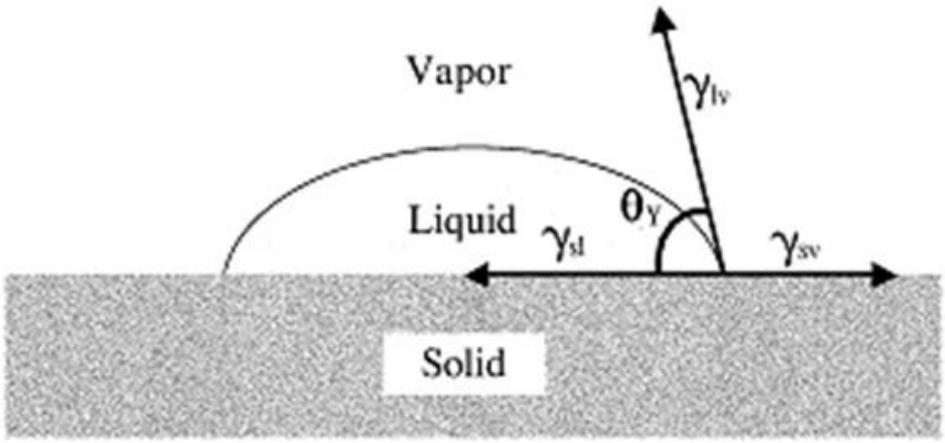


***Figure 15**: Static contact angle measurement with the sessile drop method [53]*

The drop's profile is being changed depending on the physico-chemical characters of the solid surface, on the adhesion forces newly created at the interface solid/liquid and on the cohesion forces of the liquid. This change will affect the contact angle value revealing the surface state (hydrophobic or hydrophilic, rough or smooth, homogeneous or heterogeneous…) and the different forces occurred are linked together according to Young's equation:

$$\gamma_{sv} = \gamma_{sl} + \gamma_{lv}.\cos\theta$$

Where $\gamma_{sv}$, $\gamma_{sl}$ and $\gamma_{lv}$ represent respectively the "surface tensions" of the interface solid/gas, solid/liquid and liquid/gas, respectively, and $\theta$ represents the contact angle.

The sessile drop method was used to examine the PLLA wettability through the different configurations. The contact angle measurements are made by placing a drop of the liquid on a surface and viewing it with magnifying lens, as shown in figure 16. The angle is then optically measured, using a specific software. The static contact angle technique and the Drop Shape Analysis System were applied. The wettability measurement were performed at room temperature. The preparation of the samples and the protocol are described in annex E.

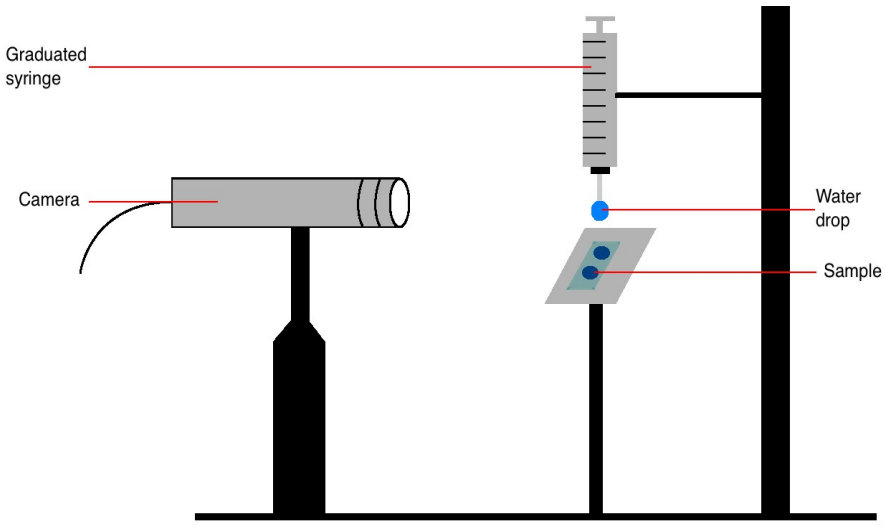


***Figure 16**: Schematic representation of the goniometer used for the contact angle measurement*

## 4.5 X-Ray diffraction – XRD

**Working principle**

X-ray diffraction corresponds to the elastic scattering of a X-ray photons by the periodic structure of a solid material. Practically the photons are diffracted by the electron of the atoms. The electrons are then accelerated in the field of the transversally polarized electromagnetic wave, and the accelerated charges emit electromagnetic waves with the same polarization and wavelength. In other words, there is absorption of a photon by an electron, followed by the emission of a photon in a specific direction with conservation of the energy [68].

The incident X-ray beam, characterized by its wavelength λ, will be diffracted by a family of planes only if the path difference between two scattered waves is an integral multiple of their wavelength, i. e. if the Bragg law is verified:

$$n.\lambda = 2d.\sin(\Theta)$$

with n : order of diffraction

λ : wavelength of the X-ray beam

$d_{hkl}$ : inter planar distance, characteristic of a family of plane (hkl)

Θ : angle between the source and the sample

X-ray diffraction technique is widely used for phase identification, solid solution identification and determination of unit cell parameters of material. The X-Ray Diffraction (XRD) technique had been used successfully from long time for the crystallographic study of polymers. It is used for analyzing crystalline phases in solid materials, determining the extent of crystallinity and identifying crystalline structure. The crystalline parts give sharp narrow diffraction peaks and the amorphous component gives a very broad peak [69].

X-ray diffraction analysis was used to determine the crystalline structures of PLLA samples crystallized with different degrees of crystallinity. A monochromatized CuKa (1,54060Å) X-ray tube, operated at 45 kV and 40 mA was used, over a 2θ range of 8-30° with a step size of 2θ=0,0260°.

## 4.6 Differential Scanning Calorimetry

Differential Scanning Calorimetry (DSC) belongs to thermal analysis techniques. It consists of measuring a difference of heat flux between the sample and a reference. The use of a reference allows to increase the sensitivity of the setup compared to a simple thermal analysis technique. The reference is most of the time an empty crucible, thermally inert. The thermal flux is recorded versus the time whereas the temperature is programmed. The sample and the crucible are submitted to the same temperature program. When the sample undergoes a transition phase, its temperature response varies relative to the reference. During heating or cooling, any transition is accompanied by a heat exchange: heat release (exothermic phenomena) or heat absorption (endothermic phenomena). DSC allows determining the temperature of this transformation and quantifying the heat flux. These measurements provide quantitative and qualitative information about chemical transformations (allotropic transformation) or physical transformations (change of state).

Here is a typical thermogram obtained in DSC.

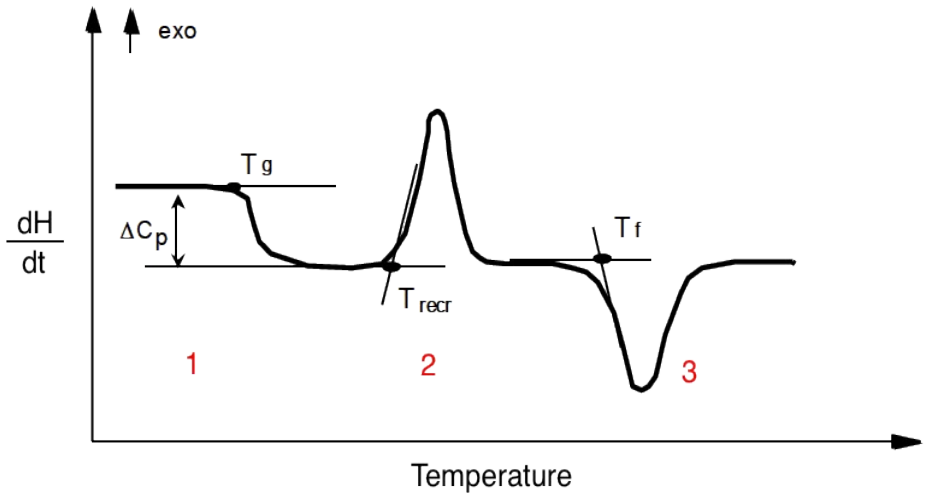


***Figure 17**: Typical DSC thermogram - the variation of enthalpy with time is determined by recording the differential heat flow between the sample and the reference*

A typical recording for a semi-crystalline polymer is shown in the figure 17.
Four phenomena can be observed. At the lowest temperatures a retaining wall (1) indicates the temperature of glass transition. The exothermic peak (2) sometimes observed then results from the crystallization of the material. Crystals formed melt around the temperature Tf (3), what appeared as an endothermic peak on the diagram.

This technique allows the determination of:

- the melting point and the glass transition temperature
- the different enthalpy of fusion and crystallization, and thus the degree of crystallinity
- the thickness of the crystalline lamellas

The enthalpy of fusion is calculated by the software from the area under the peak of fusion. The rate of crystallinity $X_c$ is then determined by the relation:

$$Xc = \frac{Hf - Hc}{H100} \times 100$$

where Hf and Hc are respectively the enthalpy of fusion and crystallization of the sample and H100 the heat of fusion for a sample of 100% crystallinity. In the study, the heating rate is equal to 10 °C/min, and a stainless steel crucible is used as reference.

# 5 Cellular biological assays

All the work described below has been done in collaboration with Ana Roque from IBIMED.

## 5.1 Preliminary steps

Prior any assays, there are some tasks that need to be done including the preparation of the wells, the sterilization of the samples and the wells, and the cell culture.

### 5.1.1 Preparation of the wells and cutout of the samples

First of all, before starting the experiments, the samples are placed in a box containing wells. This is in that box that cells will growth on the samples inside culture medium. Thus the samples were cut into 6mm (or 12mm) in diameter disks, placed in 96-well (or 24-well respectively) polypropylene plates, and fixed to the bottom of the wells using small tubes of rubber (in the case of 96 wells box) or rings (in the case of 24 wells box) as shown in figure 18. The samples need to be fixed in order to avoid them to flip because the side that is in contact with cells must be the one that was poled.

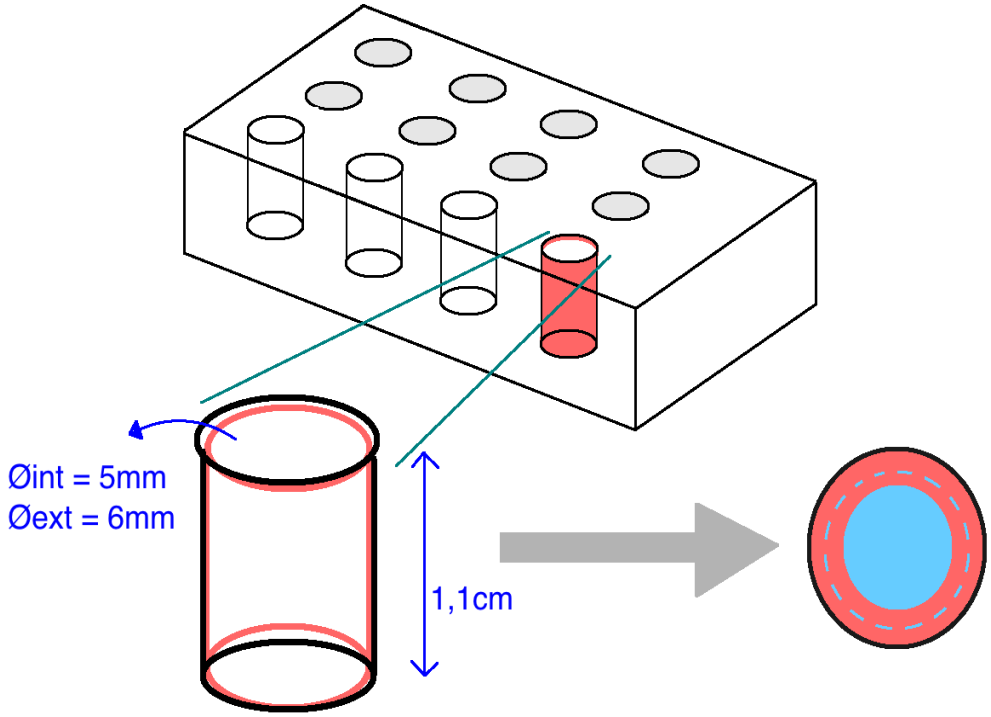


***Figure 18**: Schematic representation of the wells box – in the right corner is a top view of a well with in pink the piece of rubber which maintain the sample in the bottom of the wells*

### 5.1.2 Sterilization

Finally the last step before the bio assays is the "washing". Indeed, organisms such as bacteria, fungi, viruses, and spores are not allowed for bio studies. Moreover, in bioengineering all medical implants must be sterilized in order to ensure no bacterial contamination to the patient. In that context sterilization is defined as the process by which bacterial contamination is removed from a material and sterility is defined as less than one in one million surviving bacterial spores in the medical device prior to implantation.

There are several sterilization processes available, including autoclaving [70, 71], gamma irradiation [70, 71], electron beam method [70], strong chemical agents such as ethylene oxide gas [58, 59], gas plasma [70, 71], UV irradiation [71] and soaking in absolute ethanol [71]. Some of these techniques are briefly described in table 3.

***Table 3:*** *Summary of primary sterilization methods employed in biomaterials [70]*

| Sterilization Type | Mechanism | Benefits | Drawbacks | Applications |
|---|---|---|---|---|
| Autoclaving | High-pressure steam (121°C) disables DNA | • Efficient<br>• Easily accessible | • High temperature | • Metals<br>• Ceramics |
| Gamma irradiation | Radiation disables DNA | • Efficient<br>• Penetrating | • Radiation damage | • Metals<br>• Ceramics<br>• Polymers |
| E-beam irradiation | Accelerated electrons disable DNA | • Efficient<br>• Surface treatment | • Radiation damage<br>• Limited penetration | • Metals<br>• Ceramics<br>• Polymers |
| Ethylene oxide gas | Alkylating agent disables DNA | • No radiation damage<br>• Surface treatment | • Requires extra time for outgassing<br>• Requires special packaging | • Metals<br>• Ceramics<br>• Polymers |
| Gas plasma | Plasma chemistry disables DNA | • Low temperature<br>• No radiation damage<br>• Surface treatment | • Limited penetration<br>• Requires special packaging | • Metals<br>• Ceramics<br>• Polymers |

However one faces a major challenge: how ensure, by sterilizing, that there is no degradation to the material or its structural properties? Could the same method be employed for all materials: metal, ceramic, polymer? In general, materials that can withstand high temperatures, such as metals and ceramics, can employ any of these methods for sterilization. Polymers, because of their low melt temperatures, require low-

temperature methods such as gas plasma, ethylene oxide gas, or irradiation. However, in using irradiation for polymeric materials it is extremely important to be aware of the radiation chemistry of the specific polymer system (Birkinshaw et al., 1988; Dole et al., 1958; Pruitt, 2003). Specifically, the irradiation process can result in a chain scission or cross linking mechanism that can alter the physical structure, mechanical properties, and long-term stability of the polymeric implant; for example, gamma radiation is known to leave behind free radicals (unpaired electrons) and these free radicals are highly reactive with elements such as oxygen that may be present or may diffuse into the implant material [70].

To summarize, there are only a few suitable techniques available to sterilize the films of PLLA because most of them are susceptible to degradation and/or morphological degeneration by high temperature and pressure. A comparative study of different sterilization techniques performed on poly-L-lactide electrospun microfibers reveals that UV irradiation and hydrogen peroxide gas plasma HPGP are the most effective sterilization techniques [70]. In the context of the study HPGP is not available, therefore UV irradiation was adopted. The power of our device being less than the one specify in the study, we increased the sterilization time in order to be sure to destroy all bacteria. However, despite all that precautions, a micro-organism, fungus, attack and killed all the cells attached to PLLA films, as seen in chapter 4, figure 31. Hence, since that situation, the decision of using ethanol was taken. Ethanol 70% does not affect neither the morphology nor the molecular weight of the polymer. Yet, even if ethanol is sometimes considered as a sterilization method in some articles [71], it is unsuitable because it does not adequately eliminate hydrophilic viruses and bacterial spores [72, 73]. Ethanol is not strictly speaking a sterilization method but is more considered as a disinfection technique. Moreover it is not the first time that ethanol is used as a “sterilization” technique for PLLA [74].

The protocol regarding the “sterilization” is available in annex F.

### 5.1.3 Hob culture

The cells that were used for the study are Human osteoblast (Hob) and cancer cells (MG-63). They are both osteoblast but the second ones proliferate faster and are more resistant. Before the assays, the cells are unfrozen and cultivated. This step is described in annex G.

## 5.2 Assays

Cell line monitoring includes cell count, cell morphology checks, and the detection of calcium deposits. The different assays of viability, morphology and mineralization are described below.

### 5.2.1 Cell viability: adhesion and proliferation

The adhesion process is the first stage. It is decisive because it will mediate the cells' attachment and subsequent tissue growth. Thus the idea is to assess how cells behave, how the culture is going on, i.e. if the cells are attaching well to the substrate and if the proliferation is going on the right way. The test is performed using resazurin [75]. Resazurin (7-Hydroxy-3*H*-phenoxazin-3-one 10-oxide) is a blue dye used as an indicator in cell viability assays for bacterial and mammalian cells. Cells react with resazurin by producing a metabolite that will change the color in pink as shown in figure 19. The more cells grow, the more metabolite inside the culture media and so the pinker the solution is. In this way, one is able to evaluate the number of cells. The color detection is done by absorption spectroscopy.

Practically speaking, there are 3 replicas for each condition, plus one additive sample without cells (+1), plus an empty well where cells grow directly on plastic. The plastic well with cells is a positive control. One knows how cells behave on plastic, so one uses it to check if the experiment is progressing well. Then the extra sample without cells is used to measure the effect of resazurin directly on PLLA: it is used to calculate the background effect that is then removed to the absorbance computed with cells in the same conditions.

The protocol of the assay is given in annex H.

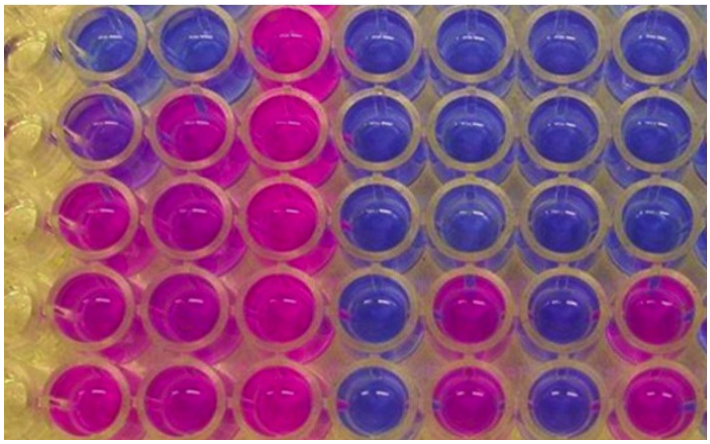

***Figure 19**: Resazurin used as colorimetric assay for cell viability [76] - Resazurin is a blue dye. Cells react with resazurin by producing a metabolite that will change the color in pink as. The more cells, the more metabolite inside the culture media and then the pinker is the solution.*

The resazurin assay was performed every day during 8 days. Every 24 hours the color is determined, introducing resazurin in the culture media, thanks to the reader and then compute the number of cells. The plate was placed inside the plate reader (TECAN i-control) and the values of resorufin were determined using the software infinite 200. The values of the resorufin inside the wells without cells were subtracted for each sample. The acquired data were then plotted and statistical analyses were conducted using the IBM SPSS statistics 22.

### 5.2.2 Cell morphology

Morphological analysis is performed in order to study the cellular organization and the state of the cells. It is the simplest and most direct method used to identify the health and stability of cells. It allows also to detect any signs of contamination. Signs of deterioration of cells include granularity around the nucleus, and detachment of the cells from the substrate.

Cell morphology was monitored by confocal microscopy (immunofluorescence) and scanning electron microscopy. Morphology can vary between cell lines depending on the health of the cells and, in some cases, the differentiation state. Morphology can change

according to the life cycle and conditions of the cells, for example with the plating density (confluence) as well as with different media. The protocol of the assay is described in annex I.

Thus samples, of 6mm in diameter, were prepared, in order to asses the morphology of the cells for two time points: 1 and 7days. The time points are end points, i.e. that the cells are "killed" and fixed to the substrate in order to observe their morphology. Two sets of samples were prepared, one for each time point, using 2 replica per cell line (Hob and MG-63).

### 5.2.3 Cell mineralization

Osteoblasts produce extracellular calcium deposits in vitro. This process is called mineralization. Calcium deposits are an indication of successful in vitro bone formation. The assessment of that mineralization process is done through the detection of Calcium deposits and quantification by staining method, using Alizarin Red S [77] as shown in figure 20. The protocol is given in annex J.

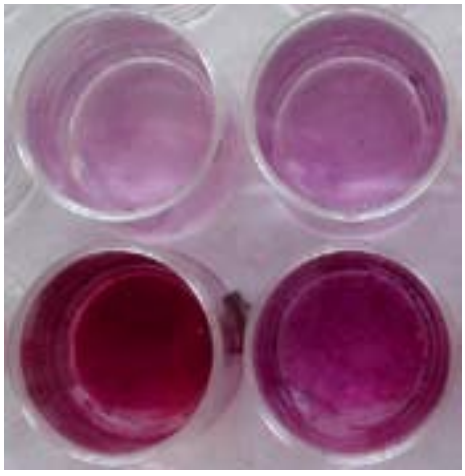

**Figure 20**: *HOB after mineralization in vitro. The negative control in HOB Growth Medium (upper row) is slightly reddish, whereas the mineralized osteoblasts in HOB Mineralization Medium show vast extra-cellular calcium deposits, stained in bright orange-red (lower row) [77]*

# Chapter 4

Results and discussion

Before presenting the results, in order to avoid any confusion and understand the results the next figures, 21 and 22 respectively, clarify the vocabularies used to qualified the different samples.

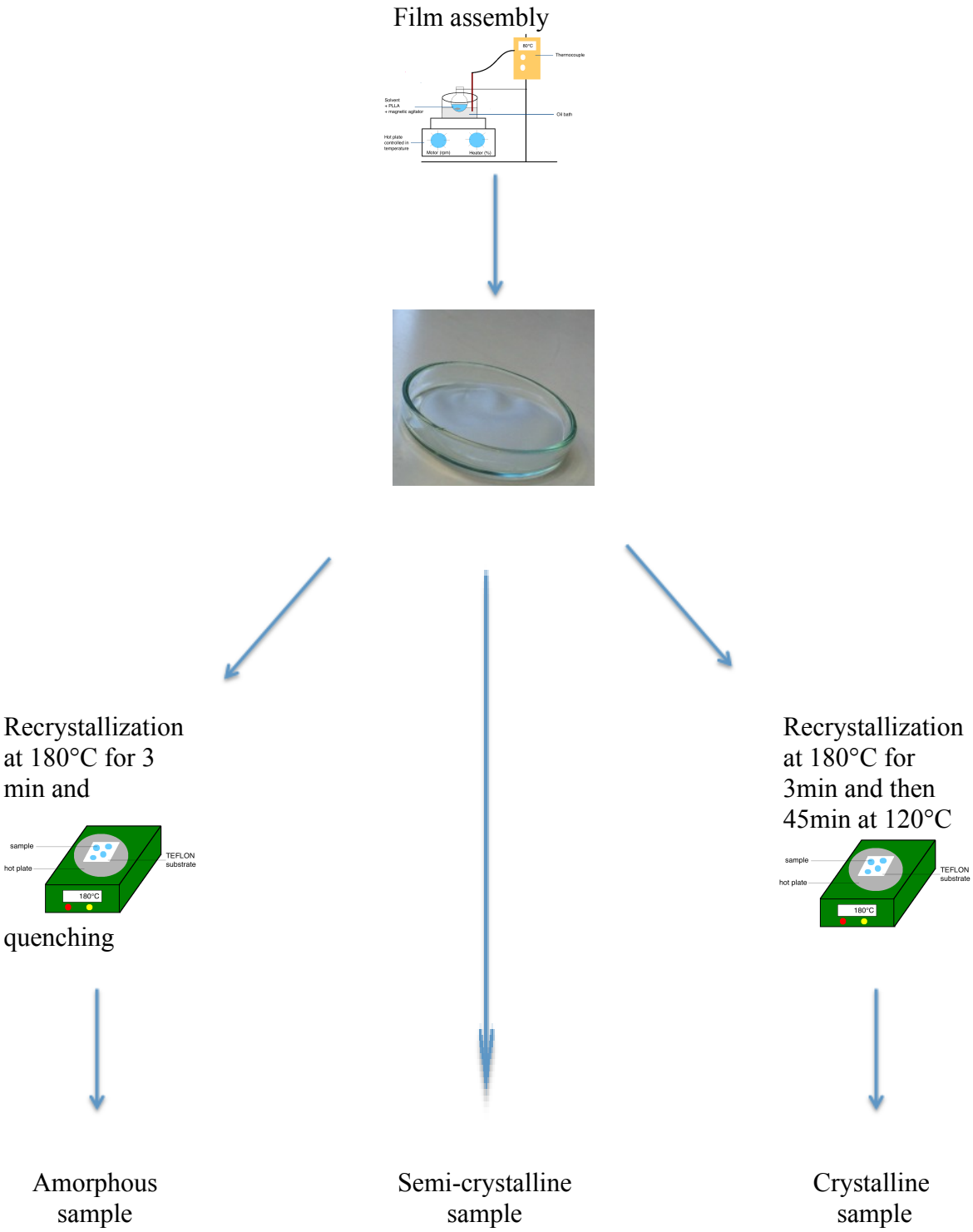


*Figure 21: Schematic representation of the processing cycles for amorphous, semi-crystalline and crystallines samples*

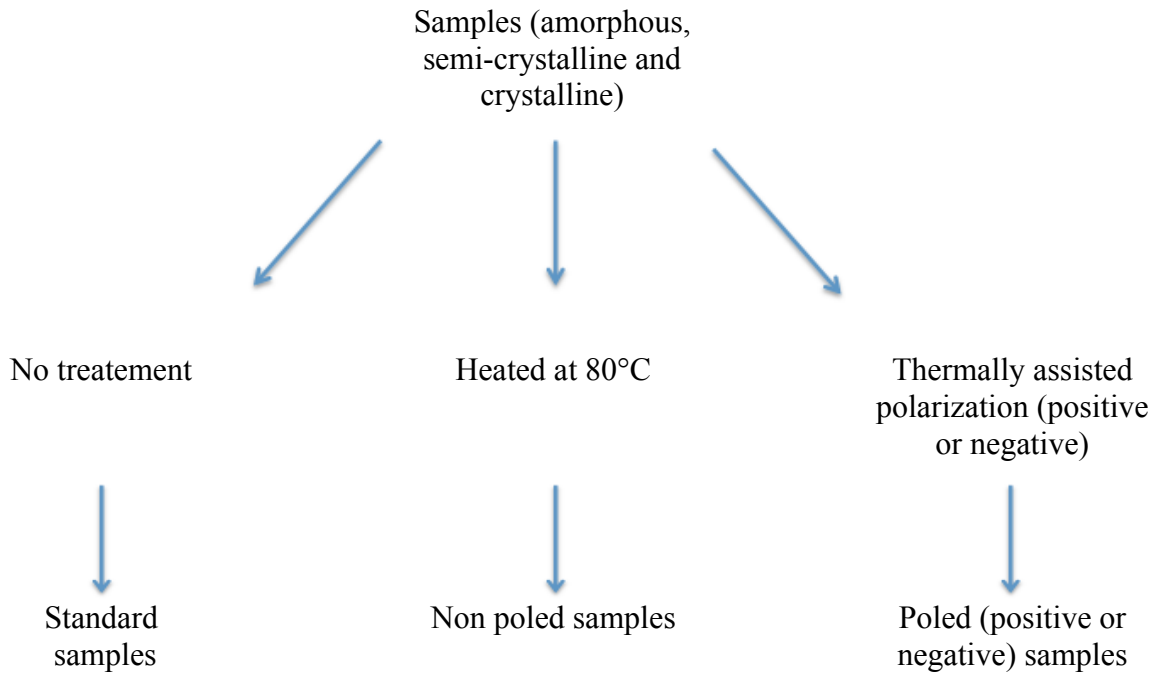


*Figure 22: Schematic representation of the poling step for standard, non poled and poled (positively or negatively) samples.*

The last figure clearly shows that standard samples are samples as prepared, without any treatment. Non poled samples are samples that only undergo the thermal treatment associated to the polarization. Finally poled samples are samples that are heated and submitted to the corona discharge.

# 1 PLLA film characterization results

In implantology, the surface properties of the implant determine its interactions with the surrounding host tissue. Physicochemical properties of the surface, like wettability and surface topography, are of prime importance for the optimization of adhesion, spreading and proliferation of cells. Since surface roughness is known to play a role in cell-biomaterial interactions, lots of effort has been put into determining the most suitable roughness parameters for implant surface characterization [78]. Thus each configuration was studied in terms of contact angle, surface roughness, XRD and DSC in order to correlate biological performances and surface properties, and then discriminate surface treatments which improve or not the osteoconductivity.

## 1.1 Micro structural study

The morphology of the films was investigated using optical and electron microscopy. It was not possible to analyze all, only some specific samples were analyzed. Moreover the polarization treatment does not imply any temperature increase and therefore no structural change. Thus, we do not expect any difference between non poled samples (i.e. only thermal treatment) and poled samples (thermal treatment + polarization) in terms of microstructure, then only standard and non-poled samples were observed. The films morphologies are depicted in the optical and SEM micrographs of figure 23 and 24, respectively.

Standard samples are samples as prepared, i.e. they did not undergone any thermal treatment after elaboration. Amorphous samples are heated until melting and quenched in water, leading to a flat and smooth surface. Whereas semi-crystalline and crystalline samples cooled down slowly their surfaces are rougher. Semi-crystalline exhibits a kind of topography made of the irregular stack of several “dots”, with the center appearing darker on the picture, giving that specific appearance and texture. Crystalline surface presents a lot of spherulites delimited by grain boundaries typical from a crystalline arrangement. Non poled samples are samples that were heated (up to 80°C) after elaboration. Overall it seems that the thermal treatment has an influence more or less important on all samples. Amorphous surface gets well organized and rougher, whereas semi-crystalline and crystallines surface become less sharp. In the case of semi-crystalline surface the material diffused and we do not observe that “dot” microstructure anymore but the peaks and valleys are still present. About crystalline surface, there is also a rearrangement and therefore the spherulites and grains boundaries are less sharp, less defined.

| | X10 | X20 |
|---|---|---|
| **Amorphous standard** | 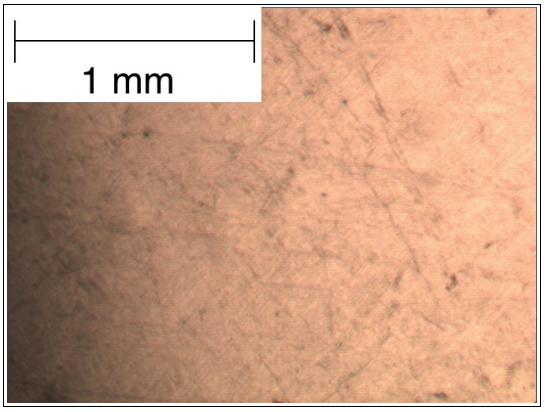  | 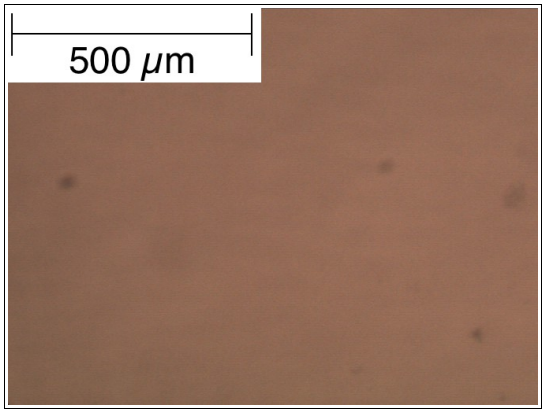  |
| **Amorphous non-poled** | 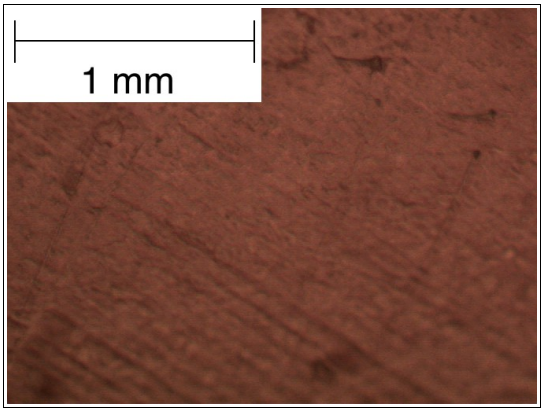  | 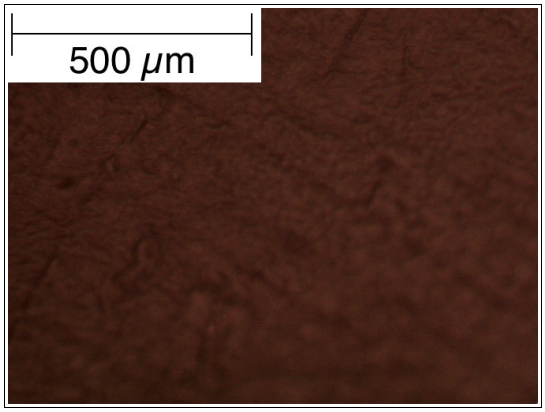  |
| **Semi-crystalline standard** | 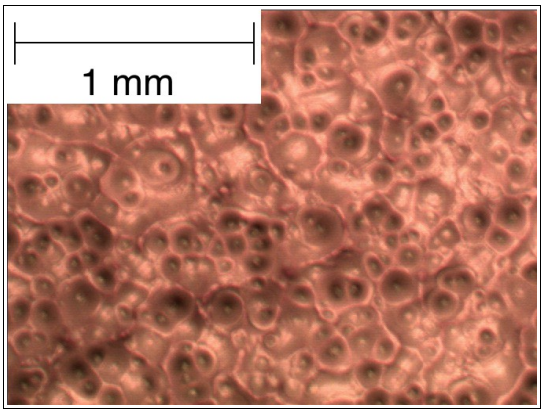  | 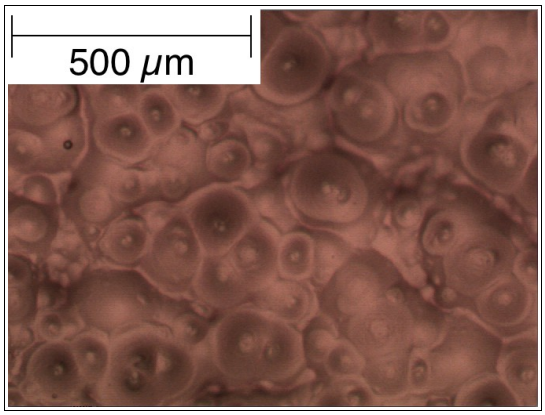  |
| **Semi-crystalline non-poled** | 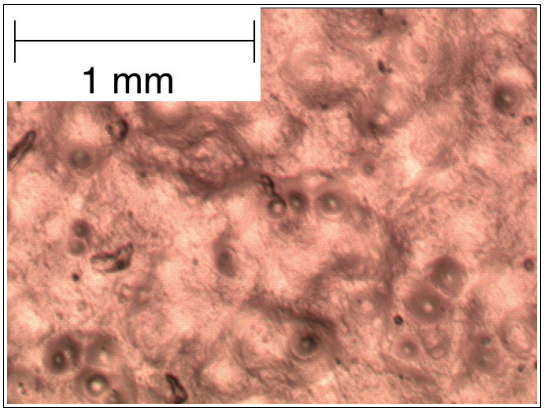  | 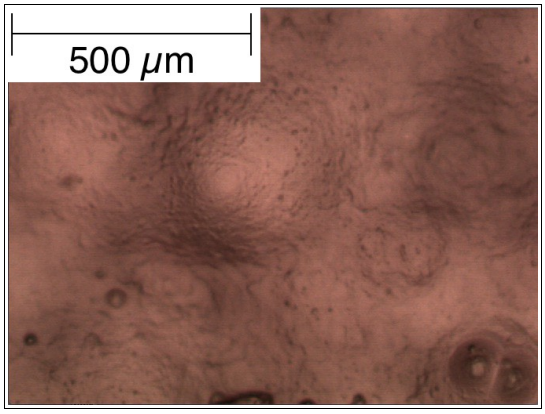  |

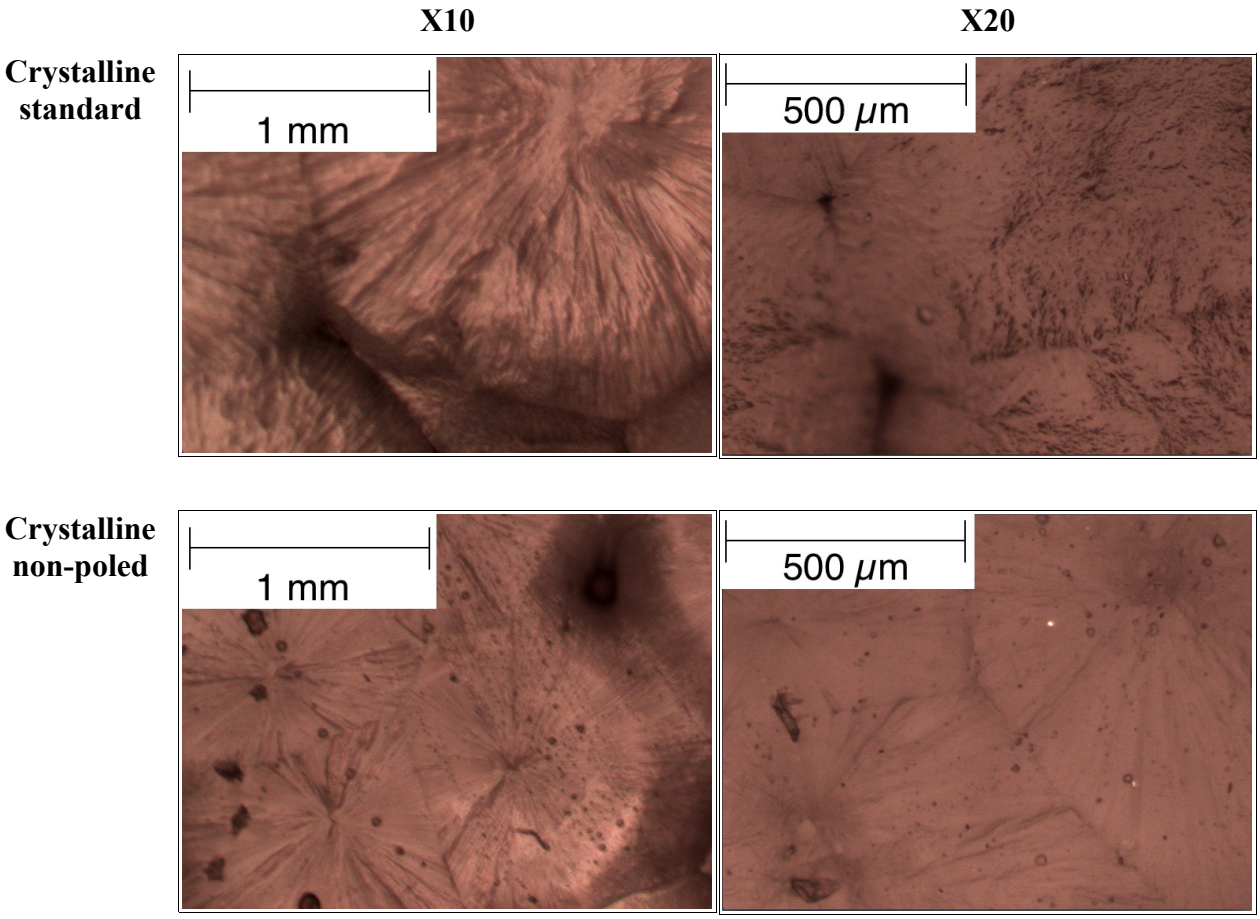


***Figure 23**: Topographic pictures of PLLA films before and after thermal treatment varying the degree of crystallinity – the pictures were acquired using a camera (Infinity 1) attached to the microscope (Nikon Microphot).*

***SEM analysis***

Samples were prepared for scanning electron microscopy (SEM) by mounting the samples on an aluminum stub covered in double-sided carbon tape, and then sputter coated with Au/Pd. The samples were analyzed using a Hitachi S-4100 SEM at 5kV.

The SEM pictures confirm what was observed with the optical microscope: standard amorphous surface is flat and smooth with no particular pattern. However after thermal treatment the texture is different; more organized. About semi-crystalline, the observed texture is what we saw with the optical microscope: a stack of "dots". With a higher magnification we notice that the dots are in reality crystallites separated by grain boundaries. After treatment, semi-crystalline sample presents less defects. The appearance of the standard crystalline samples, does not coincide with what was observed in the optical microscopy. When thermally treated, the films are deposited on a hot plate. Therefore the two faces are not submitted to the same treatment, there is a temperature gradient between the two sides. It is then possible that the observed standard crystalline sample corresponds to the side that is not in contact with the hot plate of the corona, The crystalline surface after thermal treatment exhibits grains separated by grains boundaries. Finally it seems, as stated with optical micrographs, that the thermal treatment has a great influence on all samples.

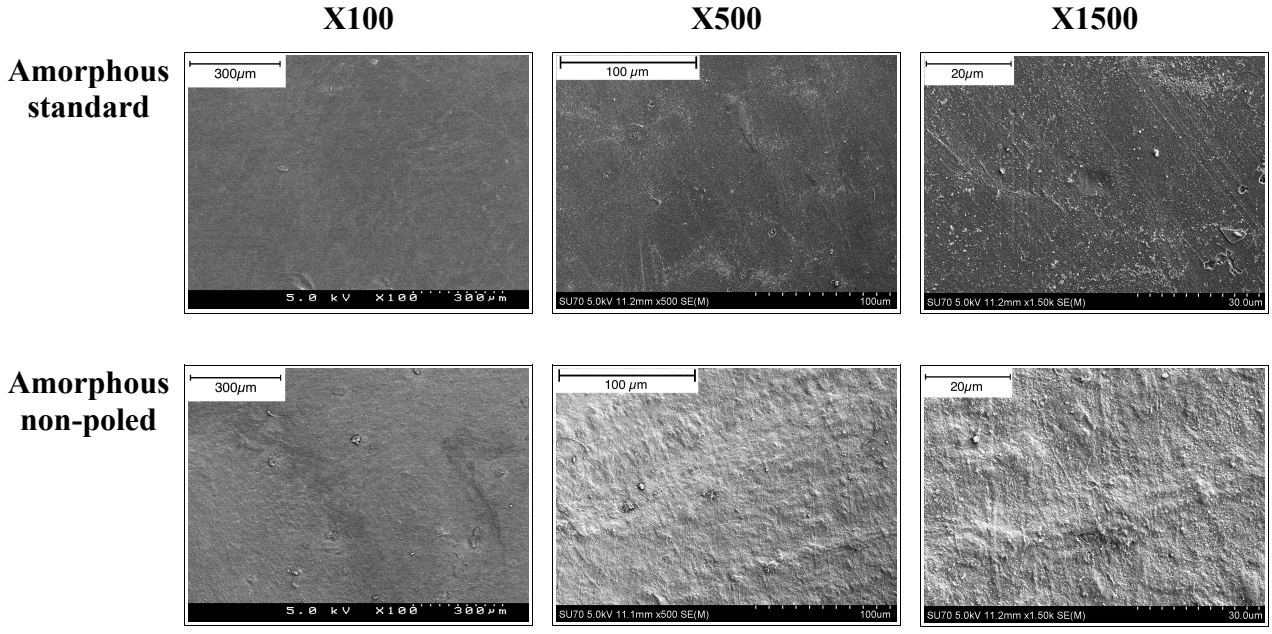

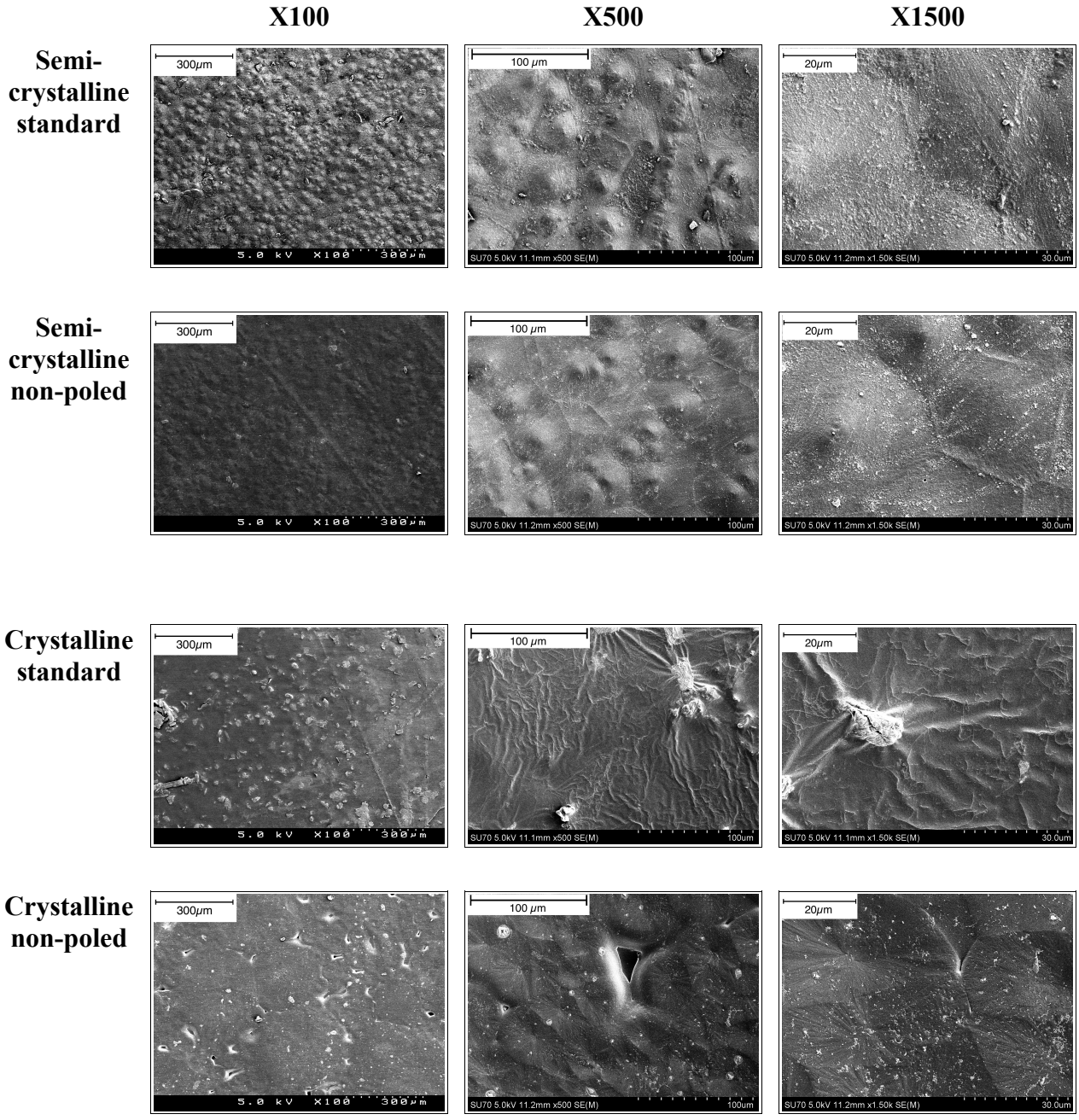


***Figure 24**: Electron micrographs of PLLA films before and after thermal crystallization varying the degree of crystallinity*

## 1.2 Surface roughness measurement

The results obtained through the surface profilometer described in Section 4,2 of chapter 3, are given in table 4. It shows the arithmetic mean surface roughness in μm, of samples measured in different configurations, i.e. the average value of the sums of all profile values measured within a determined sampling length. Although both sides are measured, the upper one being the rougher , is the one in contact with cells

***Table 4****: Surface roughness results – roughness was measured on both sides (up-facing the air and down – in contact with the substrate) of amorphous, semi- crystalline and crystalline samples*

| | Amorphous. up | Amorphous down | Semi - crystalline up | Semi - crystalline down | Crystalline up | Crystalline down |
|---|---|---|---|---|---|---|
| Standard | 0.055 μm ± 0.008 μm | 0.129 μm ± 0.036μm | 0.493 μm ± 0.052 μm | 0.090 μm ± 0.019 μm | 0.273 μm ± 0.079 μm | 0.122 μm ± 0.024 μm |
| Non poled | 0.143 μm ± 0.022 μm | 0.147 μm ± 0.028 μm | 0.431 ± 0.051 μm | 0.200 μm ± 0.016 μm | 0.425 μm ± 0.084 μm | 0.118 μm ± 0.019 μm |
| Poled - | 0.145 μm ± 0.042 μm | 0.148 μm ± 0.018 μm | 0.433 ± 0.045 μm | 0.158 μm ±0.021 μm | 0.429 μm ± 0.096 μm | 0.159 μm ± 0.043 μm |
| Poled + | 0.144 μm ± 0.035 μm | 0.140 μm ± 0.026 μm | 0.429 ± 0.022 μm | 0.151 μm ± 0.037 μm | 0.448 μm ± 0.061 μm | 0.132 μm ± 0.029 μm |

***Standard samples (samples as prepared)***

As expected, according to the microstructural study, the amorphous surface is the smoother, and the semicrystalline one the rougher. The down value of standard semi-crystalline samples are smoother to the values of the down values of amorphous and crystalline, probably because semi-crystalline samples were made on glass substrate, which is smoother than the teflon substrate of amorphous and crystalline samples. Moreover amorphous and crystalline have similar values. Indeed they were synthesized with the same substrate.

***With thermal treatment***

The values of roughness after thermal treatment, with and without polarization are really similar what confirms the hypothesis that the polarization step does not imply considerable change in the microstructure of the films. Regarding the up side, all results are really similar whereas the spreading is higher in the case of the down side. This may come from the fact that the up side is the one in contact with the hot plate in the Corona setup and the down side, the one in contact with air in the Corona. Then the results show larges changes of the roughness with thermal treatment, in all configurations, and especially in the case of crystalline samples.

***Conclusion***

There is a difference between the two surfaces: up and down. It is therefore important to pay attention to the surface which will be exposed to polarization and then to cells. Moreover the results match what is observed in the microscope. In the case of standard samples, amorphous surface is the smoother and semicrystalline the rougher. When submitted to the thermal treatment the roughness is shifted. Amorphous surface is slightly rougher. Semi-crystalline surface gets smoother, and surprisingly crystalline surface is getting rougher and reach the same value as semi-crystalline surface.

## 1.3 Thickness measurement

The results of cross section thickness before and after heat treatment are given in table 5.

***Table 5**: Thickness measurements. (Standard refer to as-prepared samples and non-poled refer to samples heat treated at 80°C)*

| Amorphous standard | Semi-crystalline standard | Crystalline standard |
|---|---|---|
| 121 ± 6 µm | 130 ± 4 µm | 110 ± 17 µm |
| | | |
| Amorphous non poled | Semi-crystalline non poled | Crystalline non poled |
| 114 ± 4 µm | 85 ± 3 µm | 174 ± 10 µm |

The results indicate, first that there are differences between samples with different degrees of crystallinity; and then that after thermal treatment there are significant differences of thickness, especially regarding semi-crystalline and crystalline samples. The elaboration process is not controlled at such an accurate scale. For example the environment (water content, etc) is not monitored; and the cast method is dependent on the operator and not controlled. Thus there are a lot of parameters that more or less can influence the thickness of the films. The same may happen with the recrystallization process, even if the exact same conditions are applied to all samples. Therefore it is not possible to conclude about the influence of the thermal treatment on the thickness of the samples. To quantify it, a statistical study made on perfect replica should be done.

## 1.4 Wettability – Contact angle measurement

The results of contact angle measurements are given in table 6.

***Table 6**: Contact angle results in water– the contact angles were measured on both sides (up – facing air and down – in contact with the substrate) of amorphous, semi-crystalline and crystalline samples*

| | Amorphous. up | Amorphous down | Semi - crystalline up | Semi - crystalline down | Crystalline up | Crystalline down |
|---|---|---|---|---|---|---|
| Standard | 92.7 ± 3.8 ° | 80.2 ± 0.9 ° | 75.9 ± 1.5 ° | 87.8 ± 4.2 ° | 91.4 ± 1.9 ° | 87.0 ± 1.6° |
| Non poled | 88.7 ± 6.3 ° | 70.7 ± 3.9 ° | 81.5 ± 3.7 ° | 79.8 ± 5.4 ° | 77.9 ± 3.1 ° | 93.7 ± 5.2 ° |
| Poled - | 82.3 ± 3.4 ° | 76.0 ± 8.7 ° | 92.3 ± 4.8 ° | 73.4 ± 8.4 ° | 81.9 ± 11.1 ° | 85.4 ± 9.8 ° |
| Poled + | 88.7 ± 7.8 ° | 81.4 ± 6.9 ° | 100.8 ± 2.2 ° | 79.7 ± 5.7 ° | 105.1 ± 7.1 ° | 69.0 ± 6.0 ° |

As stated in chapter 3, wettability measurements enable to characterize the affinity of a surface towards a liquid; and is performed by assessing the equilibrium of the system through the measurement of the static contact angle θ between the drop of liquid and the solid surface. Static contact angle, opposed to dynamic contact angle, is measured when the droplet is standing on the surface and the three-phase boundary is not moving. Low values of θ indicate a strong liquid–solid interaction and the liquid tends to spread on the solid, or wets well, while high θ values indicate weak interaction and poor wetting.

The results indicate, for standard samples, that water has more affinity with semi-crystalline surface, than amorphous and crystallines surfaces. Then it seems that there is no effect of the thermal treatment, except for crystalline surface that changes from 91,4 ° to 77,9 ° and gets really wettable. About the effect of polarization, there are large changes between the standard angle value and the angle after polarization for semi-crystalline and crystalline. It seems that the polarization makes the semi-crystalline and crystalline surfaces hydrophobic. However these results have to be carefully considered and discussed. Indeed, even if the sessile drop method is accurate, the measurement is subjective enough to bring incertitude about the values. Therefore it is not possible to conclude about the influence of the thermal treatment and of the polarization on the wettability of the samples. To quantify it, a statistical study made on perfect replica should be done.

**Conclusion**

From a general point of view we are not able to notice any significant differences before and after polarization, except for semi-crystalline and crystalline poled positive.

## 1.5 Thermal analysis

The obtained films were characterized in terms of thermal behavior and crystallinity. DSC thermograms of PLLA films are compared in figure 25, and their respective degrees of crystallinity computed. DSC measurements were performed using a scanning range from 25 °C to 230 °C and a heating rate of 10 °C/min. Only standard and non poled samples have been studied. Standard samples are as-prepared films and non-poled samples are standard films that have been heated at 80 ºC for 30 min, mimicking the heating cycle in the Corona hot plate while poling the samples. Both positive and negative poled samples are still under experiment.

Amorphous standard

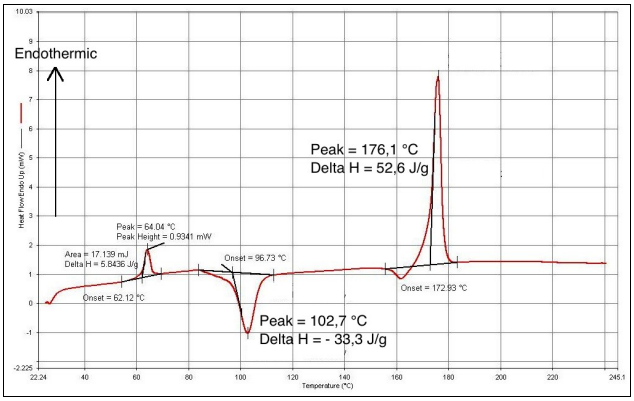


Amorphous non poled

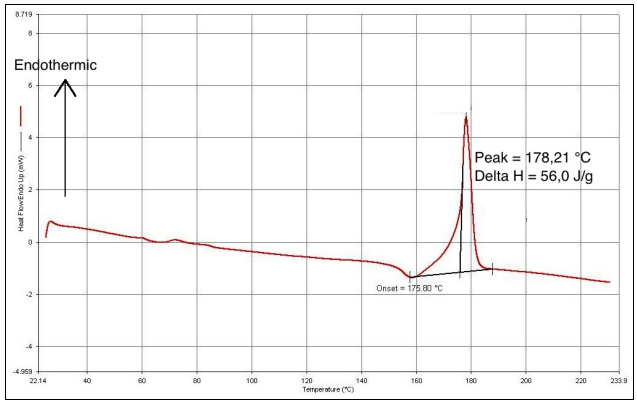


Semi-crystalline standard

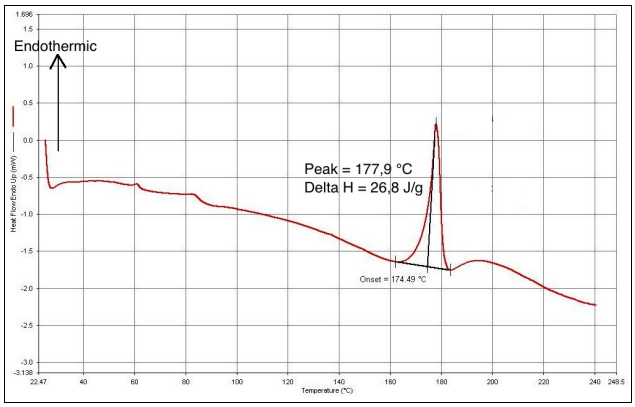


Semi-crystalline non poled

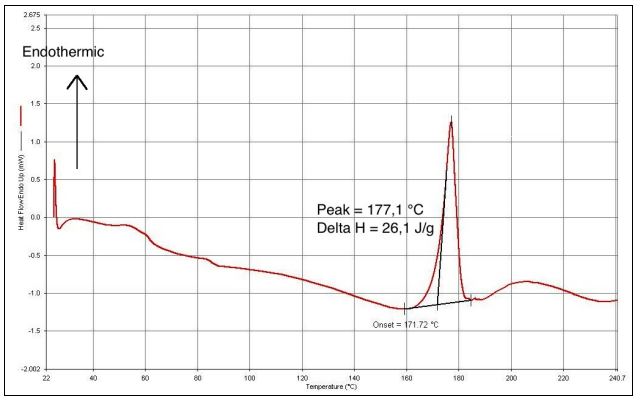


Crystalline standard

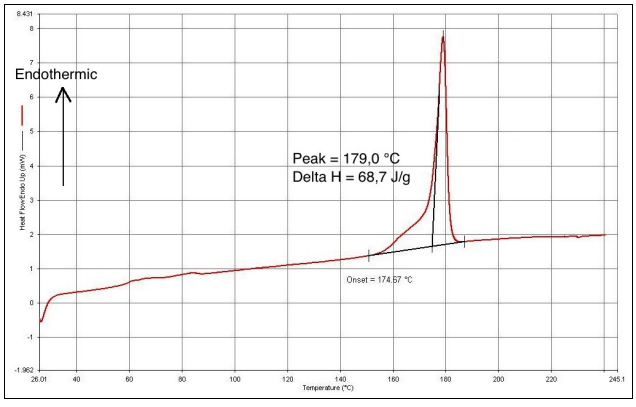


Crystalline non poled

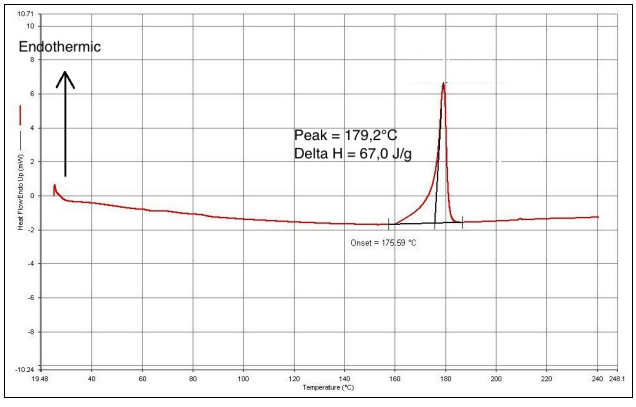


***Figure 25**: DSC curves of amorphous, semi-crystalline and crystalline PLLA films for standard and non poled configurations*

These thermograms allow us to quantify the degree of crystallinity of each sample. However we can distinguish several phenomena that are interesting to discuss. Indeed, in figure 26, we note the presence of three peaks at 62 °C, 102 °C and 176 °C corresponding respectively to the glass transition, the crystallization and the melting of the polymer. All these phenomena appear in all samples but are well defined in the case of standard amorphous, detailed in figure 26, and are in agreement with the existing literature [79]: Tg around 60 °C, the Tc peak between 80 and 120 ºC, and the melting point around 170 °C.

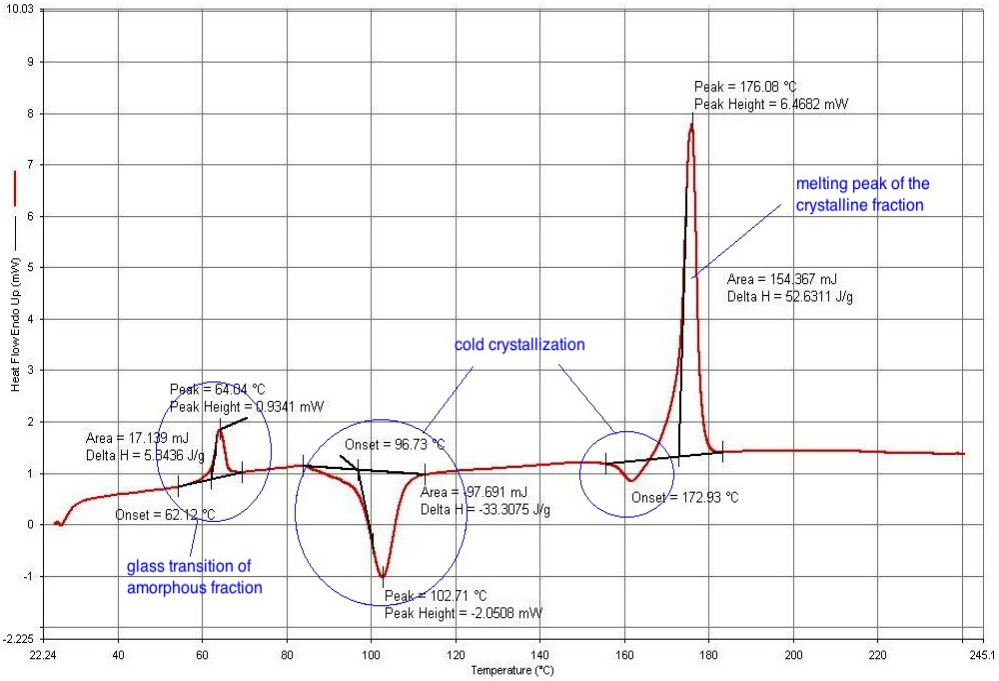


***Figure 26**: Standard amorphous DSC thermogram*

The degree of crystallinity $X_c$ is determined by the relation:

$$Xc = \frac{Hf - Hc}{H100} \times 100$$

With ΔH=Hf-Hc, the difference between the enthalpy of fusion Hf and the enthalpy of crystallization Hc. Then ΔH is the heat released by the part of the sample which was already crystalline before the polymer was heated above the crystallization temperature. In order to know which part of PLLA was crystalline before heating to make it crystalline, the enthalpy of crystallization has to be subtracted from the enthalpy of fusion. Hf and Hc were calculated by the software from the area under the peak of fusion and crystallization

respectively, displayed on the thermograms, and H100 the enthalpy of fusion of the sample with 100% crystallinity. The theoretical heat of fusion of pure crystalline PLLA is equal to 91 J/g [80]. Considering this value and making the suitable calculations, the crystallization degrees and respective enthalpies are obtained, table 7.

***Table** 7: Enthalpies and degrees of crystallinity of PLLA films*

| **Films** | ***Hf*** | ***Hc*** | ***ΔH*** | **Xc** |
|---|---|---|---|---|
| Amorphous standard | 49,6 J/g | 31,9 J/g | 17,7 J/g | 19,5 % |
| Amorphous non poled | 56,9 J/g | 0 J/g | 56,9 J/g | 62,5 % |
| Semi-crystalline standard | 26,8 J/g | 0 J/g | 26,8 J/g | 29,5 % |
| Semi-crystalline non poled | 29,4 J/g | 0 J/g | 29,4 J/g | 32,3 % |
| Crystalline standard | 68,7 J/g | 0 J/g | 68,7 J/g | 75,5 % |
| Crystalline non poled | 67,0 J/g | 0 J/g | 67,0 J/g | 73,6 % |

Table 7 shows that amorphous samples, in standard configuration, exhibit a high degree of crystallinity, about 20%. Then they are very influenced by the thermal treatment, the degree of crystallinity dramatically increases from 19,5 to 62,5%. This is easily explained by the fact that the glass transition temperature (60 °C) is inferior to the working temperature (80 °C) used during polarization. In addition the cooling of the sample is slow, what allows the crystallization of the sample. Physically after the thermal treatment amorphous samples are opaque, which confirms that there is crystallization. About semi-crystalline and crystalline samples, we see on the thermograms that the glass transition phenomenon is very weak, either inexistent. Thus the degree of crystallinity after polarization is only slightly changed.

## 1.6 X-ray diffraction studies

XRD patterns of standard, non poled, and poled PLLA samples crystallized at different degrees of crystallinity are reported in Figure 27 and 28. For easier comparison, all the diffraction patterns are normalized using the strongest (200/110) reflection intensity [80]. The indexation of the observed reflections is based on the crystal structure reported by Cocca et al. [81]. For information, crystallization of PLLA from the melt or solution results in its most common and stable polymorph, the α form, in an orthorhombic unit cell [82]. The other two forms, β and γ are developed under special processing conditions [81]. In our study we are dealing with the α form of PLLA.

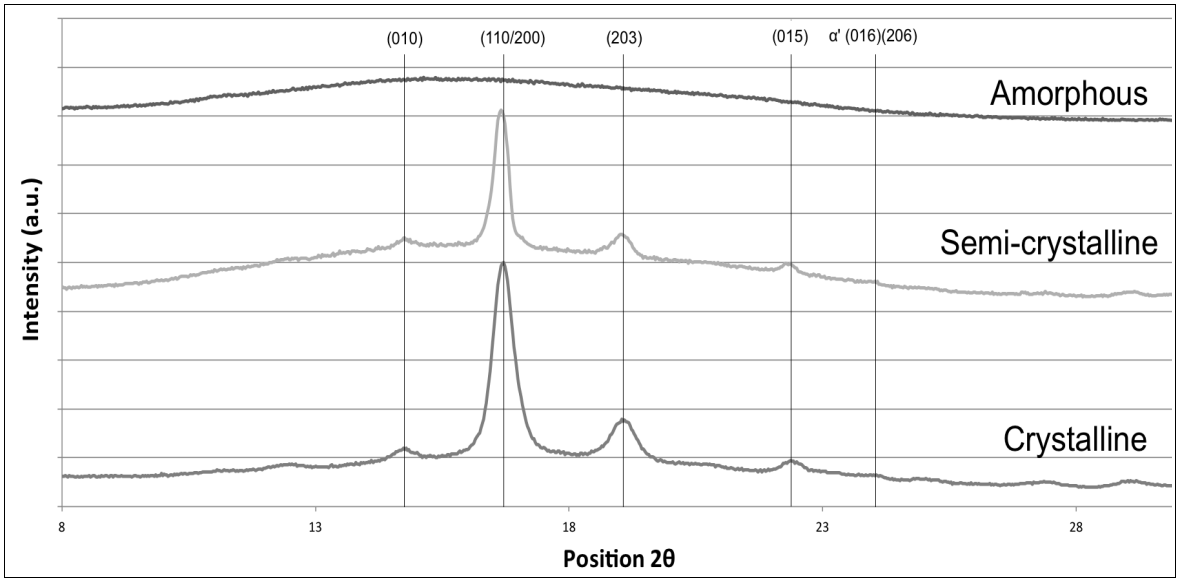


***Figure 27**: X-Ray diffractogram for amorphous, semi-crystalline and crystalline samples, in standard configuration, i.e. as prepared - for easier comparison, all the diffraction patterns are normalized using the strongest (200/110) reflection intensity*

Differences in XRD patterns are observed between crystalline, semi-crystalline and amorphous PLLA samples. First amorphous samples are characterized by a hump, typical of the absence of organized structures, associated with no reflection. Then the same peaks are observed on semi-crystalline and crystalline samples but much bigger and sharper for crystalline sample, characteristic of a higher degree of crystallinity. We can also distinguish that peaks appear at a position slightly higher for crystalline than semi-crystalline, respectively 16,65 and 16,7° for the (110/200) peak. In polymeric structures

crystallization is associated with the alignment of molecular chains that grow and orient themselves giving rise to ordered regions. A variation in peak position is thus quite plausible.

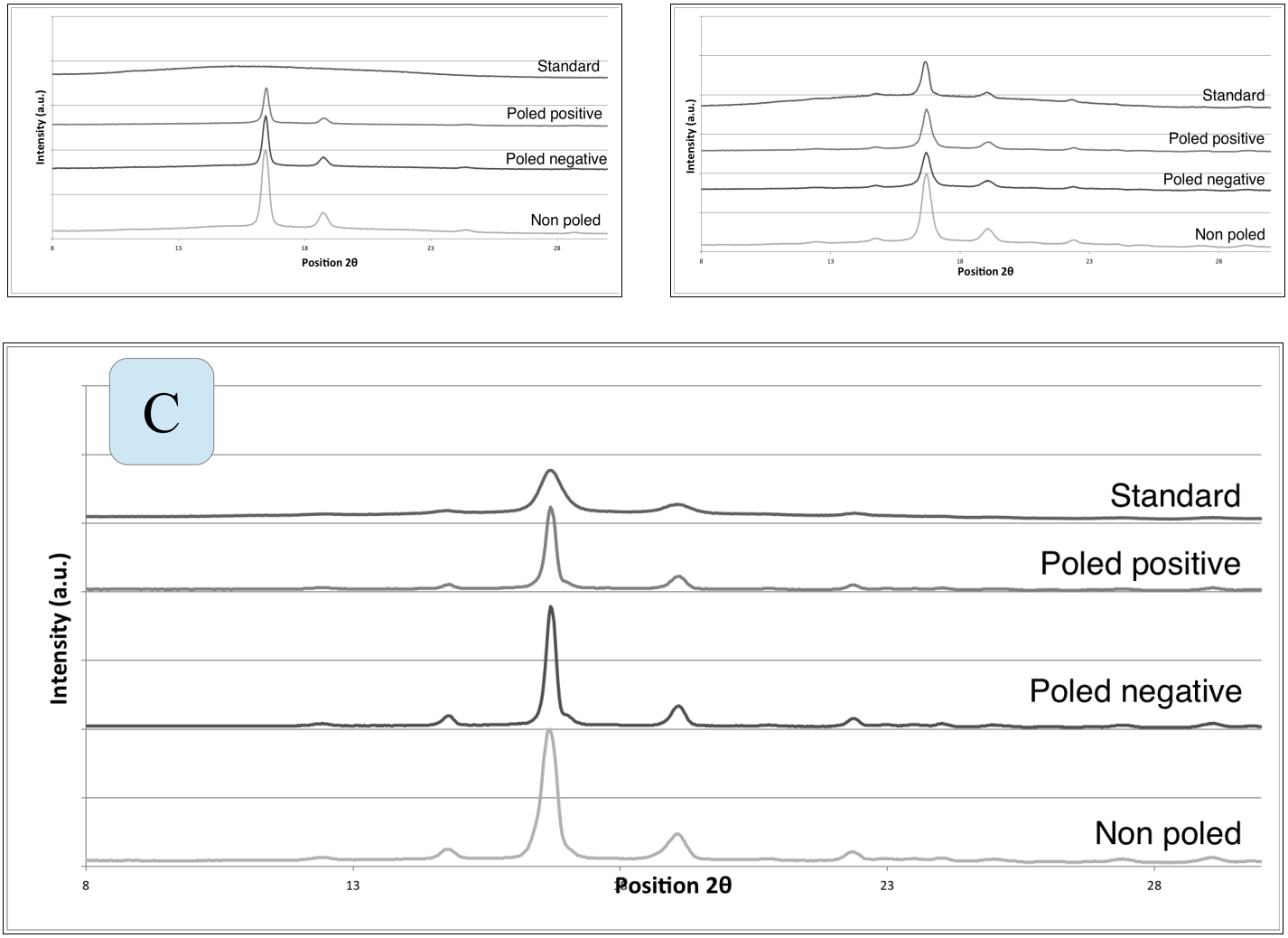


***Figure 28**: X-Ray diffraction patterns for non poled, poled positive, poled negative and standard for different cases **a)** amorphous, **b)** semi-crystalline, and **c)** crystalline samples - for easier comparison, all the diffraction patterns are normalized using the strongest (200/110) reflection intensity*

From diffraction patterns in figure 28 several readings may be taken. First amorphous samples become crystalline after undergoing the thermal treatment for polarization, although still less than semi-crystalline and crystalline, because amorphous samples do not show peaks around 14 and 22° as in the cases of semi-crystalline and crystalline. Then

semi-crystalline and crystalline samples are also getting more crystalline thanks to that treatment.

About the influence of the polarization, we note that there is not any shift between peaks, leading to the conclusion that the polarization does not change the structure of the polymer, it is the same crystallographic plans that are diffracting. Nevertheless we observe that the sharpest peak is always the non poled one, and the poled positive and poled negative peaks have similar values except in the case of crystalline samples. This indicates that the number of diffracting centers are more important in the case of non poled samples. From that we can make three hypothesis: 1) the differences between poled and non poled correspond to the standard deviation and there is therefore no significant differences between the two cases; 2) the corona effects heats locally the sample leading to a less effective recrystallization; 3. by orientating the dipoles the C=O bond rotates slightly leading to a less effective rearrangement than in the case of only thermally treated. A DSC experiment would tell us more about the possible influence of the polarization.

## 1.7 Cellular bio assay results

### 1.7.1 Cell viability onto PLLA films

The results of cell viability obtained through the methodology described in Section 5.2.1, Chap 3, are given in figure 29 and 30, for Hob and MG-63 respectively.

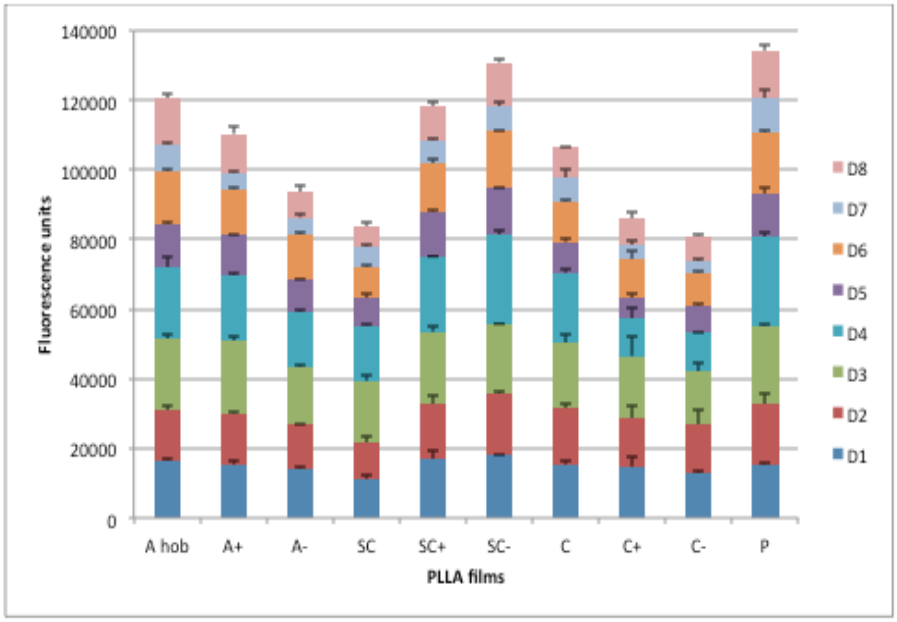


***Figure 29**: Graph of resazurin measurements for 8 days. HOB cells were grown on different PLLA films polarized and non-polarized and plastic.*

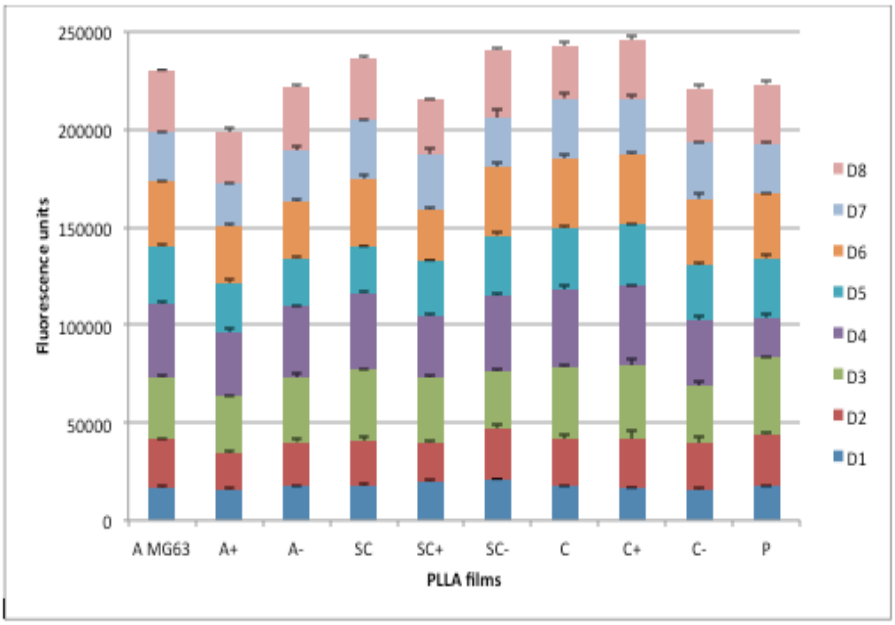


***Figure 30**: Graph of resazurin measurements for 8 days. MG-63 cells were grown on different PLLA films polarized and non-polarized and plastic.*

***Legend:** A) Amorphous; A+) Amorphous positively-charged; A-) Amorphous negatively-charged; SC) Semi-crystalline; SC+) Semi-crystalline positively-charged; SC-) Semi-crystalline negatively-charged; C) Crystalline; C+) Crystalline positively-charged; C-) Crystalline negatively-charged; P) Plastic; D*)Day number **

The plastic well boxes are made of black polystyrene. This specific material has been treated and optimized for cell culture and suitable measurement such as fluorescence common in biology. Thus the attachment and growth of cells on this surface is optimal. In this kind of assay, there is always an empty well, i.e. with no sample, were the cells are growing directly in the plastic on the well. This serves as a positive control. It allows first to check if the cells are going well on a known surface, and then it allows subsequently to compare the results of the assay with a reference.

First we notice that the number of counts for MG-63 is twice more important than the number of fluorescence units of Hob. This is explained by the fact that cancer cells are more resistant and duplicate twice faster than Hob. Then from this assay we can see that all the surfaces are viable for both kind of cells (Hob and MG-63). About Hob, we observe a kind of trend; for example semi-crystalline poled negative exhibits uniform variations of results, reaching the same value as the plastic well. Amorphous non poled and semi-crystalline poled positive also reach high values. On the other hand semi-crystalline non poled, crystalline poled positive and negative have the lower value of fluorescence what means that less cell grew on these surfaces. In order to know if these differences are significant to discriminate a particular surface, which would induce osteoconductivity, a statistical analysis has to be performed. Moreover we can also note that there are differences between days; for instance day 5 and day 7, there are much less cells that duplicate compared to the other days. This is related to biological phenomena that we will not discuss here.

About MG-63, it is impossible to distinguish any kind of trend, all the surface exhibit high viability and proliferation. Moreover it is impossible to correlate these results with the results of Hob because, for example, crystalline poled positive which was one of the "worse" surfaces for the proliferation of Hob is here the best, even better than plastic. Here again a statistical analysis will be done soon Another assay of viability and proliferation, of 21 days, is currently under experiment. By combining the future results with the ones of 8 days, we expect to be able to establish in a more sensible way, the relationship between degree of crystallinity/surface features with cells response in contact with PLLA.

1.7.2 Assessment of the morphology by immunofluorescence and scanning electron microscopy analysis

The morphology was assessed after 1 and 7 days by immunofluorescence and scanning electron microscopy. Unfortunately the films undergone a fungus attack and the cells were killed, what means that the aseptic technique (UV irradiation) was not suitable. The experiment was then stopped after 5 days instead of 7. However the samples have been observed by SEM, but no usable results have been found out; almost all the cells have been destroyed. Figure 31, shows cells attacked by fungus after 1 day.

The samples were fixed using 2% glutaraldheyde with 0.2% sodium cacodilate (20840-Sigma) pH 7.2-7.4 during 30 minutes at room temperature; and dehydrated. They were then prepared to be observed in SEM by coating by gold sputtering.

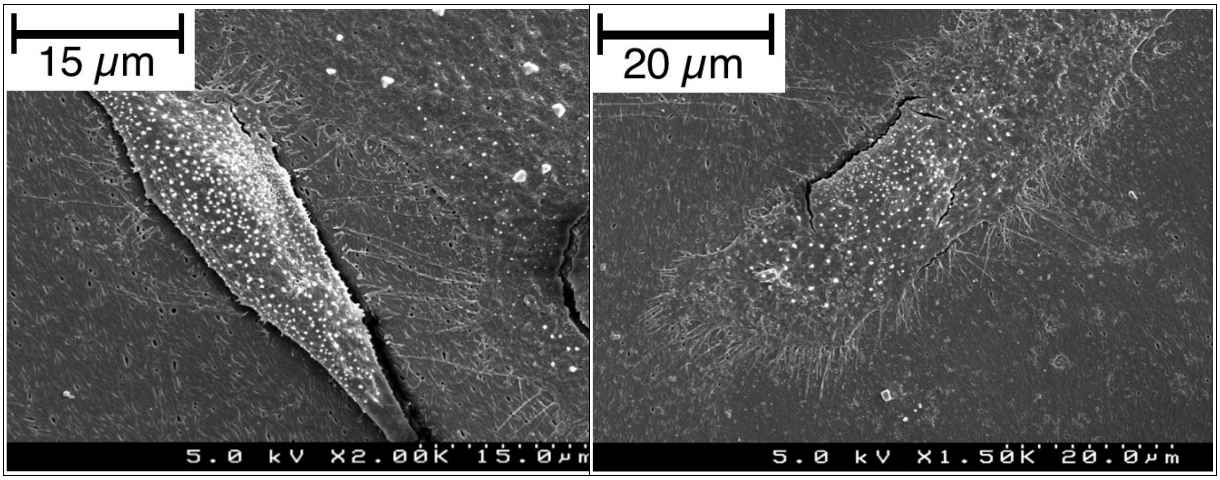


***Figure 31**: Fungus attack on cells – The small white dots are characteristic of fungus [83]*

### 1.7.3 Mineralization study

Osteoblasts can be induced to produce vast extracellular calcium deposits in vitro. This process is called mineralization. Calcium deposits are an indication of successful in vitro bone formation and can specifically be stained bright orange-red using Alizarin Red S. The detection of calcium deposit and the quantitative analysis was done by Alizarin Red Staining. Alizarin Red Staining bind to calcium ions and form orange-red complexes, whereas without extracellular calcium deposits are slightly reddish.

The experiment has been done on the 9 configurations and plastic with only cell growth media, and on plastic with cell growth media and 1mM of beta-glycerophosphate and 50 mg/mL of ascorbic acid. Glycerophosphate and ascorbic acid are inducers that are added to the standard culture medium to support the osteogenic activity of cells. In the literature there are some studies describing what should happen with cells grown on plastic under the influence of ascorbate and glycerophosphate [84]. Thus the two plastic wells are used as positive control. By comparing our results with these controls we are able to check their validity. Looking at the results, figure 32, for the Hob, we see mineralized osteoblasts, i.e. bright orange-red spots in the case of semi-crystalline and crystalline both positive and negative. Whereas undifferentiated Hob, i.e. without extracellular calcium deposits, are slightly reddish; this is the case of amorphous samples and crystalline non poled. About osteosarcoma cell line, almost no calcium deposit was detected. Amorphous and semi-crystalline poled negative, and semi-crystalline and crystalline poled positive exhibit a few small red dots. The other configurations did not produce or not significant enough amount of calcium to be detected.

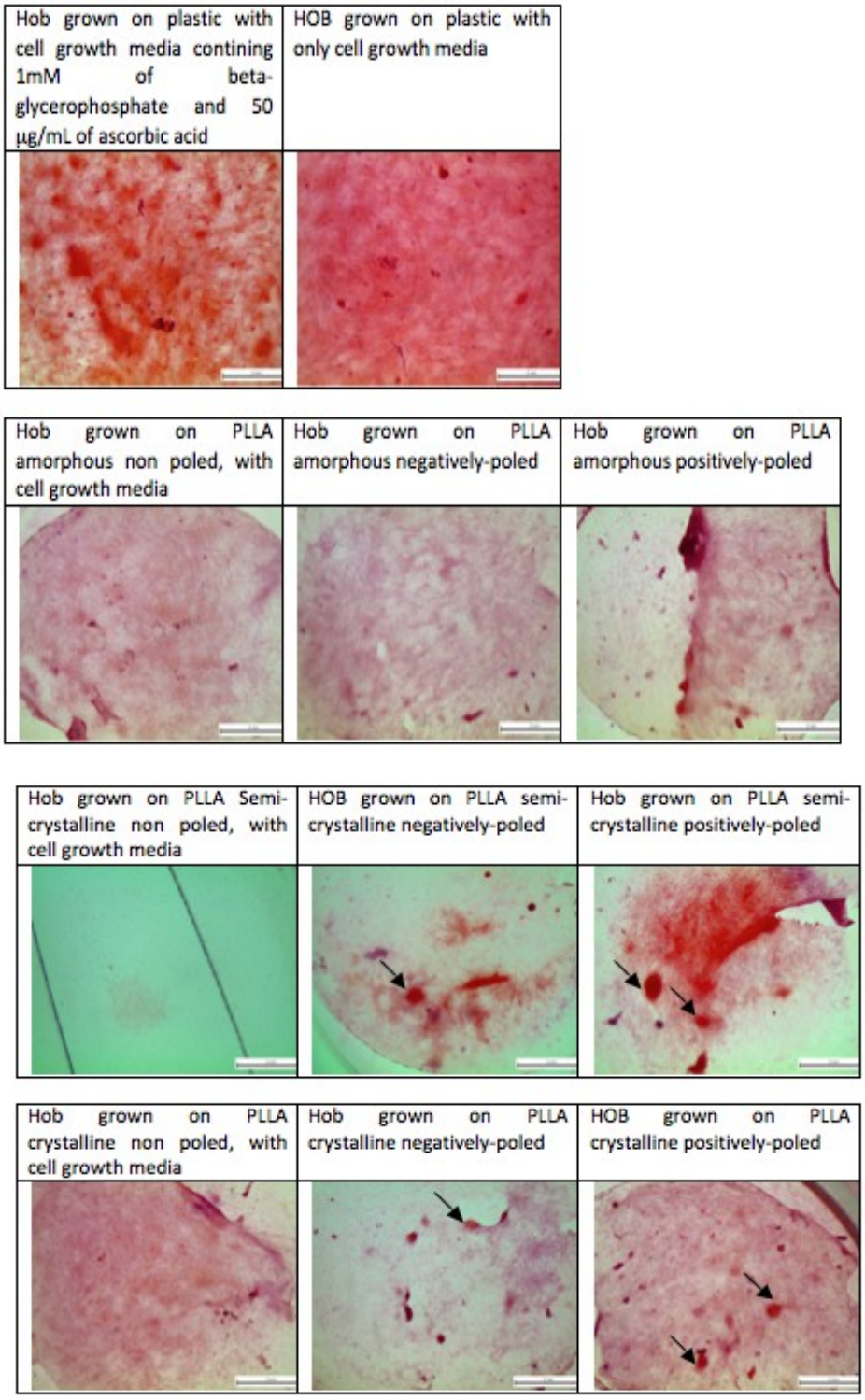


***Figure 32:*** *Images of HOB grown on different surfaces for 21 days. HOB cells were grown on different PLLA films polarized and non-polarized and plastic. Black arrows (→) show the deposits of calcium stained positively by ARS.*

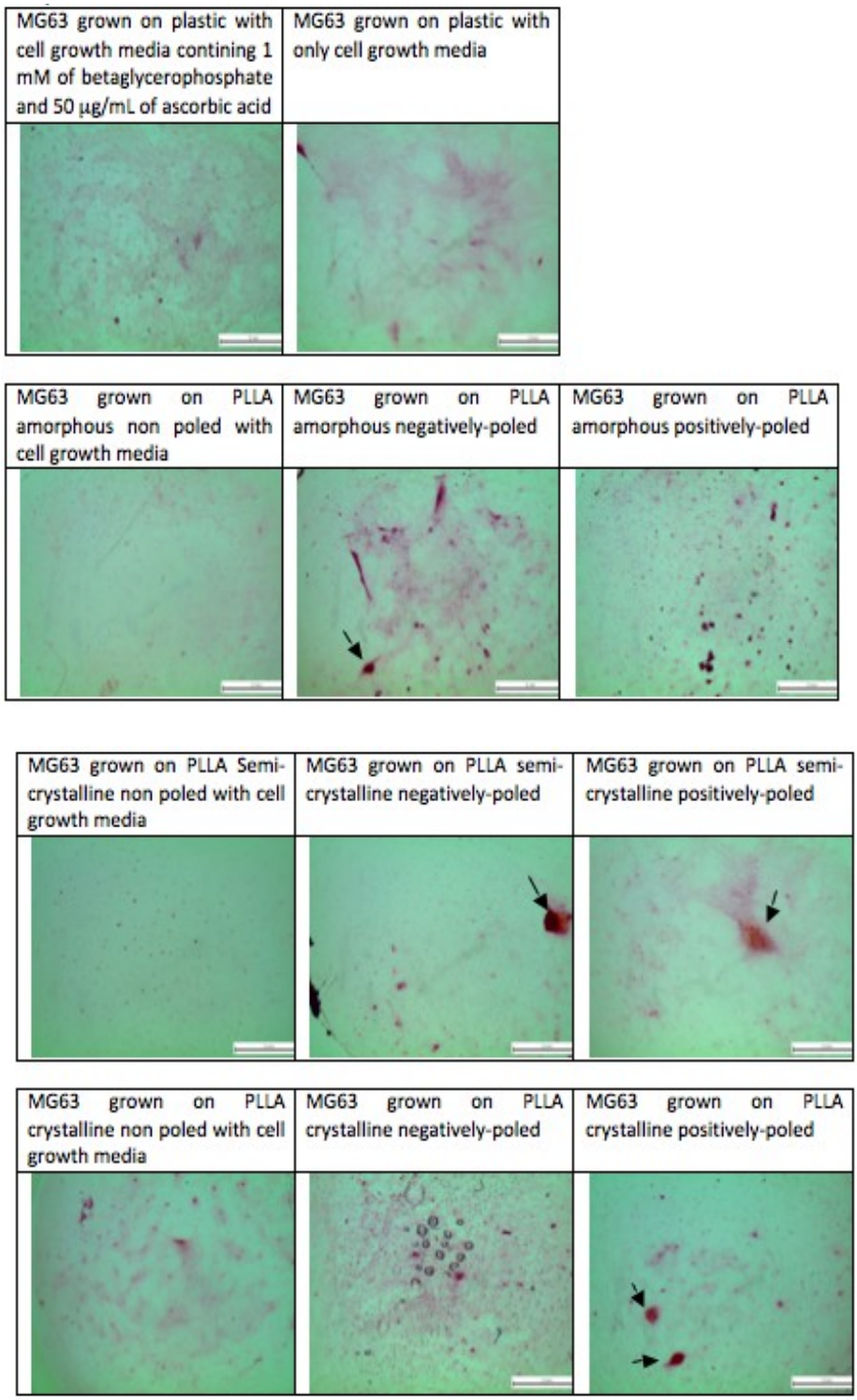


***Figure 33:*** *Images of MG63 grown on different surfaces for 21 days. MG63 cells were grown on different PLLA films polarized and non-polarized and plastic. Black arrows (→) show the deposits of calcium stained positively by ARS.*

# Conclusion and prospects

# 1 Conclusion

Piezoelectric materials have a large potential for improving bone regeneration. In this work, we suggest to study the effect of the degree of crystallinity and of the polarization of a biocompatible, biodegradable and piezoelectric polymer, Poly (L-lactic) acid (PLLA), on the viability, the proliferation, the morphology and the mineralization of osteoblasts. Especially correlations between the degree of crystallinity, the polarization and the structural properties of the polymer that could subsequently improve osteoinduction and affect the performances of the biological assay were searched. In the frame of these objectives, three degrees of crystallinity and three poling values have been tested resulting in 9 different film configurations.

Relevant knowledgements resulted from this work. First the elaboration process has been improved. The degrees of crystallinity dramatically increased, from 0 to 20% for amorphous samples, from 7 to 30% for semi-crystalline films and from 35 to 75% for crystalline samples. Then the thermally assisted poling step has been demonstrated to have a great influence on the degree of crystallinity. Indeed, even if the effect of polarization is not clear, the thermal treatment being performed above the glass transition temperature, allows the rearrangement of the molecules and therefore the crystallization of the material. Structural characterization of the films allowed the identification of noticeable differences between the configurations. For example semi-crystalline and crystalline samples have very rough surfaces compared to amorphous surface.

In parallel to the characterization study, biological assays were conducted using two types of cells, both osteoblast: Human osteoblast Hob, a primary cell culture and Human osteosarcoma MG-63 cell line. Viability assays are promising, showing that osteoblasts grew on all surfaces. Thus, according to the results, we assume that crystallinity and roughness improve cell attachment and proliferation. Although the morphology assays have failed due to a bacterial infection it was possible to perform mineralization assays. These showed the production of mineralized material on semi-crystalline and crystalline poled samples.through the detection of calcium deposit, especially on the case of Hob However all these results have to be carefully considered. Hence it is not possible to correlate cells performances and films properties and therefore discriminate which

configurations are better, but trends can be distinguished allowing to make hypothesis and orientate the next experiments with the aim of better understanding the cells/PLLA interactions.

# 2 Future work

In the future, some work can be done in order to improve the study and obtain better results. A few suggestions are given bellow.

First of all, the elaboration must be well controlled, i.e. working under controlled atmosphere in order to always have the same amount of water.. Then the elaboration process has to be improved, working with larger quantity, in order to prepare PLLA film faster and control exactly their thickness. Finally the polarization equipment needs to be changed in order to increase the area of polarization and the refrigeration speed, to pole bigger samples in a shorter period of time. Once all these parameters have been improved, the PLLA film elaboration and polarization will be much faster allowing to focus on biological assays with higher results replication.

It has been shown that both human osteoblast and osteosarcoma cells attach and proliferate on PLLA films with different degrees of crystallinity and poling configurations. It is then suggested to repeat viability and mineralization assays (what is currently under experiment), and to carry out the morphology assays that are not done yet. Statistical analysis have to be performed in order to determinate whether the differences between the configurations come from PLLA film properties or are within the standard deviation.

# References

[1] R. Langer, J P. Vacanti. (1993). "*Tissue Engineering*". Science. 260: 920-926.

[2] LG. Griffith, MA. Swartz. (2006). "*Capturing complex 3D tissue physiology in vitro*". Nature reviews. Molecular cell biology. 7: 211-24.

[3] Castells-sala, C. *et al. (2013).* "*Biochips & Tissue chips Current Applications of Tissue Engineering in Biomedicine*". Journal of Biochips & Tissue Chips.

[4] Michalopoulos, G. K. & DeFrances, M. C. (1997). "*Liver regeneration*" Science 276, 60–66.

[5] E. S. Place, N. D. Evans, and M. M. Stevens. (2009). "*Complexity in biomaterials for tissue engineering*". Nature Materials. vol. 8, no. 6, pp. 457–470.

[6] X. Zhao, J. Kim, C. A. Cezar, et al. (2011). "*Active scaffolds for on-demand drug and cell delivery"*. Proceedings of the National Academy of Sciences of the United States of America. 108(1):67-72.

[7] L. Vernon, L. Kaplan, CY. Charles Huang. (2012). "*Stem Cell Based Bone Tissue Engineering*". Bone regeneration.

[8] J. Vilches, J. I. Vilches-perez, and M. Salido. (2007). "*Cell-surface interaction in biomedical implants assessed by simultaneous fluorescence and reflection confocal microscopy*", pp. 60–67.

[9] Antranik. (2011). "Cartilage and Bones" from: http://antranik.org/cartilage-and-bones; website consulted in November 2014.

[10] M. Gomes. (2004). "*A Bone tissue engineering strategy based on starch scaffolds and bone marrow cells cultured in a flow perfusion bioreactor*". PhD thesis, Minho, Universidade do Minho, departamento de engenharia de polimeros.

[11] F. Gobeaux. (2008). "*Phases denses de collagene de type I: transition isotrope/cholesterique, fibrillogenese et mineralisation*". PhD thesis, Paris, Universite Pierre et Marie Curie.

[12] T. Moloye. (2002). "*Composite scaffolds for bone tissue engineering*". PhD thesis, University of Florida.

[13] R. Havaldar, S. Pilli, and B. Putti. (2005). "*Effects of Ageing on Bone Mineral Composition and Bone Strength*", *iosrjournals.org*, vol. 76, no. 3, pp. 207–13.

[14] R. Havaldar, S. C. Pilli, and B. B. Putti. (2012). "*Effects of Ageing on Bone Mineral Composition and Bone Strength*". vol. 1, no. 3, pp. 12–16.

[15] PromoCell GmbH, "Osteoblast Differentiation and Mineralization". Application Note.

[16] B. M. Isaacson and R. D. Bloebaum. (2010). "*Bone bioelectricity: what have we learned in the past 160 years?*", *Jornal of biomedical materials research. part A*, vol. 95, no. 4, pp. 1270–9.

[17] J-M. André, M. Catala, J-J Morère, E. Escudier, G. Katsanis, J. Poirie (2007). "Chapitre 5 - Les tissus squelettiques", Histologie: les tissus;
from : http://www.chups.jussieu.fr/polys/histo/histoP1/POLY.Chp.5.2.html; website consulted in November 2014

[18] W. Korper, D. C. Jansen, P. Saftig, V. Everts, and J. M. Delaisse. (2002). "*The Bone Lining Cell : Its Role in Cleaning Howship ' s Lacunae and Initiating Bone Formation*". Journal of Bone and Mineral Research, vol. 17, no. 1.

[19] F. Shapiro. (2008). "*Bone development and its relation to fracture repair. The role of mesenchymal osteoblasts and surface osteoblasts*". European Cells and Materials, vol. 15, pp. 53–76.

[20] R. G. Bacabac, A. D. Bakker, M. B. Group, and C. City. (2012). "*Mechanical loading and how it affects bone cells: the role of the osteocyte cytoskeleton in maintaining our skeleton*". European Cells and Materials, vol. 24, pp. 278–291.

[21] T. Bouderlique. (2012). "*Etude des propriétés ostéoinductrices et chondroinductrices de "Heparin an regulatory peptide" sur les cellules stromales mésenchymateuses humaines, application en régénération osseuse*". PhD thesis, Université Paris-Est.

[22] National Institutes of Health. (2012). "*Osteoporosis Overview*", Osteoporosis and Related Bone Diseases.

[23] C. Hamilton and D. L. Seidner. (2008). "*Metabolic bone disease in the patient on long-term parenteral nutrition*", Practical Gastroenterology, vol. 58, pp. 18–32, 2008.

[24] a Sarmiento and L. Latta. (2006). "*The evolution of functional bracing of fractures*", The Journal of bone and joint surgery. British volume, vol. 88, no. 2, pp. 141–148.

[25] N. Hallab. (2006). "*Metal sensitivity in patients with orthopedic implants*", Journal of clinical rheumatology : practical reports on rheumatic & musculoskeletal diseases, vol. 7, no. 4, pp. 215–218.

[26] "*Bone graft*", University of Maryland Medical Center
from : http://umm.edu/health/medical/ency/articles/bone-graft#ixzz3dj5YaDyS; website consulted in May 2015

[27] AS. Bose, M. Roy, A. Bandyopadhyay. (2012). "*Recent advances in bone tissue engineering scaffolds*", Trends Biotechnology, vol. 29, no. 6, pp. 997–1003.

[28] A. Ami R., L. Cato T., and N. Syam P. (2013). "Bone Tissue Engineering: Recent Advances and Challenges", *Crit Rev Biomed Eng.*, vol. 40, no. 5, pp. 363–408.

[29] F. Yang, J. Wang, L. Cao, R. Chen, L. Tang, and C. Liu. (2014). "*Injectable and redox-responsive hydrogel with adaptive degradation rate for bone regeneration*" . *J. Mater. Chem. B*, vol. 2, no. 3, pp. 295.

[30] S. Y. Kim and J.-S. Park. (2014). *"Biomineralized hyaluronic acid/poly(vinylphosphonic acid) hydrogel for bone tissue regeneration". J. Applied Polymer Science*, vol. 41194.

[31] M. Yamamoto, Y. Tabata, L. Hong, S. Miyamoto, N. Hashimoto, and Y. Ikada. (2000). "*Bone regeneration by transforming growth factor β1 released from a biodegradable hydrogel*". Journal of Control. Release, vol. 64, no. 1–3, pp. 133–142.

[32] K. Gkioni, S. C. G. Leeuwenburgh, T. E. L. Douglas, A. G. Mikos, and J. a Jansen (2010). "*Mineralization of hydrogels for bone regeneration*". Tissue Engineering. Part B. Review, vol. 16, no. 6, pp. 577–85.

[33] B. Nordell. (1988). "*The dowsing reaction originates from piezoelectric effect in bone*". Symposium on Ecological Design, Luleå University of Technology.

[34] N. Barroca, P. M. Vilarinho, M. H. V. Fernandes, P. Sharma, and A. Gruverman. (2012). "*Stability of electrically induced-polarization in poly (L-lactic) acid for bone regeneration*". Applied Physics Letters, vol. 101, no. 2, p. 023701.

[35] A. A. Marino. (1988). "Direct Current and Bone Growth". Foundation of Modern Bioelectricity. New York, pp. 657-709

[36] V. Dumas. (2010). "Réponse des ostéoblastes à des stimulations physiques basées sur des contraintes mécaniques basses amplitudes hautes fréquences. Implication en ingénierie tissulaire". PhD thesis, Saint-Etienne, Universite Jean Monnet.

[37] A. Marino and R. Becker. (1970). "*Piezoelectric effect and growth control in bone*". Nature, vol. 228, pp. 473–474.

[38] F. R. Baxter, C. R. Bowen, I. G. Turner, and A. C. E. Dent. (2010). "*Electrically Active Bioceramics: A Review of Interfacial Responses*" , Annals of Biomedical Engineering. Vol. 38, No. 6. pp. 2079 2092.

[39] L. Cen, W. Liu, L. Cui, W. Zhang, Y. Cao. (2008). "*Collagen Tissue Engineering : Development of Novel Biomaterials*". Nature, vol. 63, no. 5, pp. 492–496.

[40] K. Gelse, E. Pöschl, and T. Aigner. (2003). "Collagens - Structure, function, and biosynthesis," Adv. Drug Delivery Re*view*, vol. 55, no. 12, pp. 1531–1546.

[41] H. Lee, R. Cooper, K. Wang, and H. Liang. (2008). "*Nano-Scale Characterization of a Piezoelectric Polymer (Polyvinylidene Difluoride, PVDF)*", *Sensors*, vol. 8, no. 11, pp. 7359–7368.

[42] Chandy T. Rao G.H. Wilson R.F. Das G.S. (2001). "*Development of poly(Lactic acid)/chitosan co-matrix microspheres: controlled release of taxol-heparin for preventing restenosis*", Drug Delivery, 8:77.

[43] L. Xiao, B. Wang, G. Yang, and M. Gauthier. (2006). "Poly(Lactic Acid)-Based Biomaterials:Synthesis, Modification and Applications", Biomedical Science, Engineering and Technology, pp. 247–282.

[44] D. E. Henton, P. Gruber, J. Lunt, and J. Randall. (2005). "*Polylactic Acid Technology",* Natural Fibers Biopolymers and Biocomposites, pp. 527–578.

[45] V. la Carrubba, F. C. Pavia, V. Brucato, and S. Piccarolo. (2008). "PLLA/PLA scaffolds prepared via thermally induced phase separation (TIPS): Tuning of properties and biodegradability", International Journal of Material Forming, vol. 1, no. SUPPL. 1, pp. 619–622.

[46] Gunatillake PA and Adhikari R. (2003). "*Biodegradable synthetic polymers for tissue engineering"*, European Cells and Materials, 1-16.

[47] M. Chaubal. (2002). "*Polylactides/glycolides-excipients for injectable drug delivery and beyond*", Drug Delivery Technology, vol. 2, pp. 34–36.

[48] M. Ando, H. Kawamura, H. Kitada, Y. Sekimoto, T. Inoue, Y. Tajitsu. (2013). "*New human machine interface devices using a piezoelectric poly (L-lactic-acid) film*", 236, 239.

[49] N. Barroca, P. M. Vilarinho, A. L. Daniel-da-Silva, A. Wu, M. H. Fernandes, and A. Gruverman. (2011). "*Protein adsorption on piezoelectric poly(L-lactic) acid thin films by scanning probe microscopy*", Applied Physics Letters, vol. 98, no. 13, p. 133705.

[50] U. Siemann. (2005). "*Solvent cast technology - A versatile tool for thin film production*," Progress in Colloid and Polymer Science, vol. 130, no. June, pp. 1–14.

[51] N. Degirmenbasi, S. Ozkan, D. M. Kalyon, and X. Yu. (2009). "*Surface patterning of poly(L-lactide) upon melt processing: in vitro culturing of fibroblasts and osteoblasts on surfaces ranging from highly crystalline with spherulitic protrusions to amorphous with nanoscale indentations*", Journal of biomedical materials research. Part A. vol. 88, no. 1, pp. 94–104.

[52] D.J. Griffiths. (2007). "*Introduction to Electrodynamics*", 3rd Edition, Pearson Education. ISBN 81-7758-293-3.

[53] C.B. Parker. (1994). "*McGraw - Hill Encyclopaedia of Physics*", 2nd Edition. ISBN 0-07-051400-3.

[54] M. B. Kechiche. (2013). "*Etude et developpement de capteurs / effecteurs filamentaires de faibles diametres integrables dans des structures textiles*". PhD thesis, Mulhouse, Universite de Haute Alsace.

[55] H. P. Schwan. (1966). "*Alternating current electrode polarization*", Biophysik, vol. 3, no. 2, pp. 181–201.

[56] K. Sekimoto and M. Takayama. (2009). "*Fundamental Processes of Corona Discharge ϒ Surface Analysis of Traces Stained with Discharge on Brass Plate in Negative Corona*", J. Inst. Electrostat. Jpn., vol. 1, no. 33, pp. 38–42.

[57] J. Fraden. (2004). "*Handbook of Modern Sensors*", Physics, designs and applications.

[58] M. Goldman, a. Goldman, and R. S. Sigmond. (1985). "T*he corona discharge, its properties and specific uses*", Pure Applied Chemistry, vol. 57, no. 9, pp. 1353–1362.

[59] Hubbell Power Systems, Inc. (2004). "*What is Corona? A Clearly Explained and Illustrated Story About Three Types of Corona Discharge and Their Relationship to Radio Interference*" , Bulletin EU1234-H.

[60] Haus, Hermann A., and James R. Melcher. (1989). "*Electromagnetic Fields and Energy*". ISBN: 9780132490207.

[61] N. S. Model. (2006). "*Polymer dipoles relaxation and potential energy (New Simulation Model )*", pp. 1–15.

[62] P. K. Gallagher. (1998). "*Handbook of thermal analysis and calorimetry*", volume 1 – Principle and practice, ISBN: 0-444-82085-X

[63] Philips. Electron. Optics. (1996). "*Environmental Scanning Electron Microscopy - An Introduction to ESEM*".

[64] P. Bouchareine. (1999). "*Métrologie des surfaces*", Techniques de l'ingénieur.

[65] B. Bhushan, (2001). "*Surface Roughness Analysis and Measurement Techniques*". Modern Tribology Handbook.

[66] M. Lotfi, M. Nejib, and M. Naceur. (2013). "*Cell Adhesion to Biomaterials : Concept of Biocompatibility*", Advances in Biomaterials Science and Biomedical Applications, pp. 207–240.

[67] D. Meyers. (1999). "*Wetting and spreading, Surfaces, Interfaces, and Colloids: Principles and Applications*", chapter 17, Second Edition. John Wiley & Sons, Inc., 419.

[68] H. Stanjek and W. Häusler. (2004). "*Basics of X-ray Diffraction*", Hyperfine Interact., vol. 154, no. 1–4, pp. 107–119.

[69] S. M. Mulla, P. S. Phale, and M. R. Saraf. (2012). "*Use of X-Ray Diffraction Technique for Polymer Characterization and Studying the Effect of Optical Accessories*", *AdMet 2012*, pp. 1–6.

[70] L. A. Pruitt, A. M. Chakravartula. (2011). "*Mechanics of Biomaterials - Fundamental Principles for Implant Design"*, Cambridge University Press. ISBN: 978-0-521-76221-2

[71] A. Rainer, M. Centola, C. Spadaccio, G. Gherardi, J. a. Genovese, S. Licoccia, and M. Trombetta. (2010). "*Comparative study of different techniques for the sterilization of poly-L-lactide electrospun microfibers: Effectiveness vs. material degradation*" , Int. J. Artif. Organs, vol. 33, no. 2, pp. 76–85.

[72] C. E. Holy. (2001). "*Optimizing the sterilization of PLGA scaffolds for use in tissue engineering*", Biomaterials, vol. 22, 25-31.

[73] M. Vaubourdolle. (2007). "*Infectiologie*", 3rd edition. ISBN: 978-2-915585-40-7

[74] J. E. Schechter, D. Ph, and S. C. Yiu. (2009). "Microporous Poly(L-Lactic Acid) Membranes Fabricated by Polyethylene Glycol Solvent-Cast/Particulate Leaching Technique", Tissue Engineering. Part C, Methods, vol. 15, no. 3.

[75] T. L. Riss, A. L. Niles, and L. Minor. (2004). "*Cell Viability Assays*", Assay Guidance Manual, pp. 1–23.

[76] S. Singh, P. Kumar, S. Sharma, F. Mumbowa, A. Martin, N. Durier. (2012). "*Rapid identification and drug susceptibility testing of mycobacterium tuberculosis: standard operating procedure for non-commercial assays: part 3: colorimetric redox indicator*", DOI: 10.4103/0974-2727. 105594

[77] "*Influence of topography and wettability on biocompatibility*", Application Note 17 , from: www.attension.com; website consulted in April 2015.

[78] M. a. Fernández-Rodríguez, A. Y. Sánchez-Treviño, E. De Luna-Bertos, (2014). "Wettability and osteoblastic cell adhesion on ultrapolished commercially pure titanium surfaces: the role of the oxidation and pollution states", Journal of Adhesion Science and Technology, vol. 28, no. 12, pp. 1207–1218.

[79] Di Lorenzo. (2006). "The Crystallization and Melting Processes of Poly(L-lactic acid)", Macromol. Symp., 234 : p. 176–183.

[80] J. Zhang, K. Tashiro, H. Tsuji, AJ. Domb. (2008). "Disorder-to-order phase transition and multiple melting behavior of poly(L-lactide) investigated by simultaneous measurements of WAXD and DSC", Macromolecules, 41(4):1352–7.

[81] M. Cocca, M. L. Di Lorenzo, M. Malinconico, and V. Frezza. (2011). "*Influence of crystal polymorphism on mechanical and barrier properties of poly(l-lactic acid)*" European Polymer Journal, vol. 47, no. 5, pp. 1073–1080.

[82] W. Hoogsteen, AR. Postema, AJ. Pennings, G. Ten Brinke, P. Zugenmaier. (1990). "*Crystal structure, conformation and morphology of solution-spun poly(L-lactide) fibers*", Macromolecules; 23(2):634–42.

[83] A. Allaire, M. X. Luong, and K. P. Smith. (2010). "*Basics of Cell Culture*" Human Stem Cell Technology and Biology: A Research Guide and Laboratory Manual, pp. 17–31, 2010.

[84] F. Langenbach and J. Handschel. (2013). "*Effects of dexamethasone, ascorbic acid and β-glycerophosphate on the osteogenic differentiation of stem cells in vitro*," Stem Cell Research and Therapy, vol. 4, no. 5, p. 117.

# Annexes

# Annex A: Film assembly protocol

***Materials***

- 50mL flask (better to use round-bottomed flask in order to avoid any deposition that would disturb the homogeneity of the solution)
- Magnetic agitator (homogenization of the heat and composition)
- 0,55g of PLLA ( PLLA38 Pursaborb: 3,8mL of dioxane per mg of PLLA; hydroscopic: absorb humidity so avoid prolonged exposure with air)
- 7,8 g of dioxane (Penreac)
- Hot plate
- Thermocouple
- Silicon oil bath
- Plastic pipette
- Ø5cm petri dish

***Protocol***

- Switch on the hot plate to heat up the oil until 80°C. The melting temperature of PLLA is around 70 °C. By working above it we ensure a good mixing. Tune the *heater* button on 50% max;
- Insert the 0,55 g of PLLA on a 50 mL flask;
- Add the solvent;
- Insert the magnetic agitator;
- Close the flask with the vial stopper, thus no vapor can escape but do not put it too deep, by heating up the pressure will increase what would eject it;
- Place the flask on the oil bath. Pay attention: the flask must not touch the plate;
- The working time is 2h30. After this period, when the PLLA is dissolved in the solvent, remove the flask and pour the solution inside a petri dish. Put as more as possible and, apply a rotary movement to the small plate in order to spread homogeneously the solution;
- Place the petri dish in the oven at 37°C in order to evaporate the solvent and after keep it always in a desiccator.

# Annex B: Crystallization protocol

***Materials***

- Hot plate
- Substrate
- Carbon tape
- Stamp (∞1,4cm)
- Chronometer
- Ω5cm film

***Protocol***

***Recrystallization***

*Amorphous samples*

- Adjust the set point to 180°C;
- Wait for the hot plate to reach this temperature;
- Place the substrate with the samples on the hot plate;
- Wait for 3 min, from the moment the sample starts to melt;
- Quench the substrate with the samples for 5 s in water;
- Remove the sample from the substrate.

*Crystalline samples*

- Adjust the set point to 180°C;
- Wait for the hot plate to reach this temperature;
- Place the substrate with the samples on the hot plate;
- Wait for 2 min;
- At the end of the 2 min, change the set point to 120°C (it will takes about 5 min to reach 120°C);
- Wait 45 min at 120°C;
- Remove the samples and leave it in a vacuum chamber (or dessicator) for 5-6 h.

# Annex C: Polarization protocol

### *Preparation of the sample*

***Materials***

- Aluminum sheet (square of 5x5cm)
- Carbon tape
- Sample
- Scissors
- Twizzers


***Figure 34***: *Equipment used for the preparation of the sample for polarization*

***Protocol***

| | |
|---|---|
| 1 . Place the sample at the center of the aluminum sheet | 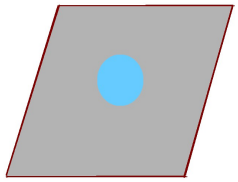 |
| 2. Use the carbon tape to fix the samples, applying it all around and leaving at least an inner circle of 1cm$^2$ - the PLLA sample should stay in close contact with the foil to avoid air layer in between them | 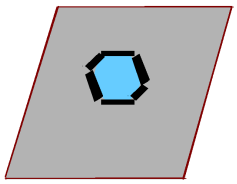 |
| 3 . Fold the aluminum foil, making small angles all around the sample in order to obtain a flat disc | 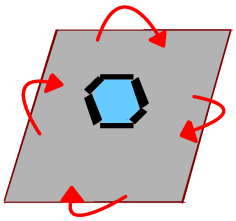 |
| 4. After preparation, store the sample in a dessicator box until the polarization step | 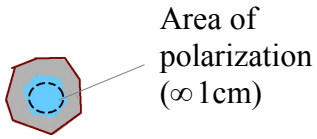 |

***Figure 35**: Schematic representation of the different steps of preparation of the sample for polarization*

### *Poling*

***Materials***

- Faraday cage
- Corona needle and plate
- Multimeter
- Temperature controller unit
- High voltage supply unit (positive or negative according to the source)

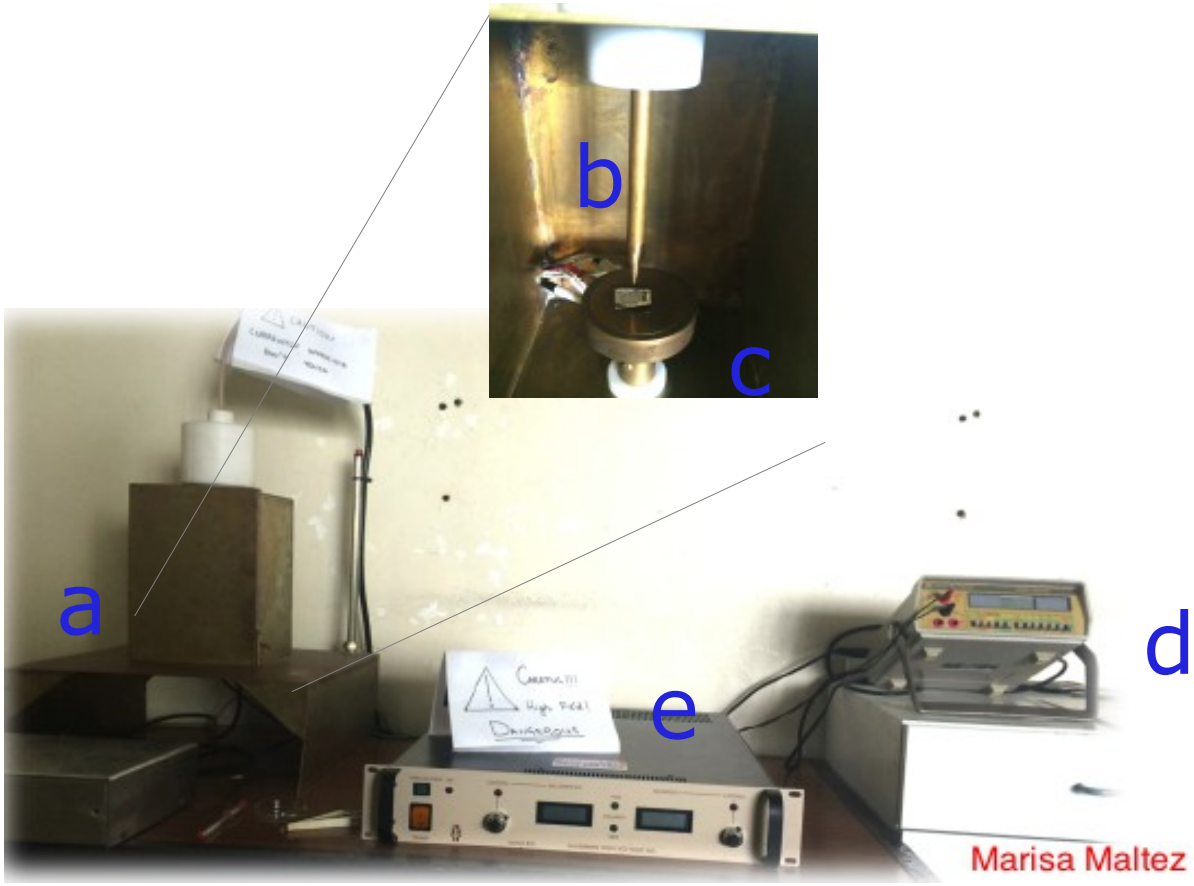


***Figure 36**: Corona polarization setup including a Faraday cage (**a**), a Corona needle and a Corona plate (**b** & **c**), a multimeter (**d**), and and a power supply unit (**e**)*

***Protocol (from Marisa Maltez)***

- Place the sample onto the plate, centered under the needle (the polarization only occurs in a Ø1cm area below the needle, the positioning of the sample is therefore paramount to ensure a good and homogeneous polarization)
- Close the Faraday cage (pay attention to the fact that the cage is properly closed, if the box is not fully closed the high voltage will not be applied for safety reasons)
- Switch on the temperature unit (by connecting the cable in the back part of the device) and adjust the set point to 80°C
- When the temperature reaches 80°C (it will take approximately 45min), switch on the multimeter and the power supply unit, adjust the output voltage to 9,5kV in order to obtain a reading around 6mV on the multimeter
- Apply a constant potential for 30 min, at a constant temperature (80°C)
- After 30 min, disconnect the temperature unit and leave the sample to cool down while still applying the constant potential
- When the temperature reaches the room temperature (~25°C), adjust slowly the output voltage to 0kV and then disconnect the high voltage unit
- Wait for 30s before opening the Faraday cage in order to avoid any electrical discharge
- Open the Faraday cage, remove the sample, write on the back the date and place it inside the dessicator

# Annex D : Surface roughness measurement protocol

## *Preparation of the sample*

**Materials**

- Sample
- Tape
- Micro slide for microscope

***Protocol***

- Wash the glass slide with ethanol
- Put on the sample on the clean surface
- Apply plastic tape on the side of the sample in order to immobilize it

***Comments***

- The sample needs to be immobilized otherwise it is moving during the measurements
- Double side tape can be used but then only one side of the sample can be measured, thus regular tape would be preferred

## *Roughness measurement*

***Materials***

- Sample ready to be measured
- Roughness measurement device (Hommel tester T1000)

***Protocol***

- Put the glass slide with the sample on a flat surface
- Place the tip of the tester above the sample. Pay attention to the needle path. The needle has to scan only the sample, otherwise the measurement will be wrong.
- Press start
- Write the result and repeat the same operation at least three times per sample

***Comment***

- The device is ready to used, it does not need to be calibrate
- The tip scratch the sample. Thus, when repeating the measurement you have to pay attention to not cross already probed lines, otherwise the results will be wrong
- Because the tip scratch the surface, the sample cannot be used anymore
- In order to be statistically representative, each configuration (degree of crystallinity and polarization) is tested on three samples, with at least 5 measurements per each sample, on several directions (horizontal, vertical and diagonal)

# Annex E: Wettability measurement protocol

## *Preparation of the sample*

### ***Materials***

- Sample
- Tape
- Glass micro slide

### ***Protocol***

- Wash the glass slide with ethanol
- Put on the sample on the clean surface
- Apply plastic tape on the side of the sample in order to immobilize it ensuring it to fit the surface in order to have a flat surface

### ***Comments***

- The sample needs to be immobilized in order to avoid it moving during the measurements
- Double side tape can be used but then only one side of the sample can be measured, thus regular tape would be preferred
- Flatness of the sample is important for two reasons: 1) to not introduce “mistakes” in the measurement; 2) to focus properly the camera on the surface

### *Contact angle measurement*

***Materials***

- Sample ready to be measured
- Contact angle goniometer

***Protocol***

- Adjust the levelness of the instrument and of the sample holder is necessary using a bubble leveler
- Clean the syringe and needle using distilled water
- Suck the liquid into the syringe
- Fix the syringe into the the holder of syringe pump
- Adjust the needle position
- Place the glass slide with the sample on the sample holder
- Dose a drop of liquid of 2 µL moving the needle down but drop end side does not touch the solid sample
- Focus the objective of the camera on the plan containing the water drop and the sample using the small screws
- Start recording
- Approach the drop of water to the surface of the sample
- Once the drop is in contact with the sample, go up until the water drop detach completely from the syringe
- Stop recording
- Repeat the same operation at least twice per sample

***Comment***

- The "videos" which have been recorded are then processed. Each video is fragmented in pictures. One is able then to determine the right image when the vibrations stop, and perform the measurement, by drop shape analysis, which corresponds to the static situation
- In order to be statistically representative, each configuration (degree of crystallinity and polarization) is tested on 3 samples, with at least 2 measurements per sample

# Annex F: Sterilization protocol

The next protocol is in english and translated from the portuguese version which was previously established by Ana Roque.

***Protocol***

1. PLLA samples have been previously introduced in the wells box
2. Keep samples in 70% ethanol for 15 min
3. Wash 5 times with distilled water
4. Wash 5 times with PBS pH 7,4
5. Wash once with cell culture medium

Phosphate Buffered Saline (PBS) is a buffer solution commonly used in chemistry for bio-research. It is a water-based salt solution containing sodium phosphate and sodium chloride. This solution is called buffer because it allows maintaining the pH at a constant value of 7,4 – pH of the blood of the human body. In general it is used for a wide variety of cell culture applications including washing cells before dissociation, transporting cells or tissue, diluting cells for counting, and preparing reagents.

# Annex G: Cell culture protocol

The next protocol is an english version translated from the portuguese version which was previously established by Ana Roque. This step was performed by Ana Roque IBIMED.

**A. Preparation of the culture flasks to Hob**

1. Remove the Hob growth medium from the refrigerator and decontaminate it with 70% ethanol
2. Pipette 15 ml of Hob growth medium at room temperature to a T-75 flask (ideally keep a ratio of 1 mL per 5cm$^2$)

**B. Defreezing and adhesion of Hob**

1. Remove the cryopreserved flask from the storage tank of liquid nitrogen
2. Defreeze quickly the cells bu putting the lower part of the flask in a bath at 37°C for 1 min
3. Remove the flask from the bath, dry and decontaminate the outside with 70% ethanol
4. In the flow chamber, remove carefully the vial stopper
5. Resuspend the cells in the vial, slightly pipetting the cells five times with a pipette of 2mL
6. Pipette the cell suspension (1mL) of the vial to the T-75 flask containing 15mL of Hob growth medium
7. Cap the bottle and shake slowly to distribute well the cells;
8. Place the flask in the incubator (37°C, 5%$CO_2$, wet atmosphere)
9. Replace the medium 24 hours later in order to remove all traces of DMSO
10. Change the medium every day until the cells reach a confluence of 60%
11. Double the volume of medium when the cell culture has reached a confluence > 60%, or growth during the weekend
12. Split cells when the cell culture reaches 80% of confluence

**C. Preparation of the neutralizing solution of Trypsin**

*For 200 mL of 5% buffer FBS without calcium and magnesium*

1. Prepare HBSS;
2. Inactivated FBS: 30min at 56°C (cool in refrigerator overnight);
3. Add 10mL of inactivated serum to 190mL of HBSS - store at 4°C.

**D. Split Hob**

*Trypsinize cells at room temperature. There is no heating of the reactants at 37°C*

4. Pipette 15mL of culture medium for new T-75 flasks
5. Remove the medium from the flasks with confluent Hob by aspiration
6. Wash cells with HBSS and remove the solution by aspiration
7. Pipette 6 ml of Trypsin/EDTA (solution) for the T-75 flask. Blend slowly the flask in order to ensure that the solution covers all cells
8. Close the flask and follow the process of trypsinization at room temperature using inverted microscope. Usually the cells become round after 2-4min
9. Release the cells from the flask surface, tapping the flask sides with the hand
10. Pipette 5mL of neutralizing solution of Trypsin to inhibit tryptic activity
11. Transfer the cell suspension into a 50mL sterile flask
12. Wash the flask with additional 5mL of trypsin neutralizing solution and transfer to the same flask of 50mL
13. Centrifuge the tube at 220g for 5 minutes to pellet the cells
14. Aspirate and throw the supernatant
15. Resuspend the cell pellet in 5mL of Hob growth medium by slowly pipetting
16. Count the cells on hemocytometer. Inoculate 10000 cells per $cm^2$ for growth fast or 5000 per $cm^2$ for normal growth

# Annex H: Viability and proliferation assay

The next protocol was kindly provided by Ana Roque from the biology IBIMED.

1. PLLA films were prepared in DEMAC by Mathieu Paradis and Marisa Costa.
2. For viability assay using resazurin, three samples of each condition were prepared. Each film has 0.2cm$_2$.
3. The films were placed into 96-well plates (Greiner, 96 Flat Bottom clear Polystyrene). In each film was placed an O-ring to immobilize it in the bottom of the well.
4. The diagram of the plate is presented below.

| | Added cells to each well | | | | | | | | | No cells added | | |
|---|---|---|---|---|---|---|---|---|---|---|---|---|
| MG63 | A | A | A | A+ | A+ | A+ | A- | A- | A- | A | A+ | A- |
| | SC | SC | SC | SC+ | SC+ | SC+ | SC- | SC- | SC- | SC | SC+ | SC- |
| | C | C | C | C+ | C+ | C+ | C- | C- | C- | C | C+ | C- |
| | P | P | P | - | - | - | - | - | - | P | P | P |
| HOB | A | A | A | A+ | A+ | A+ | A- | A- | A- | A | A+ | A- |
| | SC | SC | SC | SC+ | SC+ | SC+ | SC- | SC- | SC- | SC | SC+ | SC- |
| | C | C | C | C+ | C+ | C+ | C- | C- | C- | C | C+ | C- |
| | P | P | P | - | - | - | - | - | - | P | P | P |

***Legend:*** *A) Amorphous; A+) Amorphous positively-charged; A-) Amorphous negatively-charged; SC) Semi-crystalline; SC+) Semi-crystalline positively-charged; SC-) Semi-crystalline negatively-charged; C) Crystalline; C+) Crystalline positively-charged; C-) Crystalline negatively-charged; P) Plastic.*

5. The assays were performed by Ana Roque at IBIMED. Films were incubated with 70% ethanol for 15 minutes. The ethanol was removed and samples were washed 5x with dd$H_2O$. After remove the water, films were rinsed 1x with PBS pH7.4. PBS was washed off, and films were rinsed 1x with the respective cell culture media (HOB growth media (Sigma) and MEM media for MG63). (sterilization process, see annex F).
6. Each cell type was prepared separately. Briefly, the cell media of each plate was removed and the cells were washed 1x with PBS pH7.4. Then, the PBS was washed off and 5-8mL of Trypsin-EDTA 1x was added to each plate containing the cells.

Cells were incubated with trypsin for 3-5 minutes at room temperature (until all the cells are in suspension).

The cells were recovered to falcon tubes and 1mL of the respective cell culture media containing serum was added to each falcon tube to stop the action of trypsin. Cells were centrifuged at 1000rpm for 3 minutes at room temperature. The supernatant was discarded and the cell pellet resuspended in 1mL of the respective cell culture media. Cells were counted using hemocytometer.

7. To each well were added 1200 cells (30% confluent) in 100microliters of media. The plate was placed in the incubator at 37ºC, 5%$CO_2$.
8. The resazurin assay was performed every day during 8 days (100% confluent)
9. After 24h of incubation, the cell culture media was removed and 150 micro liters of PBS was added to each well. The PBS was removed and 100 micro liters of 10% of resazurin in PBS pH 7.4 was added to each well. The plate was placed in the incubator for 4 hours. After that time, the solution of resazurin was removed and added to a black 96-well plate (Greiner, 96 Flat Bottom Black Polystyrene). The plate was placed inside the plate reader (TECAN i-control) and the values of resorufin were determined using the software infinite 200. The readings were performed using the Mode: Fluorescence Top reading; multiple reads per well (circle filled): 2x2; Multiple reads per well (border): 600µm; Excitation wavelength: 560nm and Emission wavelength: 590nm; excitation bandwidth: 9nm; emission bandwidth: 20nm; Gain: 107(100%); number of flashes: 25; integration time: 20µs; initial shaking of 10 seconds.
10. The values of the resorufin inside the wells without cells were subtracted for each sample.
11. The data was plotted and statistical analyses were conducted using the IBM SPSS statistics22.

# Annex I: Morphology assay

The next protocol was kindly provided by Ana Roque from the biology IBIMED.

1. PLLA films were prepared in DEMAC by Mathieu Paradis and Marisa Costa.
2. For Cell morphology, two samples of each condition were prepared. Each film has 0.2cm2. One film was used for Immunofluorescence and the other film for SEM.
3. The films were placed into 96-well plates (Greiner, 96 Flat Bottom clear Polystyrene). In each film was placed an O-ring to immobilize it in the bottom of the well.
4. Films were sterilized by U.V during 20 min (only the films) plus 10 min (films and the O-rings) at DEMAC.
5. The diagram of the plate is presented below.

| Day 1 | | | | | | | | | | | | |
|---|---|---|---|---|---|---|---|---|---|---|---|---|
| MG63 | P | P* | | P | P* | | P | P* | | | | |
| | A | A | | SC | SC | | C | C | | | | |
| | A+ | A+ | | SC+ | SC+ | | C+ | C+ | | | | |
| | A- | A- | | SC- | SC- | | C- | C- | | | | |
| HOB | P | P* | | P | P* | | P | P* | | | | |
| | A | A | | SC | SC | | C | C | | | | |
| | A+ | A+ | | SC+ | SC+ | | C+ | C+ | | | | |
| | A- | A- | | SC- | SC- | | C- | C- | | | | |

***Legend:*** *A) Amorphous; A+) Amorphous positively-charged; A-) Amorphous negatively-charged; SC) Semi-crystalline; SC+) Semi-crystalline positively-charged; SC-) Semi-crystalline negatively-charged; C) Crystalline; C+) Crystalline positively-charged; C-) Crystalline negatively-charged; P) Plastic; P*) without O-ring.*

| Day 7 | | | | | | | | | | | | |
|---|---|---|---|---|---|---|---|---|---|---|---|---|
| MG63 | P | P* | | P | P* | | P | P* | | | | |
| | A | A | | SC | SC | | C | C | | | | |
| | A+ | A+ | | SC+ | SC+ | | C+ | C+ | | | | |
| | A- | A- | | SC- | SC- | | C- | C- | | | | |
| HOB | P | P* | | P | P* | | P | P* | | | | |
| | A | A | | SC | SC | | C | C | | | | |
| | A+ | A+ | | SC+ | SC+ | | C+ | C+ | | | | |
| | A- | A- | | SC- | SC- | | C- | C- | | | | |

***Legend:*** *A) Amorphous; A+) Amorphous positively-charged; A-) Amorphous negatively-charged; SC) Semi-crystalline; SC+) Semi-crystalline positively-charged; SC-) Semi-crystalline negatively-charged; C) Crystalline; C+) Crystalline positively-charged; C-) Crystalline negatively-charged; P) Plastic; P*) without O-ring.*

6. The biology assays were performed by Ana Roque at IBIMED. Films were rinsed 1x with the respective cell culture media (HOB growth media (Sigma) and MEM media for MG63).
7. Each cell type was prepared separately. Briefly, the cell media of each plate was removed and the cells were washed 1x with PBS pH 7.4. Then, the PBS was washed off and 5-8mL of Trypsine-EDTA 1x was added to each plate containing the cells. Cells were incubated with trypsine for 3-5 minutes at room temperature (until all the cells are in suspension). The cells were recovered to falcon tubes and 1mL of the respective cell culture media containing serum was added to each falcon tube to stop the action of trypsine. Cells were centrifuged at 1000rpm for 3 minutes at RT. The supernatant was discarded and the cell pellet resuspended in 1mL of the respective cell culture media. Cells were counted using hemocytometer. To each well were added 1200 cells (30% confluent) in 100 microliters of media. The plate was placed in the incubator at 37ºC, 5%CO2.

**A. Immunofluorescence**

1. After 1, and 7 days remove the cell media and rinse cells once with PBS pH 7.4 briefly to remove media components;
2. Prepare a fresh solution of 4% paraformaldehyde in PBS pH 7.4 (4g paraformaldehyde in 100ml dH2O. Heat to ~60°C. Add 1 drop of 1M NaOH. Filter stock thru 0.2 μm filter);
3. The cells grown on PLLA films were fixed using 4% of paraformaldehyde in PBS pH 7.4 for 15 minutes at room temperature;
4. Wash the cells three times with PBS pH 7.4;
5. Permeabilize the fixed cells by incubating in 0.1% Triton X-100 in PBS for 1 minute at room temperature;
6. Rinse gently in PBS with four changes over 5 minutes;
7. The cells were incubated with Rhodamine-phalloidin (Molecular Probes) diluted 1:500 in PBS for 30 minutes at room temperature in the dark. (Phalloidin binding requires the F-actin to have a protein structure near native);
8. Rinse 3 times in PBS, 5 minutes per wash;
9. Mount for microscopy using DAPI-plus VECTASHIELD (Vector laboratories) as mounting medium;
10. The preparations were observed under a confocal microscope.

**B. Scanning Electron microscopy**

1. The samples were fixed in 2% glutaraldheyde com 0.2% sodium cacodilate (20840-Sigma) pH 7.2-7.4 during 30 minutes at room temperature;
2. After fixation, the fixative was aspirated into a waste container for disposal. The samples were washed three times in 1ml 0.2% sodium cacodilate to remove excess fixative, and the waste liquid was discarded.
3. For the dehydration process, 1 ml of 25% ethanol was added into each well and incubated for 15 min at room temperature. The ethanol was aspirated and discarded. The last step was repeated using increasing concentrations of ethanol: 50 %, 75 %, 96% (2 times) and 100 % and finally absolute ethanol.
4. Hexamethyldisilazane (sigma-440191) was added to the samples for 10 minutes at room temperature;
5. The samples were placed at 4ºC prior to gold sputter coating.

# Annex J: Mineralization assay

The next protocol was kindly provided by Ana Roque from IBIMED.

1. PLLA films were prepared in DEMAC by Mathieu Paradis and Marisa Costa.
2. For mineralization assay using Alizarin red, two samples of each condition were prepared. Each film has 1cm$_2$.
3. The films were placed into 24-well plates (Orange, 24 Flat Bottom clear Polystyrene). In each film was placed an O-ring to immobilize it in the bottom of the well.
4. The diagram of the plate is presented below.

| | | | | | | |
|---|---|---|---|---|---|---|
| MG63 | A | A | A+ | A+ | A- | A- |
| | SC | SC | SC+ | SC+ | SC- | SC- |
| | C | C | C+ | C+ | C- | C- |
| | P | P* | - | - | - | - |

***Legend:*** *A) Amorphous; A+) Amorphous positively-charged; A-) Amorphous negatively-charged; SC) Semi-crystalline; SC+) Semi-crystalline positively-charged; SC-) Semi-crystalline negatively-charged; C) Crystalline; C+) Crystalline positively-charged; C-) Crystalline negatively-charged; P) Plastic; P*) Osteogenesis induction.*

| | | | | | | |
|---|---|---|---|---|---|---|
| HOB | A | A | A+ | A+ | A- | A- |
| | SC | SC | SC+ | SC+ | SC- | SC- |
| | C | C | C+ | C+ | C- | C- |
| | P | P* | - | - | - | - |

***Legend:*** *A) Amorphous; A+) Amorphous positively-charged; A-) Amorphous negatively-charged; SC) Semi-crystalline; SC+) Semi-crystalline positively-charged; SC-) Semi-crystalline negatively-charged; C) Crystalline; C+) Crystalline positively-charged; C-) Crystalline negatively-charged; P) Plastic; P*) Osteogenesis induction.*

The biology assays were performed by Ana Roque at IBIMED. Films were incubated with 70% ethanol for 15 minutes. The ethanol was removed and samples were washed, 5x with ddH2O. After remove the water, films were rinsed 1x with PBS pH7.4. PBS was washed off, and films were rinsed 1x with the respective cell culture media (HOB growth media (Sigma) and MEM media for MG63).

5. Each cell type was prepared separately. Briefly, the cell media of each plate was removed and the cells were washed 1x with PBS pH7.4. Then, the PBS was washed off and 5-8mL of Trypsin-EDTA 1x was added to each plate containing the cells. Cells were incubated with trypsin for 3-5 minutes at room temperature (until all the cells are in suspension). The cells were recovered to falcon tubes and 1mL of the respective cell culture media containing serum was added to each falcon tube to stop the action of trypsin. Cells were centrifuged at 1000rpm for 3 minutes at RT. The supernatant was discarded and the cell pellet resuspended in 1mL of the respective cell culture media. Cells were counted using hemocytometer.
6. To each well were added 6000 cells (30% confluent) in 1.5mL of media. The plate was placed in the incubator at 37ºC, 5%CO2.

   The cells were maintained in culture for 21 days at 37ºC, 5%CO2, with changes of medium every 2 or 4 days in case of MG63 or HOB, respectively.

**A. osteogenesis**

Mineralization was **only** induced on confluent monolayer (day 13) of HOB or MG63 attached on plastic (P*) by addition of HOB growth media or MEM containing 10% (v/v) FBS, 100 µg/mL streptomycin, 100U/mL penicillin, and 2mM glutamine with osteogenic supplements, 1mM sodium glycerophosphate, 50µg/mL L-ascorbate (all Sigma–Aldrich), respectively. Cultures were incubated at 37 °C with 5% CO2 with changes of medium every 2 or 4 days for MG-63 an HOB cells, respectively.

**B. Detection and quantification of mineralization**

*Protocol adapted from: An Alizarin red-based assay of mineralization by adherent cells in culture: comparison with cetylpyridinium chloride extraction*. Carl A. Gregory, W. Grady Gunn, Alexandra Peister, and Darwin J. Prockop. Analytical Biochemistry 329 (2004) 77–84.

1. Monolayer in 24-well plates (~ 1cm2/well) were washed with PBS;
2. Then, they were fixed in 10% (v/v) formaldehyde (Sigma–Aldrich) at room temperature for 15 min;
3. The monolayer were washed **twice** with excess dH2O prior to addition of 500µL of 40mM Alizarin Red S (pH 4.1) per well;

Alizarin red S solution preparation:

- Add 40 ml dH2O to 500 mg alizarin red S;
- Adjust pH to 4.1 using 10% of ammonium hydroxide;
- Make up to 50 ml with dH2O (final concentration is 40mM)

4. The plates were incubated at room temperature for 20 min with gentle shaking;
5. After aspiration of the unincorporated dye, the wells were washed **four** times with 4mL dH2O while shaking for 5min;
6. The plates were left at an angle for 2 min to facilitate removal of excess water, re-aspirated, and then stored at -20 °C prior to dye extraction;
7. Stained monolayer were visualized by Light microscopy;
8. After capture the images, the staining was quantified using the following protocol:

**Protocol for quantitative analysis of Alizarin Red Staining**

Quantitative analysis of Alizarin Red Staining can be performed by determining OD405 values of a set of known Alizarin Red concentrations and comparing these values to those obtained from unknown samples. This protocol is particularly versatile in that the dye can be extracted from the stained monolayer and quantified directly. The sensitivity of the assay is improved by the extraction of the calcified mineral at low pH and, since the mineral is already stained in a quantitative manner, there is no requirement for an additional colorimetric quantification step.

1. Add 200µL 10% acetic acid (v/v) to each well of a 24-well plate and incubate for 30 minutes with shaking;
2. The monolayer will now be loosely attached. With the aid of a cell scraper, gently scrape the cells from the plate and transfer the cells and acetic acid to a 1.5mL micro-centrifuge tube;
3. Vortex vigorously for 30 seconds;
4. Heat to 85°C for 10 minutes. (**Note: To avoid evaporation, micro-centrifuge tube should be sealed with para-film)**;
5. Transfer tube to ice for 5 minutes. Note: Take care not to open the tube until fully cooled;
6. Centrifuge the slurry at 20,000xg for 15 minutes;
7. While centrifuging, make up Alizarin Red standards (Note: the standards can be prepared directly in the 96-well plate, as shown below, or in eppendorf tubes and then add 100µL/well):

[Alizarin Red S]stock solution= 20mg/ml

**A) 1mg/ml**: 10µl of [Alizarin Red S]Stock Solution + 190µl H2O ; vf=100µL/well

**B) 500µg/ml**: 100µl of **A** + 100µl H2O

**C) 250µg/ml**: 100µl of **B** + 100µl H2O (Discard 20µl to have a final volume of 100µl/well)

**D) 100µg/ml**: 80µl of **C** + 120µl H2O

**E) 50µg/ml**: 100µl of **D** + 100µl H2O

**F) 25µg/ml**: 100µl of **E** + 100µl H2O

**G) 10µg/ml**: 80µl of **F** + 120µl H2O (Discard 20µl to have a final volume of 100µl/well)

**H) 5µg/ml**: 100µl of **G** + 100µl H2O

**I) 0µg/ml**: 100µl H2O

9. When centrifugation is finished, remove 200µL of the supernatant and transfer to a new 1.5mL micro-centrifuge tube;
10. Neutralize the pH with 10% Ammonium hydroxide. Take a small aliquot and test pH to ensure it falls within the range of 4.1 -4.5;
11. Add 100µL of the standard or sample (in duplicate) to an opaque-walled, transparent bottom 96-well plate;
12. Read at OD405;
13. Plot Alizarin Red concentration vs. OD405.